THE ABSORPTION OF ULTRASOUND IN AQUEOUS SOLUTIONS OF BOVINE SERUM ALBUMIN AND POLYETHYLENE GLYCOL

BY

LAWRENCE WOLFE KESSLER
B.S.E.E., Purdue University, 1964
M.S., University of Illinois, 1966

THESIS

Submitted in partial fulfillment of the requirements
for the degree of Doctor of Philosophy in Electrical Engineering
in the Graduate College of the
University of Illinois, 1968

Urbana, Illinois

ACKNOWLEDGEMENT

The author wishes to express his grateful appreciation to his advisor Professor Floyd Dunn for suggesting the problem and for his continued interest and guidance throughout this investigation. Appreciation is also extended to Mr. William O'Brien for his invaluable assistance in the experimental work and to Mr. James Robertson for his contributions to the fabrication of the mechanical instrumentation used in this research. The helpful discussions with Professor Gregorio Weber are greatly appreciated. The author especially wishes to thank his wife for her patience and understanding throughout this difficult period.

TABLE OF CONTENTS

CHAPTER 1

INTRODUCTION

Propagation of an acoustic wave results in time dependent changes in the thermodynamic variables of the transmitting medium such as pressure and density. The wave motion is described by equations which are analogous to those which describe the general phenomena of waves provided that the amplitude of the wave is infinitesimally small (Kinsler and Frey, 1950). Sound waves above approximately 20 kHz are referred to as ultrasonic waves since they are beyond the limit of human auditory perception. The medium through which the sound wave propagates is characterized by its acoustic impedance Z which, for plane wave propagation, is equal to the product of the density and the speed of sound in the material. For propagation in a "lossless" material, Z is constant and is equal to a real number. However in a lossy material, Z, is a complex quantity dependent on frequency and energy is transferred from the sound wave to the propagating medium where it is dissipated as heat. This results in a decrease in amplitude of the sound wave as it continues to propagate in the lossy medium, and this process is known as absorption. The ultrasonic absorption coefficient is a characteristic of the transmitting medium which describes the amount of attenuation an acoustic wave undergoes per unit distance. The determination of the ultrasonic absorption coefficient as a function of frequency is called ultrasonic spectroscopy and it provides a useful method for studying fast reactions having time constants in the range from 10^{-9} sec to 10^{-4} sec.

The mechanism of interaction of high intensity, noncavitating ultrasonic waves ($>>$ 1 w/cm^2) and biological media is not well understood (Dunn, 1958). Alteration of irradiated cells occurs almost instantaneously

as observed by loss of physiological function, yet it is not until approximately 15 min later that histological signs of cellular damage become apparent. Thermal processes have been shown not to be the primary mechanism by which damage occurs. In experiments using infant mice whose body temperatures were decreased below the normal temperature of the adult, the local temperature of the irradiated tissues never reached damaging levels although physiological function was irreversibly altered. Further, a theory postulating that unidirectional forces which are caused by the acoustic wave may produce elastic failure of structural components of tissue (Welkowitz, 1955) is not supported by experiment (Dunn, 1957). A possible explanation for these observed effects is that the site of the physical action of the sound wave is at the molecular level, however, it was shown recently (MacLeod and Dunn, 1966) that high intensity, non-cavitating ultrasound could produce no inactivation of selected enzymes, nor could it interfere with their specific activity during reactions even though enough energy was absorbed by the solution to have completely denatured the enzyme molecules if a major portion of the available energy was coupled to molecular bonds. Since all the acoustic energy is apparently not coupled to the bonds of the enzyme molecules, the question arises regarding what kinds of processes are responsible for the observed absorption. In general terms, any process which results in a phase difference between acoustic variables such as pressure and density, can lead to absorption. Specific mechanisms which cause such phase differences are discussed in Chapter II, though the magnitude of the observed absorption in protein solutions remains unaccounted for quantatively by any theory presently available.

It has been shown that the absorption of sound arising from a suspension of intact red blood cells is largely due to the protein content of the cells (Carstensen, et al., 1953) implying that the absorption of sound in tissue may be due largely to the protein content. However, Hawley et al. (1965) observed that in addition to proteins, contributions by other large macromolecules which assume different molecular configurations in aqueous solution may also play a significant role in the absorption in tissue.

In order to elucidate the important mechanisms of absorption in aqueous solutions of biologically important macromolecules, it is necessary to examine the significance of molecular configuration. This can be accomplished by comparing the ultrasonic spectrograms of different macromolecules which possess structural similarities and relating their acoustic properties with known structural simplicity are useful since the relationship between acoustic and structural properties may be more easily determined.

There are three basic spacial configurations that a long chain macromolecule can assume in solution depending upon the solvent and solute interactions (Tanford, 1961). Molecules are said to be randomly coiled if all possible configurations of the chain can occur with equal probability. In this case, the macromolecule is best described by an average configuration. However, true random coils do not exist experimentally since complete flexibility is not possessed by the molecular chains and strong attractive interactions exist between sites on the solute and solvent molecules. A macromolecule can assume the shape of a helical rod if strong attractive intramolecular interactions are present between specific, regularly spaced sites along the chain and such interactions are more

probable than interactions with solvent molecules. The third configuration is that of a compact, rigid, globular mass. If the probable interactions in the solute-solvent system are attractive forces between various non-specific portions of the chain, in addition to strong intermolecular solvent attractions, the molecule will assume a configuration which minimizes the number of solvent-solute contacts. If, in addition, a few strong attractions exist between solvent molecules and sites along the solute molecule, the resulting configuration will maximize the number of probable solvent-solute contacts and minimize others.

To date, only a few biologically important macromolecules have been subjected to thorough ultrasonic examination. For both hemoglobin (Carstensen and Schwan, 1959b), a globular protein, and dextran (Dessler, 1966; Hawley and Dunn, 1968), a random coil molecule, the interaction between solvent and solute has been suggested as the principal contributor to the observed absorption. The pressure variations associated with the sound wave is thought to perturb the equilibrium distribution of solvent molecules that are weakly bonded to the solute. Polyglutamic acid, a synthetic polypeptide that can be made to undergo a configurational change from the helix form to the random coil form as a function of pH has been examined by Schwartz (1965) and Lewis (1965). While the first investigator has attributed the excess absorption to the helix coil transition, the latter attributes it again to interaction between solvent and solute. Zana et al. (1963) have measured the absorption in nonaqueous solutions of several synthetic polypeptides that were made to undergo helix coil transitions. Although the results obtained do not show any direct evidence of the helix coil transition being responsible for the observed absorption, a

definite change in the absorption is found as the molecular structure is changed.

One purpose of this investigation is to explore further the use of ultrasonic spectroscopy as an investigative probe for observing molecular conformal changes and to provide additional evidence that may be necessary to associate directly the magnitude of the ultrasonic absorption with interactions between solvent and solute. Bovine serum albumin, a globular protein which can be made to undergo a conformal change, was chosen for this study because many of its physical and chemical properties have been rather well characterized by numerous investigations (Foster, 1960) and therefore acoustic parameters would be easier to correlate with the known characteristics of the molecule. Chapter 4 contains a brief summary of the present state of understanding of the conformal changes that occur in bovine serum albumin outside the pH range $4.3 \leq pH \leq 10.5$ but generally speaking, the molecule has a compact globular form within the stated pH region and an expanded form outside that region. Bovine serum albumin, Fraction V, was used in this investigation since it is more readily available than the purest fraction in the large quantities necessary for ultrasonic absorption measurements as specified in Chapter 3.

An additional purpose of this investigation is to determine if similarities exist in the ultrasonic absorption spectra of different molecules that assume similar structural configurations in solution. For this purpose, polyethylene glycol, a synthesized long chain flexible molecule, which assumes a random coil configuration in aqueous solution was chosen. Several narrow molecular weight fractions are commercially available from the highly polymerized form (Mw 20,000) to the monomer, ethylene glycol (Mw 62), thereby enabling the investigation of the effect

of polymerization on the absorption coefficient and the comparison to that obtained for dextran (Hawley and Dunn, 1968).

This thesis is organized in the following manner: Chapter 2 presents a selection of the theories of absorption of ultrasound in pure liquids and solutions which are considered to be important for this investigation. Solutions of randomly coiled molecules and solutions of dense compact irregular particles are given special attention. Absorption processes are considered from the frictional losses in a purely viscous liquid and from the molecular standpoint. Chapter 3 is concerned with the principles and techniques used to obtain information on the absorption and velocity of sound in liquid media. Each technique employed is discussed from the standpoint of its usefulness and limitations. The instrumentation designed and fabricated for these experiments is also described. The results of the investigations on aqueous solutions of bovine serum albumin and on aqueous solutions of polyethylene glycol are presented in Chapter 4 and the discussions of the results follows in Chapter 5. Concluding remarks that can be made as a result of the present investigation are presented in Chapter 6. For possible future reference and completeness, tabulations of the data and the detailed electronic circuitry of instruments designed during this investigation are included in the appendix.

CHAPTER 2

THEORIES OF ULTRASONIC ABSORPTION

A. Classical Absorption Mechanisms

1. Viscoelastic Mechanisms

The propagation of an acoustic wave through a compressible medium is accompanied by changes in instantaneous pressure, density, particle displacement, particle velocity and temperature. The term "particle" refers to a volume element of the medium which is sufficiently small such that the acoustic variables are constant throughout, yet sufficiently large to be characterized by macroscopic characteristics such as density, compressibility, etc. For a perfectly elastic, invisid medium, i.e., one in which applied stress and resulting strain are proportional and in which the viscosity is zero, energy is not dissipated in the wave propagation process. On the other hand, in a viscous fluid, i.e., one in which an applied stress and the resulting rate of strain are proportional, and in a general viscoelastic medium, energy is dissipated due to the frictional resistance to flow and results in attenuation of the acoustic wave. This process is referred to as absorption, and several specific processes by which it occurs will be considered below. In general, absorption results when density variations do not remain in phase with pressure variations as the wave propagates.

The behavior of a viscoelastic liquid in response to a sinusoidal compressional stress, T_V, of angular frequency ω can be described by the complex bulk modulus K^*, an intrinsic property of the medium,

$$K^* = \frac{T_V}{S_V} = \frac{K_o + j\omega K_\infty \tau_V}{1 + j\omega \tau_V} \tag{2-1}$$

where S_V is the compressional strain, K_o is the static bulk modulus of the liquid, K_∞ is the limiting bulk modulus at infinitely high frequency and τ_V is the relaxation time, i.e., the time required for the strain to reach within 1/e of its final value following a step change in compressional stress. If a sinusoidal shear stress is applied, the behavior of the viscoelastic liquid can be described by an equation analogous to (2-1) for the complex shear modulus G^*,

$$G^* = \frac{T_s}{S_s} = \frac{j\omega\tau_s G_\infty}{1 + j\omega\tau_s} \tag{2-2}$$

where $G_o = 0$ since a liquid cannot support a static shear stress. Under the assumption of infinitesimally small sinusoidal variations of the acoustic variables, the one dimensional wave equation for plane, longitudinal waves is

$$c^{*2} \frac{\partial^2 q}{\partial x^2} + \omega^2 q = 0 \tag{2-3}$$

where q represents any one of the acoustic variables and c^* is the complex velocity of propagation

$$c^{*2} = \left[\frac{4/3G^* + K^*}{\rho_o}\right] = \left[c + jc''\right]^2 \tag{2-4}$$

and ρ_o is the undisturbed density of the fluid. A solution to (2-3) for a wave propagation in the positive x direction in an unbounded, homogeneous medium is

$$q = Q_o e^{-\alpha x} e^{j(\omega t - kx)} \tag{2-5}$$

where α is the absorption coefficient and k is the wave number. If $\alpha/k << 1$, the absorption coefficient and the real part of the velocity are found to be

$$\alpha = \frac{1}{2c}\left[\frac{\dfrac{K_r\omega^2\tau_V}{1+\omega^2\tau_V^2} + \dfrac{4/3\ G_\infty\omega^2\tau_s}{1+\omega^2\tau_s^2}}{K_o + \dfrac{K_r\omega^2\tau_V^2}{1+\omega^2\tau_V^2} + \dfrac{4/3\ G_\infty\omega^2\tau_s^2}{1+\omega^2\tau_s^2}}\right] \tag{2-6}$$

$$c^2 = \frac{1}{\rho_o}\left[K_o + \frac{K_r\omega^2\tau_V^2}{1+\omega^2\tau_V^2} + \frac{4/3\ G_\infty\omega^2\tau_s^2}{1+\omega^2\tau_s^2}\right] \tag{2-7}$$

where $K_r = K_\infty - K_o$. At low frequencies such that $\omega\tau_V \to 0$ and $\omega\tau_s \to 0$, (2-6) and (2-7) reduce to

$$\alpha = \frac{\omega^2}{2\rho_o c^3}(\eta_V + 4/3\ \eta_s) \tag{2-8}$$

$$c = \sqrt{\frac{K_o}{\rho_o}} \tag{2-9}$$

$$\eta_V = \frac{1}{\omega}\,\mathrm{Im}\{K_V^*\} \tag{2-10}$$

$$\eta_s = \frac{1}{\omega}\,\mathrm{Im}\{G^*\} \tag{2-11}$$

where η_V and η_s are the bulk and shear viscosities of the fluid, respectively. Stokes (1845), who was the first to consider the effect of viscosity on absorption of sound set $\eta_V = 0$ since he had no method for dealing with it and derived an equation which is otherwise identical to (2-8). It remains today that the only method for measuring η_V is to measure α. The relaxation times for both shear and bulk processes in water are thought to be the same order of magnitude (Hirai and Eyring, 1958) and have been estimated to be about 10^{-12} sec (Hall, 1948) which

is not within the range of acoustical experimentation. Therefore (2-8) and (2-9) adequately describe the absorption coefficient and velocity of sound in water. Equation (2-9) is useful for determining the bulk modulus of liquids when ρ_o and c are known. If the fluid is a mixture of two homogeneous phases, for example, a solution of large molecules, a generalization of (2-9) can be used to calculate the bulk modulus of the large particles in solution. Urick (1947), under the simplifying assumption that the sound wave could not distinguish fine structure within the mixture and thus be reflected off boundaries at the solute solvent interfaces, derived the following equation

$$(2\text{-}12) \qquad (c/c_x)^2 = \left[1 + \phi \frac{K_o - K_1}{K_o}\right] \left[1 + \phi \frac{\rho_1 - \rho_o}{\rho_o}\right]$$

where c_x is the velocity of sound in the solution, ϕ is the volume fraction of solute particles in solution, K_1 is the static bulk modulus of the particles and ρ_1 is the density of the particles.

2. Heat Conduction Effects

Kirchhoff (1868) showed that the heat conductivity of the medium is, in part, responsible for absorption of energy from a propagating acoustic wave. At a particular instant of time during the passage of a sound wave, neighboring regions of different temperatures may exist, specifically, at the condensation of the wave, wherein the temperature is elevated above that of the undisturbed medium, while at the adjacent rarefaction the temperature is less than that of the undisturbed medium. Heat flows from the high temperature to the low temperature regions thus decreasing the temperature differential, and because of the PVT relationship, decreases the sound pressure, and thereby leading to absorption. The absorption

due to heat conduction is

$$\alpha = \frac{(\gamma - 1)k\omega^2}{2\rho_o c^3 c_p} \tag{2-13}$$

where γ is the ratio of the specific heat at constant pressure, c_p, to that at constant volume.

When the magnitude of the observed absorption in a liquid is small, the total absorption coefficient α_T can be considered to be the sum of the absorption coefficients due to each process acting alone. The term "classical absorption" refers only to the mechanisms of shear viscosity and heat conduction, viz.,

$$\alpha_{classical} = \frac{\omega^2}{2\rho_o c^3}\left[\frac{4}{3}\eta_s + \frac{(\gamma - 1)k}{c_p}\right] \tag{2-14}$$

It has been determined, however, that for most liquids, except liquid metals (Herzfeld and Litovitz, 1959) that the relative contribution of heat conduction is only about one percent compared to that of shear viscosity. Further, heat radiation contributions to absorption are entirely negligible.

B. Molecular Absorption Mechanisms

1. Discussion of General Relaxation Phenomena

The absorption of ultrasonic waves in aqueous solutions of macromolecules is not fully accounted for by the classical mechanisms and thus it is necessary to consider other mechanisms to account for the excess absorption. At the molecular level, the acoustic transmission medium can no longer be considered homogeneous and the acoustic wave must be considered to produce fluctuations of the average kinetic energy of the molecules. If molecules can reside in more than one energy state, it is

possible for the population distribution between states to be perturbed from equilibrium by the sound wave. The energy necessary for the molecules to overcome potential energy barriers and populate higher energy states is supplied by the sound wave.

The magnitude of absorption that occurs depends on the time required for the energy level transition to occur, compared with the period of the sound wave as well as the energy level difference between the states. For simplicity, consider a system which allows only two energy states denoted by A and B where A > B. If the time constant associated with a transition from A to B, or vice versa, is τ_{AB} and if the period of the acoustic wave $T >> \tau_{AB}$, the population of state A will increase during the condensation of the wave since work is done on the liquid and that of state B will increase during the rarefaction. Absorption occurs since a finite amount of time is required for the molecules to change energy states, resulting in a phase lag between applied pressure and the resulting population distribution. If, on the other hand, $T << \tau_{AB}$, the acoustic parameters will change more rapidly than the molecules can change states and little or no energy will be extracted from the wave process. When $\tau_{AB} = \frac{T}{2\pi}$, there is maximum interaction between the acoustic wave and the population distribution which results in maximum absorption per wavelength. Single relaxation mechanisms which involve only two energy states are not yet known to occur in aqueous solutions of macromolecules leading to the more complex situation wherein multiple relaxation times are present.

For a single relaxation process, the total absorption per wavelength can be expressed as

$$\alpha\lambda = B\omega + 2(\alpha_\lambda)_{max} \frac{\omega\tau}{1 + \omega^2\tau^2} \qquad (2\text{-}15)$$

where $(\alpha\lambda)_{max}$ is the maximum value attained by the function $(\alpha\lambda - B\omega)$ over all ω, B represents absorption contributions due to classical mechanisms and all other mechanisms that have characteristic relaxation times much smaller than τ. The parameter $(\alpha\lambda)_{max}$ and τ can be directly related to the molecular relaxation process (Lamb, 1965). Specifically $(\alpha\lambda)_{max}$ is a function of the difference in the energy levels between A and B while τ is a function of both the rate constant of the reaction and the magnitude of the potential energy barrier which a molecule must overcome before it can change states.

The square of the velocity of propagation for a single relaxation process is

$$c^2 = c_o^2 + \frac{2}{\pi} (\alpha\lambda)_{max} c_o c_\infty \frac{\omega^2 \tau^2}{1 + \omega^2 \tau^2} \tag{2-16}$$

where c_o and c_∞ are the limiting values for the velocity at very low and very high frequencies, respectively. Equation (2-16) shows that velocity dispersion accompanies relaxational behavior. However, in aqueous solutions of macromolecules the magnitude of the dispersion appears to be very small, on the order of 1 m/sec. For other liquids, however, it may be larger, e.g., in pure glycerol, the dispersion is 1850 m/sec (Piccirelli and Litovitz, 1957).

In the general, there may be N discrete relaxation processes occurring, though acting independently of one another, and the absorption per wavelength for such a system can be described by

$$\alpha\lambda = B\omega + \sum_{i=1}^{N} K_i \frac{\omega\tau_i}{1 + \omega^2 \tau_i^2} \tag{2-17}$$

where the K_i's are constants for each process. In practice it may not be

possible to distinguish a finite number of processes, whose relaxation times are of the same order of magnitude, from a continuous distribution. Also, since the absorption coefficient must be determined over more than one decade of frequency to characterize adequately a single process, many decades are necessary to characterize adequately a distribution of relaxation processes.

2. Structural Relaxation

Structural relaxation occurs when an acoustic wave perturbs the equilibrium distribution of molecules within their possible configurational states. Usually more than two energy levels exist (Litovitz and Davis, 1965) and, therefore, more than one relaxation time is necessary to describe the process. Liquid water, for example, consists of a mixture of instantaneously distinguishable species which have been shown to correspond to ice-like formations, or clusters of water molecules, suspended in a more dense packed state. Nemethy and Scheraga (1962a,b,c) propose that five energy levels must exist in order to account for the observed properties of water, while Hall (1948) suggests that only two may be necessary. The number of water molecules which makes up a cluster varies as a function of temperature, decreasing from about 91 molecules at 0° C to about 25 molecules at 70°C (Nemethy and Scheraga, 1962a,b,c). The clusters are in a dynamic state of breaking apart and reforming, each having a lifetime of about 10^{-12} sec according to the "flickering cluster" model of Frank and Wen (1957).

Macromolecules in aqueous solution provide additional structuring of the medium due to the fact that water molecules form hydration layers about each solute molecule. These hydration layers are believed to be

held together by networks of hydrogen bonds and to be attached to the solute through hydrogen bonds. When the hydration layer becomes extensive, as with proteins, where each gram of dry protein has 0.2 grams of hydration, the outermost regions in contact with the solvent are not as stable as the region that is bonded to the solute. The outer regions are in a dynamic state similar to cluster formations, and their equilibrium distribution may be perturbed by a sound wave.

Structural relaxation generally occurs in polar liquids and results in a bulk viscosity contribution to the absorption coefficient (Litovitz and Davis, 1965). Both the bulk and shear viscosities decrease as a function of increasing temperature, though their ratio remains relatively constant. For example, in the hydrogen bonded liquids such as water, the ratio η_V/η_s is three or less, and the ratio changes by only about 10% over a temperature variation of 60°C (litovitz, 1963).

3. Thermal Relaxation

Thermal relaxation occurs when an existing molecular equilibrium is perturbed by the periodic temperature fluctuation associated with the sound wave. All thermal relaxations that have been observed thus far have been single processes (Lamb, 1965) and the magnitude of the velocity dispersion that occurs is very small. For these processes, $\eta_V/\eta_s > 20$ and there is no obvious correlation between the temperature dependences of η_V and η_s. Thermal relaxation generally occurs in the non-polar liquids such as benzene and thus may not be expected to play a significant role in aqueous solutions.

4. Viscoelastic Relaxation of Randomly Coiled Polymers in Solution

The Shear viscosity exhibited by a dilute solution of long chain flexible polymers results from the frictional resistance of solvent molecules to flow past the polymer segments and the amount of energy that is required to perturb the configurational equilibrium of the polymer. The frequency of the periodic stress which is applied to the solution will influence the behavior of the motions of the polymer segments, and therefore the viscosity. Rouse (1953) determined exactly the coordinated motions of the polymer segments for the simplified case of an ideal gaussian polymer, i.e., a chain whose segments are distributed throughout space in such a way that the probability of finding ρ segments per unit volume a distance r from the center of mass of the polymer is given by

$$\rho = K e^{-\beta^2 r^2} \tag{2-18}$$

where K and β are constants related to the statistical dimensions of the polymer chain. The model for the polymer chain used in the theoretical analysis consists of a linear arrangement of N + 1 identical beads each having mass m connected alternately by N massless ideal springs. If complete flexibility is allowed at each bead, each segment is completely free to rotate. If $\bar{b}_o^2$ is the mean squared segment length, then the mean squared distance between the ends of the chain, $\bar{L}^2$, is given by the statistical random walk result for large N (Philippoff, 1965).

$$\bar{L}^2 = \bar{b}_o^2 N \tag{2-19}$$

For non-gaussian chains, $\bar{b}_o^2$ is replaced by $\bar{b}^2_{\text{effective}}$ for several reasons (Tanford, 1961), all of which affect the mean squared end to end distance: 1) The chemical bond, which is represented in the model by a

freely jointed spring, in reality maintains a constant angle in space and rotation about this bond angle is restricted; 2) The presence of one segment excludes the possibility of another segment occupying the same space (excluded volume effect); 3) In a solvent that is somewhat less than ideal, the distribution of polymer segments is more spread out; 4) Electrostatic interactions whether attractive or repulsive will further limit the possible configurations of the polymer; 5) The hydrodynamic flow at one bead is modified due to the presence of other beads; 6) Internal viscosity opposes the dynamic movements of the polymer molecule.

The solution of a set of N simultaneous differential equations which describes the motion of each bead when acted upon by thermal, viscous, and restoring forces, describes N modes of coordinated segment motions, each denoted by a characteristic relaxation time. The simple gaussian chain is "free draining" since the solvent molecules within the region of the center of mass are free to travel independently of the polymer segments. The solution to the equations for this case is given by both Rouse (1953) and Zimm (1956). However, when hydrodynamic interactions are present, the solution is somewhat more complex (Zimm, 1956) and this case is called "non-free draining" since solvent molecules become immobilized in the central region of the polymer. A third case is that in which the extension of the polymer is taken into account (Bloomfield and Zimm, 1966). In the following, η_s is the viscosity of the pure solvent and η^* is the complex viscosity of the solution. η_s is a real quantity since the elasticity of the solution is assumed to be entirely due to the presence of the polymer.

a) Free Draining Polymer (Rouse, 1953; Zimm, 1956)

For the free draining polymer

$$\eta^* - \eta_s = \frac{cN_a}{M_w} kT \sum_{k=1}^{N} \frac{\tau_K}{1 + j\omega\tau_K} \tag{2-20}$$

where c is the concentration of polymer molecules in units of trams per centimeter cubed of solution, M_w is the molecular weight of the polymer, N_a is Avagadro's number, T is the absolute temperature, k is Boltzmann's constant and the summation is carried out over all N segments of the polymer. The relaxation time τ_K for each mode is given by (2-21).

$$\tau_K = \frac{6M_w\eta_s[\eta]_o}{\pi^2 N_a kTK^2} \tag{2-21}$$

and is valid for values of K less than the number of segments of the chain divided by 5. The intrinsic (also designated as limiting) viscosity at $\omega = 0$, $[\eta]_o$, is a real quantity defined for infinitely dilute solutions as

$$[\eta]_o = \lim_{c \to 0} \frac{\eta^* - \eta_s}{c\eta_s} = \frac{\eta^* - \eta_s}{c\eta_s} \tag{2-22}$$

From (2-20), it has been shown (Zimm, 1956) that

$$[\eta]_o = \frac{N_a N^2 b_o^2 \rho_f}{36 M_w \eta_s} \tag{2-23}$$

where ρ_f is a frictional constant.

The first relaxation time, τ_1, corresponds to the "primary mode" of the polymer in which the ends of the molecule move in opposite directions while the center of mass remains stationary (Zimm, 1960). This is the primary contributor to the dynamic viscosity for all angular frequencies such that $\omega\tau_1 << 1$. The second relaxation time, τ_2, describes a mode in which both ends of the molecule move in the same direction while the

center of mass moves in the opposite direction. Each succeeding relaxation mode after the first corresponds to a smaller number of segments of the chain and each individually contributes less to the viscoelasticity of the solution.

b) Non-Free Draining Polymer (Zimm, 1956)

The expression for the intrinsic viscosity for this case is

$$[\eta]_o = \frac{\bar{L}^3 \pi^{3/2} N_a}{4\sqrt{3}\, M_w} \sum_{K=1}^{N} \frac{1}{\lambda_K'} \frac{1}{1 + j\omega\tau_K'} \tag{2-24}$$

where λ_K' is related to the K^{th} eigenvalue of the N simultaneous equations. The first five values of λ_K' are 4.04, 12.79, 24.2, 37.9, and 53.5 and correspond to the first five modes respectively. The relaxation time is a function of λ_K' and is given by

$$\tau_K' = \frac{M_w \eta_s [\eta]_o}{0.586 RT \lambda_K'} \tag{2-25}$$

When $\omega = 0$,

$$[\eta]_o = 2.84 \times 10^{23} \frac{\bar{L}^3}{M} \tag{2-26}$$

If (2-24) is put in a form similar to (2-20), the appropriate constants, save the relaxation time, are identical to that of the free draining molecule. Thus consideration of hydrodynamic interactions appears to affect only the distribution of relaxations times, viz.,

$$\eta^* - \eta_s = \frac{cN_a kT}{M_w} \sum_{K=1}^{N} \frac{\tau_K'}{1 + j\omega\tau_K'} \tag{2-20a}$$

c) Non-Free Draining, Extended Polymer Chain (Bloomfield and Zimm, 1966)

If $\bar{b}_{eff}^2 > \bar{b}_o^2$, then an expansion parameter ε is defined as

(2-27) $$\overline{b_{eff}^2}\, N = \overline{b}_o^{\,2}\, (N)^{1+\varepsilon}$$

The equation for the viscosity of an expanded polymer chain, including hydrodynamic interactions also reduces to the same form as (2-20) with the K^{th} relaxation time replaced by τ_K'' where

(2-28) $$\tau_K'' = \frac{M_w n_s [\eta]_o}{\left(\sum_{K=1}^{N} \frac{1}{\lambda_K''}\right) RT \lambda_K''}$$

and values for λ_K'' depend upon ε. For $\varepsilon = 0$, the relaxation times are approximately the same as those given for λ_K', as is expected. However, for $\varepsilon \neq 0$, the values of λ_K'' are tabulated in Table 2-1.

TABLE 2-1. TABLE OF EIGENVALUES FOR EXTENDED NON-FREE DRAINING POLYMERS (Bloomfield and Zimm, 1966)

	K						
ε	1	2	3	4	5	6	$\sum_{K=1}^{\infty} \left(\frac{1}{\eta_K''}\right)$
0.0	4.099	12.87	24.27	37.91	53.42	70.61	0.5810
0.1	5.078	16.37	31.47	49.81	70.94	94.60	0.4382
0.2	6.312	20.89	40.90	65.63	94.45	127.0	0.3341
0.3	7.930	26.92	53.69	87.29	127.0	172.3	0.2515
0.4	10.19	35.48	71.91	118.7	174.4	238.7	0.1875
0.5	13.11	46.82	96.80	161.5	239.9	330.9	0.1395

5. Viscoelastic Relaxation of Ellipsoidal Particles in Solution

The viscosity of a dilute solution of rigid spherical particles has been shown to be

(2-29) $$\eta = n_s (1 + 2.5\phi)$$

where ϕ is the volume fraction of solution occupied by the spheres (Einstein, 1920). If the particles are assymetric, the viscosity of the solution is greater in magnitude than for spheres of the same volume fraction, and is dependent on the degree of assymetry. Velocity gradients due to flow or produced by the passage of an acoustic wave tend to orient the particles, resulting in non-Newtonian behavior (Scheraga, 1955), i.e., the viscosity is not independent of the velocity gradient. Brownian motion of the ellipsoid will oppose any orienting force, and when the period of the acoustic wave becomes comparable to the time required for an oriented particle to reassume random behavior maximum absorption per wavelength occurs. The rotary diffusion constant, θ, is a measure of the time required for an external force to orient an assymetric particle which is under the influence of Brownian forces (Tanford, 1961).

Globular proteins at, or near their isoelectric point, assume a very compact dense structure which is impenetrable to solvent. Molecules of serum albumin, for example, can be represented by solid prolate ellipsoids that have an axial ratio, $p = a/b$, of about five (Tanford, 1961), where a is the semiaxis of revolution and b is the equatorial radius of the ellipsoid. The frequency dependence of viscosity in a dilute solution of rigid ellipsoids was given by Cerf (1952) who modified the theories of Saito (1951), Jeffery (1922), and Peterlin (1938). Scheraga (1955) then computed the general equations for the viscosity as a function of axial ratio and as a function of the amplitude of the velocity gradient. Since the viscosity of a solution of assymetric particles depends on the degree of assymetry, (2-29) can be generalized to

$$\eta^* = \eta_s(1 + \nu^*\phi), \tag{2-30}$$

where

(2-31) $$\nu^* = \nu - j\nu''.$$

ν^* is a complex shape factor, which for spheres is a real quantity independent of frequency, i.e., $\nu^* = 2.5$. For assymetric particles (Scheraga, 1955),

(2-32) $$\nu = \lim_{\phi \to 0} \frac{\eta^* - \eta_s}{\phi \eta_s}$$

or in terms of the intrinsic viscosity

(2-33) $$\nu = [\eta]_o \left(\frac{M_w}{N_a V_s}\right)$$

where V_s is the volume of a solute particle. Cerf (1952) has shown that under the condition $G_V = 0$, where G_V is the velocity gradient, the frequency dependence of ν^* can be written as

(2-34) $$\nu = \nu_A + \frac{\nu_B}{1 + \omega^2\tau^2}$$

(2-35) $$\nu'' = \frac{\omega\tau\nu_A}{1 + \omega^2\tau^2}$$

where $\tau = 1/6\theta$, $\nu_A = 3.434$ and $\nu_B = 2.372$ for $p = 5$. For other values of p, the reader is referred to the tabulation in Scheraga's (1955) paper. To justify the applicability of this equation to acoustic measurements, it must be shown that the velocity gradients present are negligibly small. Consider an extreme case for the present instrumentation where the frequency is 100 MHz and the acoustic intensity is 0.01 watts/cm^2. The normalized velocity gradient, $G_{V/\theta} = 0.4$, where the value of θ was taken as 0.84×10^6 (Tanford, 1961). At this velocity gradient, the shape

factor differs by less than 0.2% from the ideal case at zero velocity gradient. Substituting the proper values of ν_A and ν_B in (2-23) and (2-34)

$$\frac{\eta^* - \eta_s}{c\eta_s} = \frac{N_a V_s}{M_w}\left[3.434 + \frac{2.372}{1 + j\omega\tau}\right] \tag{2-36}$$

where τ, the rotational relaxation time is given by Perrin (1934) for $p > 5$.

$$\tau = \frac{\pi \eta_s L^3}{9kT(2 \ln 2p - 1)} \tag{2-37}$$

where $L = 2a$ is the length of the major diameter of the ellipsoid.

6. Relative Motion and Scattering Losses

If the general hydrodynamic wave equation is solved completely, the existence of both longitudinal (compressional) waves and transverse (shear) waves is allowed. In an elastic medium, both waves propagate readily. In a viscous medium such as water, on the other hand, the absorption coefficient for shear waves is greater than that for longitudinal waves by a factor greater than 10^6 at 1 MHz and thus shear waves are almost immediately degraded into heat through the absorption process. In a solution of spherical particles, whose diameter is small compared to the wavelength of sound, partial conversion of the propagating longitudinal wave, to transverse waves takes place at the particle boundaries resulting in absorption. The most general treatment of this problem has been given by Epstein (1941) who considered the above absorption mechanism in addition to the following mechanisms. A frictional loss results when the suspended particles do not follow the oscillatory motion of the solvent in phase, and absorption results from frictional losses due to relative motion

between the solvent and solute. Scattering is also considered as a source of absorption wherein the acoustic wave impinges on particles of a different acoustic impedance than the solvent and the scattering occurs since the particles are excited to vibrate in particular modes and reradiate energy spatially determined by that mode of vibration. This mechanism does not involve dissipation of acoustic energy directly but merely a redistribution throughout space which, due to the nature of experimental techniques appears as an absorption. The relative contribution by scattering to the total absorption coefficient in the solutions considered here is insignificant since the wavelength of sound is always much larger than the particle diameter (Hawley, 1966; Carstensen and Schwan, 1959a). Other investigators (Urick, 1948; Lamb, 1945; Fry, 1952) have also considered relative motion and have obtained results equivalent to those of Epstein.

The absorption coefficient derived by Epstein (1941), with scattering neglected is, to a first approximation,

$$\alpha = \frac{2}{3} \pi a^3 n k (\delta - 1) \text{ Re} \left\{ \frac{j + b - jb^2/3}{\delta - jb\delta - (2 + \delta)b^2/9} \right\}, \tag{2-38}$$

where n is the number of particles per cubic centimeter, δ is the ratio of the density of the solvent to that of the suspended particles, and b is defined as

$$b^2 = j\omega \frac{\rho_s}{\eta_s} a^2 \tag{2-39}$$

where ρ_s is the density of the solvent and a is the radius of the particle. Following the treatment by Carstensen and Schwan (1959), (2-38) can be put into the following form

$$\alpha = \frac{V_p}{2c} \left(\frac{\delta - 1}{\delta}\right)^2 \cdot \frac{m}{Me} \cdot \frac{\tau_o \omega^2}{1 + \omega^2 \tau_o^2} \tag{2-40}$$

(2-41) $$V_p = 4/3\ \pi\ a^3 n$$

(2-42) $$Re = 6\pi a \eta_s [1 + \gamma\omega^{1/2}]$$

(2-43) $$Me = M + m[1/2 + 9/4\ \frac{1}{\gamma\omega^{1/2}}]$$

(2-44) $$\gamma^2 = \frac{\rho_s a^2}{2\eta_s}$$

(2-45) $$\tau_o = \frac{Me}{Re}$$

where M is the mass of the solute particles, m is the mass of an equivalent volume of the solvent, and c is the velocity of propagation of sound.

CHAPTER 3

EXPERIMENTAL

A. Measurement Techniques

1. General

The amplitude of a plane, progressive, sinusoidal wave decays exponentially as it propagates through a lossy, homogeneous, infinitely extended medium according to (3-1)

$$P(x) = P_o\, e^{-\alpha x} \tag{3-1}$$

If, however, the acoustic wave is normally incident on a plane boundary of different acoustic impedance, located at x_o, a standing wave results. In this case, the amplitude of the wave must be extracted from the following expression for the instantaneous pressure.

$$P(x,t) = P_1\, e^{-\alpha x}\, e^{j(\omega t - kx)} + P_2\, e^{-\alpha(x_o - x)}\, e^{j(\omega t + kx_o - kx)} \tag{3-2}$$

where P_1 and P_2 are constants which depend on the acoustic impedances of the two media. In order to determine the absorption coefficient, α, $P(x,t)$ must be determined as a function of x and, in order to measure the phase velocity, c, the wavelength of the sound in the medium must be determined. A relatively complete summary of various methods used to measure α and c is given by Markham et al. (1951).

The pulse technique, which is employed in this study to measure the absorption coefficient can simulate the free field condition described by (3-1). It was first described by Pellam and Galt (1946) and was adapted from WWII radar technology. The basic pulse echo system consists of a piezoelectric transducer which emits a short pulse of sound into the

liquid to be measured. An acoustic reflector is set parallel to the transducer to produce reflection of the emitted sound back to the transducer. After emitting an acoustic pulse, the transducer is switched electronically to receive the reflected energy, but because of the large impedance mismatch between the liquid and the transducer, most of the sound is reflected again. The amount of acoustic energy coupled to the transducer, however, produces an electrical signal which is proportional to the pressure wave amplitude. The received signal is amplified and displayed in such a way that the signal amplitude can be measured. The transducer is attached to a moveable mount and when the path length is changed, the amplitude of the received pulse changes accordingly, since the pulse travels different distances between reflections. Since no standing waves exist, the amplitude changes in accordance with (3-1), and a plot of the pressure amplitude as a function of twice the transducer-reflector distance permits determination of α. The velocity of sound can be computed if the time difference between two successive reflections is measured and the distance between the transducer and reflector is known. The pulse technique has the advantage that the duty cycle of the acoustic pulse can be made small so that the average intensity of the acoustic wave will not be great enough to cause any appreciable temperature rise in the liquid.

2. Diffraction Effects

The discussion thus far has assumed plane wave propagation and the experimental justifications of this assumption and limitations will now be discussed. Guided mode propagation will be ignored in this discussion due to the relatively small ratio of transducer diameter to absorption chamber diameter employed in this study (Del Grosso, 1964).

A point source of acoustic waves produces wavefronts that are spherical, i.e., the instantaneous pressure amplitude of sinusoidally varying progressive waves produced by such a source obeys the following relationship (Kinsler and Frey, 1950)

$$P(x,t) = P_o/r\, e^{-\alpha r}\, e^{j(\omega t - kr)} \qquad r \neq 0 \tag{3-3}$$

where r is the distance from the point source and P_o is a constant. It can be seen that unlike plane waves, in the absence of absorption the pressure amplitude of a spherical wave decreases as 1/r. A finite size piston source such as a piezoelectric plate whose thickness varies uniformly in response to an applied electric field, produces wavefronts that depart from planarity. Consider a piston source to be represented by a circular disc on which is distributed an infinite number of point sources, all producing in phase spherical waves, then the sound pressure at any point in space is simply the superposition of the contributions of each point source. Since the relative phase of each contribution differs from that of another, interference results and the resulting nonuniformity of the pressure along a surface parallel to the piston source is known as diffraction. If the surface parallel to the piston source is a piezoelectric transducer employed as a receiver then the electrical output of the transducer is proportional to the integral of the pressure over its surface, i.e.,

$$E(x,t) = K' \int_0^{2\pi} \int_0^{a} P(r,\theta,t)\, r\, dr\, d\theta \tag{3-4}$$

where E(x,t) is the voltage output as a function of distance between source and receiver, a is the radius of the receiver, K' is a constant of proportionality and r and θ are the polar coordinates of the points along

the receiver surface. In order to determine the variation of the output voltage as a function of x in the absence of absorption, it will be assumed that a transmitting and receiving transducer, of equal dimensions are set parallel to each other coaxially and that the transmitter behaves as an ideal piston source. The most complete solution of this problem to date for circular transducers was obtained by Del Grosso (1964). Using his results, valid corrections may be made to an observed absorption coefficient provided that the loss due to diffraction is small compared to that due to the intrinsic absorption in the medium. In this case the losses may be considered additive according to

$$P(x) = P_o \, e^{-(\alpha_d+\alpha_i)x} \tag{3-5}$$

where α_d is the loss due to diffraction alone and is a function of x and α_i is the intrinsic absorption of the transmitting medium. Figs. 3-1, 3-2 and 3-3 illustrate Del Grosso's results and appropriate correction factors are obtained from tabulations from the same source.

The near field of the piston source, known as the Fresnel zone, extends approximately to a distance of a^2/λ from the source. In this region, the sound beam diverges very little and the pressure amplitude, in the absence of absorption, at a^2/λ, is about 81% of its maximum value. The far field or the Fraunhaiffer region exists beyond approximately a^2/λ. Beyond $a^2/2\lambda$, the pressure amplitude goes through several major fluctuations, and beyond about $2.4\ a^2/\lambda$ the pressure begins to fall of monotonically. When performing absorption measurements, it would be advantageous to work entirely in the near field or entirely in the far field and avoid the region between $a^2/2\lambda$ and $2.4\ a^2/\lambda$. The effects of diffraction on the velocity of propagation is much smaller than can be resolved with the

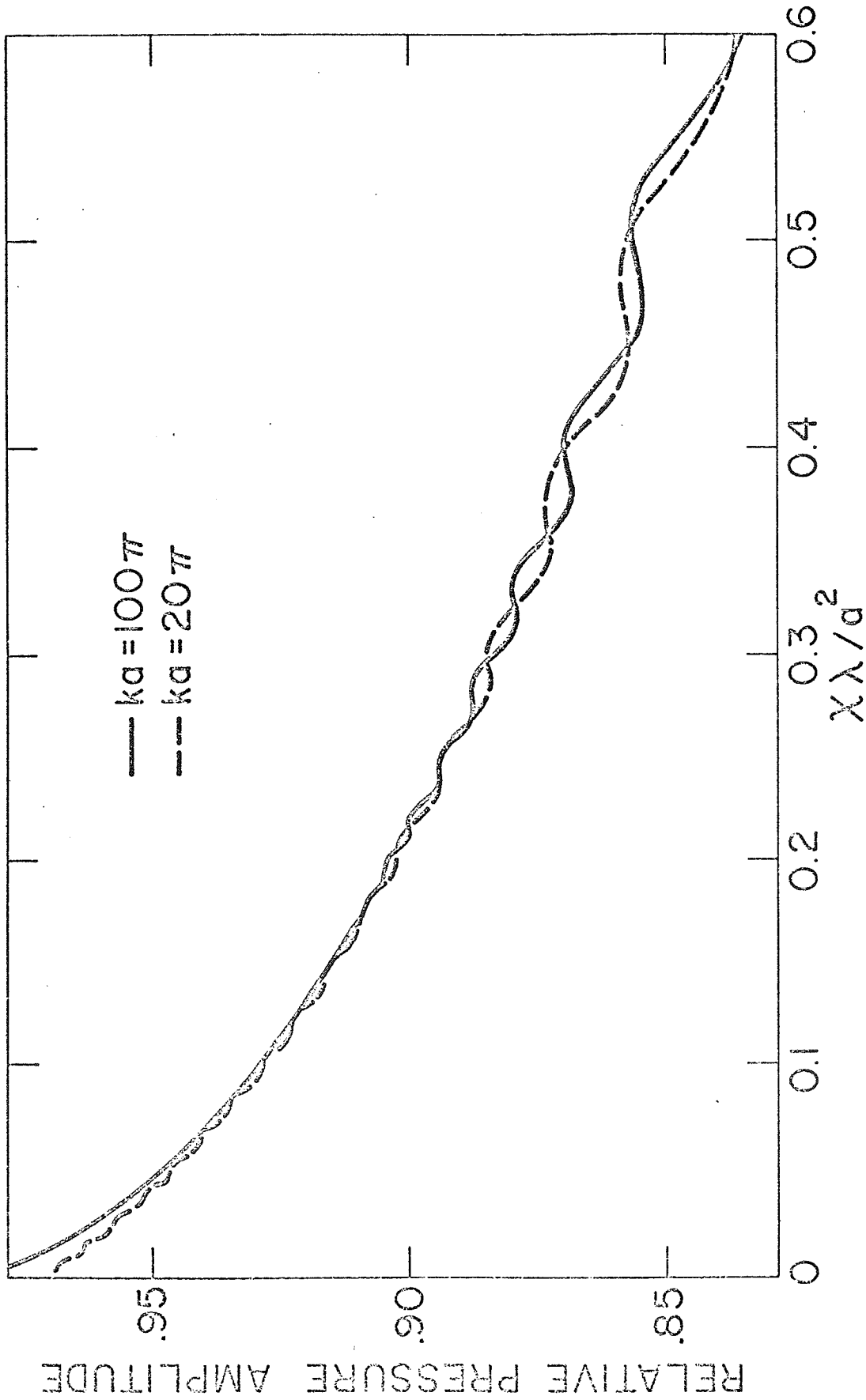

FIGURE 3-1

AVERAGE RELATIVE PRESSURE FROM A CIRCULAR TRANSDUCER OF RADIUS a IN A LOSSLESS EXTENDED MEDIUM
(Del Grosso, 1964)

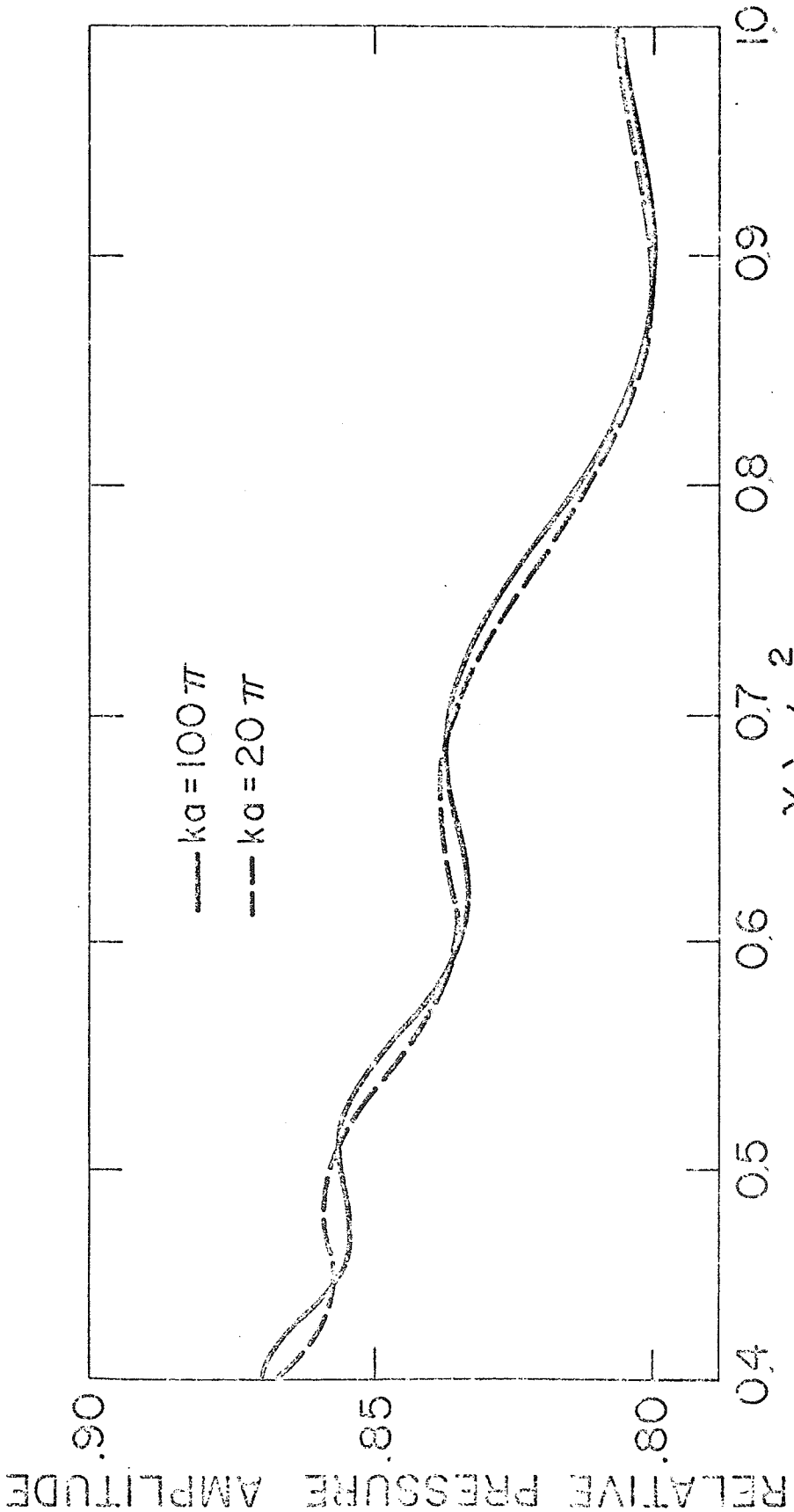

FIGURE 3-2

AVERAGE RELATIVE PRESSURE FROM A CIRCULAR TRANSDUCER OF RADIUS a IN A LOSSLESS EXTENDED MEDIUM
(Del Grosso, 1964)

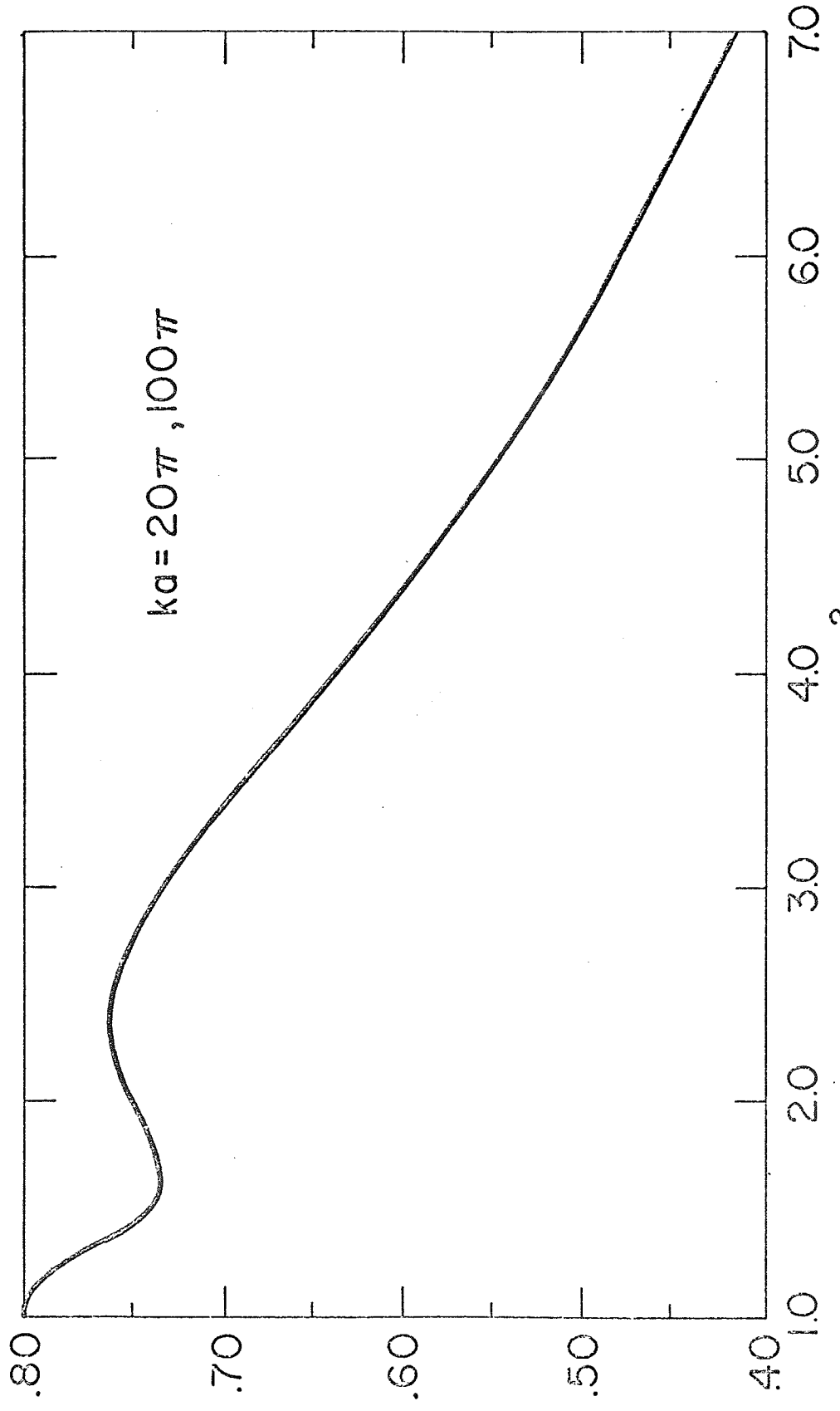

FIGURE 3-3

AVERAGE RELATIVE PRESSURE FROM A CIRCULAR TRANSDUCER OF RADIUS a IN A LOSSLESS EXTENDED MEDIUM
(Del Grosso, 1964)

present instrumentation and hence will not be considered here.

3. High Frequency Technique

Two specific techniques were employed to measure the absorption coefficient over the frequency region from 0.3 MHz to 163 MHz. The first technique for measuring the absorption coefficient in liquid media is useful where diffraction effects are negligibly small and is essentially an automated Pellam and Galt acoustic chamber that utilizes the direct pulse technique, i.e., two transducers, one for transmitting and one for receiving the acoustic pulse (Hawley, 1966). As the transducers are displaced relative to each other, the amplitude changes that occur to the first received pulse obey (3-4). The importance of the diffraction term is best seen by example. Consider a liquid which has an absorption coefficient of 500 $f^2 cm^{-1}$, i.e., 20 times greater than that of water at room temperature, and a speed of sound equal to 1550 m/sec, the resulting contributions to the total absorption are summarized in Table 3-1. For comparison, an example of liquid with properties close to those of water is also included in this table. From Table 3-1, it is evident that under certain circumstances, viz., low frequency, small transducer diameter, and small intrinsic absorption coefficient of the liquid, the diffraction effect contributes very appreciably to the overall attenuation.

Velocity measurements cannot be made with accuracies much better than 1% when the arrival time of a pulse is timed over a measured distance, unless it is done indirectly and over a fixed, accurately determined path length as is the case in the "Sing-A-Round" method (Greenspan and Tschiegg, 1962). However, if the phase of the received pulse is compared with a coherent reference signal, the periodic interference signal which

TABLE 3-1. EXAMPLES OF DIFFRACTION CORRECTIONS FOR HIGH FREQUENCY SYSTEM

		Liquid with attenuation coefficient 20 times greater than water		Water like liquid at room temperature	
Intrinsic absorption coefficient of liquid	cm^{-1}	$500 \times 10^{-17} f^2$		$25 \times 10^{-17} f^2$	
Velocity of sound	c cm/sec	1.55×10^5		1.55×10^5	
Radius of crystal	a cm	1.27		1.27	
Frequency of measurement	f Hz	10^6	10^7	10^6	10^7
Extent of near field	a^2/λ cm	10.4		10.4	
Normalized radius of crystal	$ka = \frac{2\pi a}{\lambda}$	16.4π	164π	16.4π	164π
Initial distance between transmitting and receiving crystals	x_1 cm	1		1	
Normalized	$x_1\lambda/a^2$	.0962	.00962	.0962	.00962
Final distance between transducers	x_2 cm	6		6	
Normalized	$x_2\lambda/a^2$	.0577	0.0577	0.577	0.0577
Attenuation due to intrinsic absorption coefficient	A_i db	0.217	21.7	0.0109	0.109
Attenuation due to diffraction effects above	A_d db	0.90	0.3	0.90	0.30
Total observed attenuation change observed when transducers are displaced from x_1 to x_2	A_T db	1.11	22.0	0.911	0.409

results when the transducers are moved relative to one another with a constant velocity can be used to evaluate the phase velocity of the sound wave. Fig. 3-4 shows a block diagram of the high frequency system for determining both the absorption and velocity of ultrasound in liquids and Fig. 3-5 is a schematic diagram of the high frequency instrument. The Appendix contains complete specifications for the commercially available instruments used and the circuit diagrams for the remaining electronic circuitry.

A pulse of rf is formed by gating and amplifying the output of a Measurements Corp. Model 80-R standard signal generator with an Arenberg PG650C gated amplifier. The output pulse is fed to the transmitting crystal through an attenuator and matching network. Early experiments with this system used the Arenberg PG650C instrument as a pulsed oscillator but it was found that a more accurate measurement of frequency could be made with the gated amplifier and, in addition, a reference signal is always available with which to compare the phase of the received pulse.

The received signal is amplified by a Hewlett Packard Model 460A wideband amplifier in cascade with the receiver section of a Matec Model PR201 ultrasonic attenuation comparator which altogether provides about 80 db of gain. After video detection, the signal is fed into a coincidence gate which isolates the particular pulse desired for amplitude detection from the rest of the signal. A linear pulse height detector (Sylvan, 1963) is employed to produce a DC voltage whose amplitude is directly proportional to the positive peak of the input signal. The DC output voltage is recorded on a Sargent Model SR servo logarithmic recorder which displays amplitude changes of input voltage in decibels. The chart drive motor of the recorder is synchronous to the line frequency as is the motor

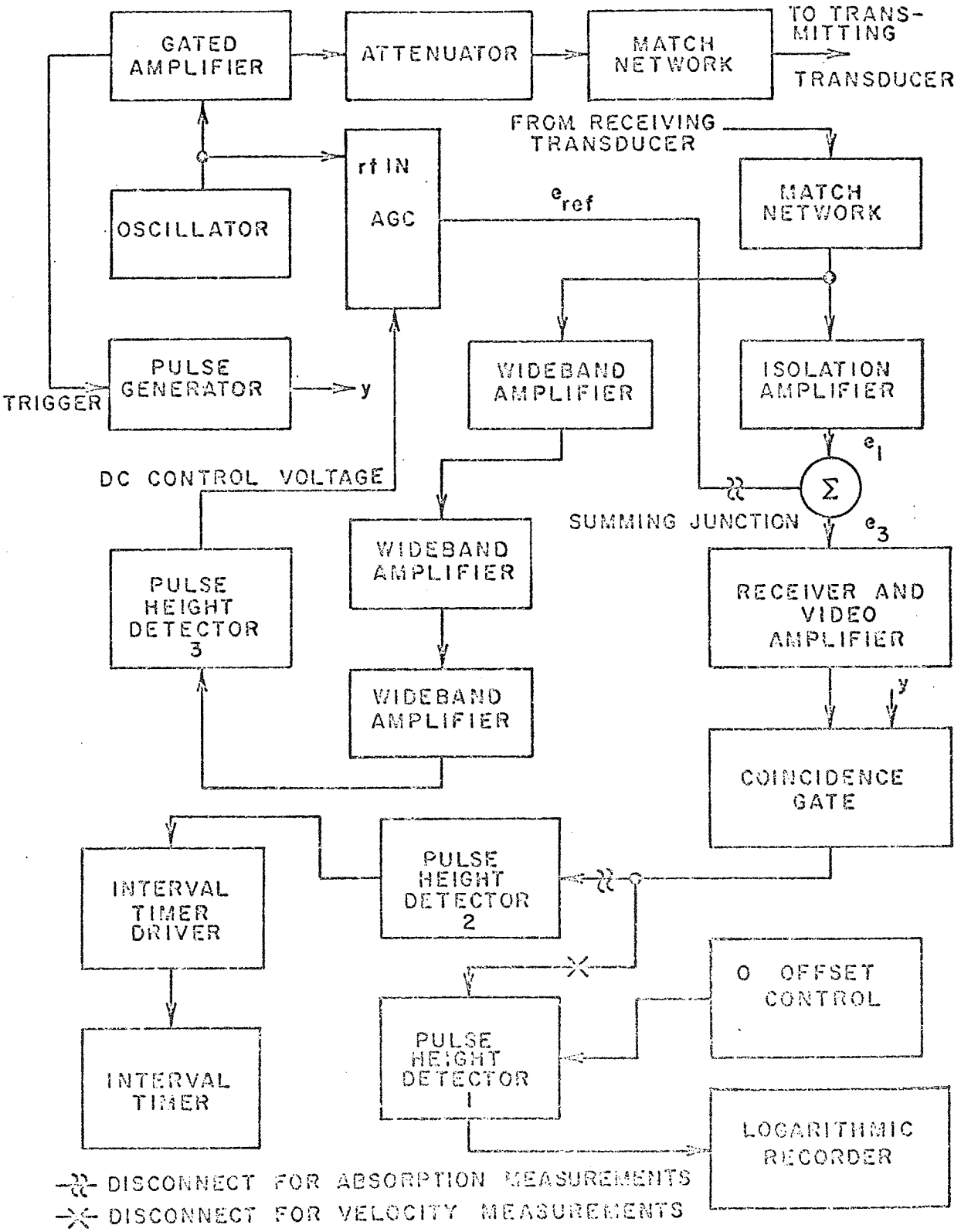

FIGURE 3-4

BLOCK DIAGRAM OF ELECTRONIC SYSTEM

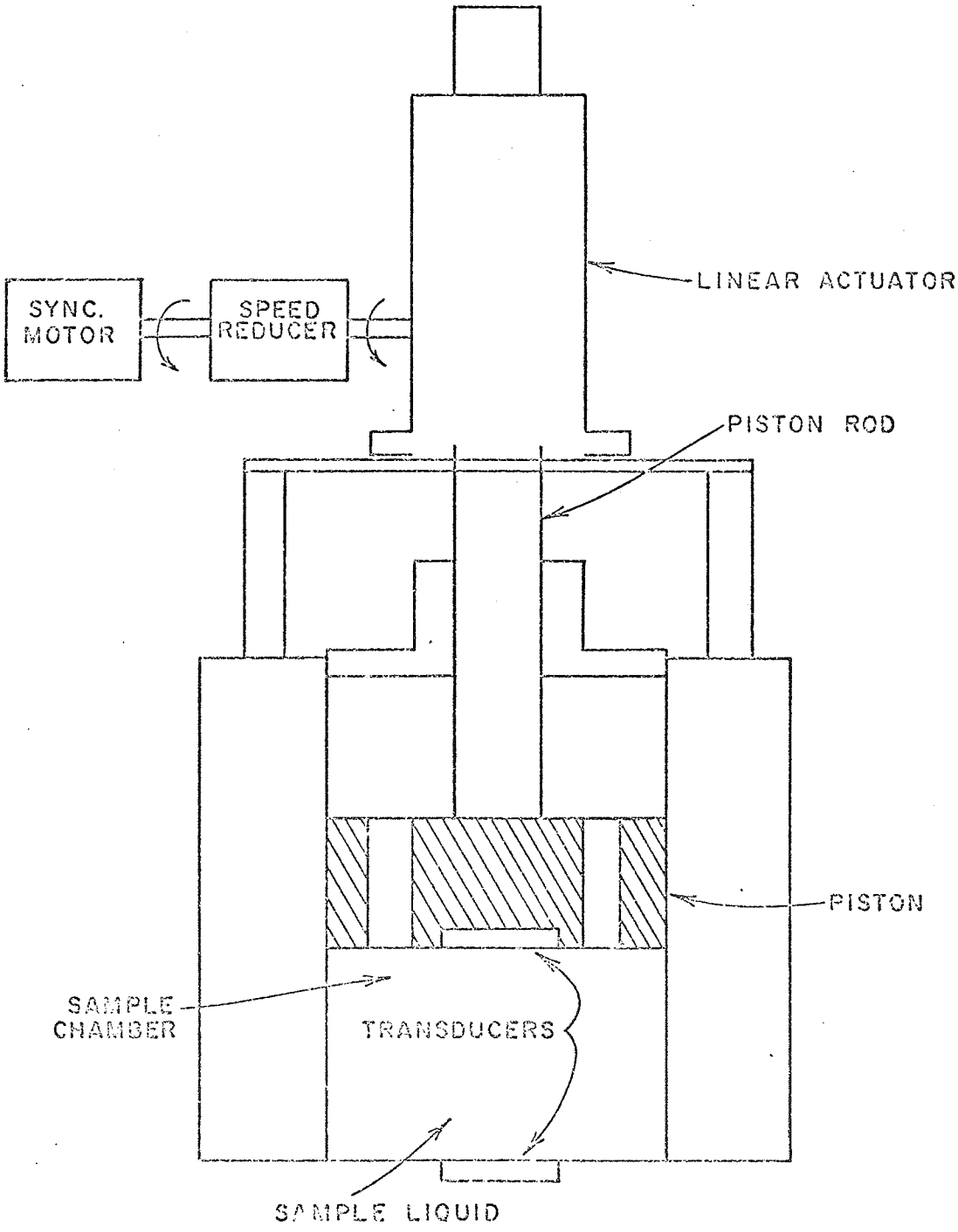

FIGURE 3-5

SCHEMATIC DIAGRAM OF HIGH FREQUENCY INSTRUMENT

which drives the piston. Therefore a displacement of the two transducers relative to each other results in a corresponding displacement of the chart and is independent of line voltage and frequency fluctuations. The absorption coefficient is measured by continuously recording the change of amplitude of the received acoustic pulse as the transducers are displaced. Since the variation of amplitude is exponential, see (3-1), the recorder draws a straight line, whose slope is proportional to α. The principal source of difficulty in obtaining precise and accurate values of the absorption coefficient is the non-linearity of the receiver, i.e., the video output voltage is not proportional to the amplitude of the input voltage. In order to render the system usable, a piecewise linear transfer function is approximated from the actual input-output transfer function of the receiver. A desirable operating region of the receiver is then selected graphically and extrapolated to zero input voltage. Since this point does not correspond to zero output voltage necessarily, the intercept on the output voltage axis is the amount of DC compensation that must be provided for at the recorder or at the pulse height detector to force the DC level of the signal being recorded to be linearly related to the amplitude of the receiver input voltage within the selected operating region.

The measurement of the ultrasonic velocity in liquids is made with the high frequency system by utilizing the acoustic chamber as a pulsed interferometer and measuring directly the wavelength of sound. The technique described by Hawley (1966) uses a double pulse arrangement of the Arenberg PG650 pulsed oscillator to record an interference signal on the chart recorder. The precision and accuracy of that method however is limited by the phase jitter between subsequent pulses and the long range

nonlinearities of the chart paper recording. An improved and automated technique which is based on the pulsed interferometer idea has been developed during the course of this investigation.

In the absence of absorption, if the amplitude of the first received pulse at the receiving transducer is added to a coherent reference signal e_{ref}, such as that obtained from the oscillator feeding the transmitting transducer, then the sum of the two signals will be a periodic function of the piston speed. That is, if

$$e_{ref} = A_o \sin \omega_o t \tag{3-6}$$

where ω_o is the angular frequency of the signal, and if the rf signal within the first received pulse is designated by e_1 and if $|e_1| = |e_{ref}|$, then

$$e_1 = A_o \sin(\omega_o t + \frac{2\pi d_o}{\lambda_s} + \frac{2\pi v_p}{\lambda_s} t) \tag{3-7}$$

where d_o is the distance which separates the two transducers at time $t = 0$, λ_s is the wavelength of sound in the liquid, and v_p is the linear velocity of the piston which is positive when the transducers are moving apart. When e_1 and e_{ref} are added together at the receiver input as shown in Fig. 3-4, the resultant signal has the following form

$$e_3 = 2 \cos (\frac{\pi v_p}{\lambda_s} t + \frac{\pi d_o}{\lambda_s}) \left[\sin((\omega_o + \frac{\pi v_p}{\lambda_s})t + \frac{\pi d_o}{\lambda_s})\right] \tag{3-8}$$

The envelope of e_3 is a full wave rectified sinusoidal waveform with a period of λ_s/v_p. Thus, the velocity of sound can be computed from the following simple formula

$$c = \frac{v_p \omega_o \Delta t}{2\pi} \tag{3-9}$$

where Δt is the time necessary for the piston to travel one wavelength.

To measure the velocity of sound, the first received pulse is selected by the coincidence gate and its amplitude is detected by a second pulse height detector whose DC output is the slowly varying envelope of e_3. This signal is then processed in the interval timer driver in such a way that each minimum of the signal, which occurs every λ_s/v_p sec., results in a pulse at the output of the circuit. The pulses are then used as start and stop signals which control the interval timer stage of a Systron Donner Model 1037 frequency counter. In order to compensate for stray noise pickup and short range nonuniformities of piston velocity, the average time between 100 pulses is measured which corresponds to the length of time required for the piston to travel 100 λ_s. In the presence of absorption, the amplitude of e_1 decreases as the transducers are separated and to compensate for this an a.g.c. circuit is placed in the path of the reference signal before the summing junction. With this arrangement the ratio $|e_{ref}|/|e_1|$ can be maintained more nearly constant than without compensation. The control voltage is derived from the amplitude of the first received pulse before the summing junction, thus the necessity for the isolation amplifier.

4. Low Frequency Technique

It has been discussed that if low values of absorption coefficients are to be determined with confidence at low frequencies, i.e., < 10 MHz, the Pellam and Galt chamber would require unreasonably large transducer elements to minimize diffraction effects. A comparison technique, first described by Carstensen (1954) is used to measure directly the difference in absorption coefficients and the difference in the velocities of sound

between two liquids. Water served as a convenient reference liquid in these experiments since its acoustic properties have been accurately determined (Pinkerton, 1949; Greenspan and Tschiegg, 1959) and are similar to those of the aqueous solutions to be studied.

Two compartments of a double chamber tank are separated by an acoustic window and are filled, respectively, with the sample and reference liquids. Two transducers, one placed in each chamber, face each other through the window and are mounted co-axially and parallel. They are supported a fixed distance apart on a sliding carriage which is mounted above and the acoustic measurements are made by varying the relative amounts of sample and reference liquids in the acoustic path. It is apparent that if the velocity of sound in both liquids is the same, then displacement of the transducer carriage would produce no change in acoustic path length and therefore no diffraction corrections would be necessary. Referring to Fig. 3-6, if $x = x_1$, is the initial position of the transducers carriage and if α_o and c_o represent the acoustic absorption and speed of sound of the reference liquid respectively, and α_x and c_x those of the sample liquid respectively, then the amplitude of the first received pulse at the receiving crystal will follow an equation of the form

$$p(x) = p_o e^{\alpha_o d} \cdot e^{-\alpha \Delta x} \tag{3-10}$$

where $\Delta\alpha = \alpha_x - \alpha_o$ and $c_o \neq c_x$. If $p(x)$ is determined as a function of x, $\Delta\alpha$ can be determined graphically and α_x is readily evaluated. An example of the contribution due to diffraction for the low frequency technique is given in Table 3-2 for the same liquid considered in Table 3-1, i.e., $\alpha/f^2 = 500 \times 10^{-17}\ f^2 cm^{-1}$ and it is clear that the contribution is much smaller.

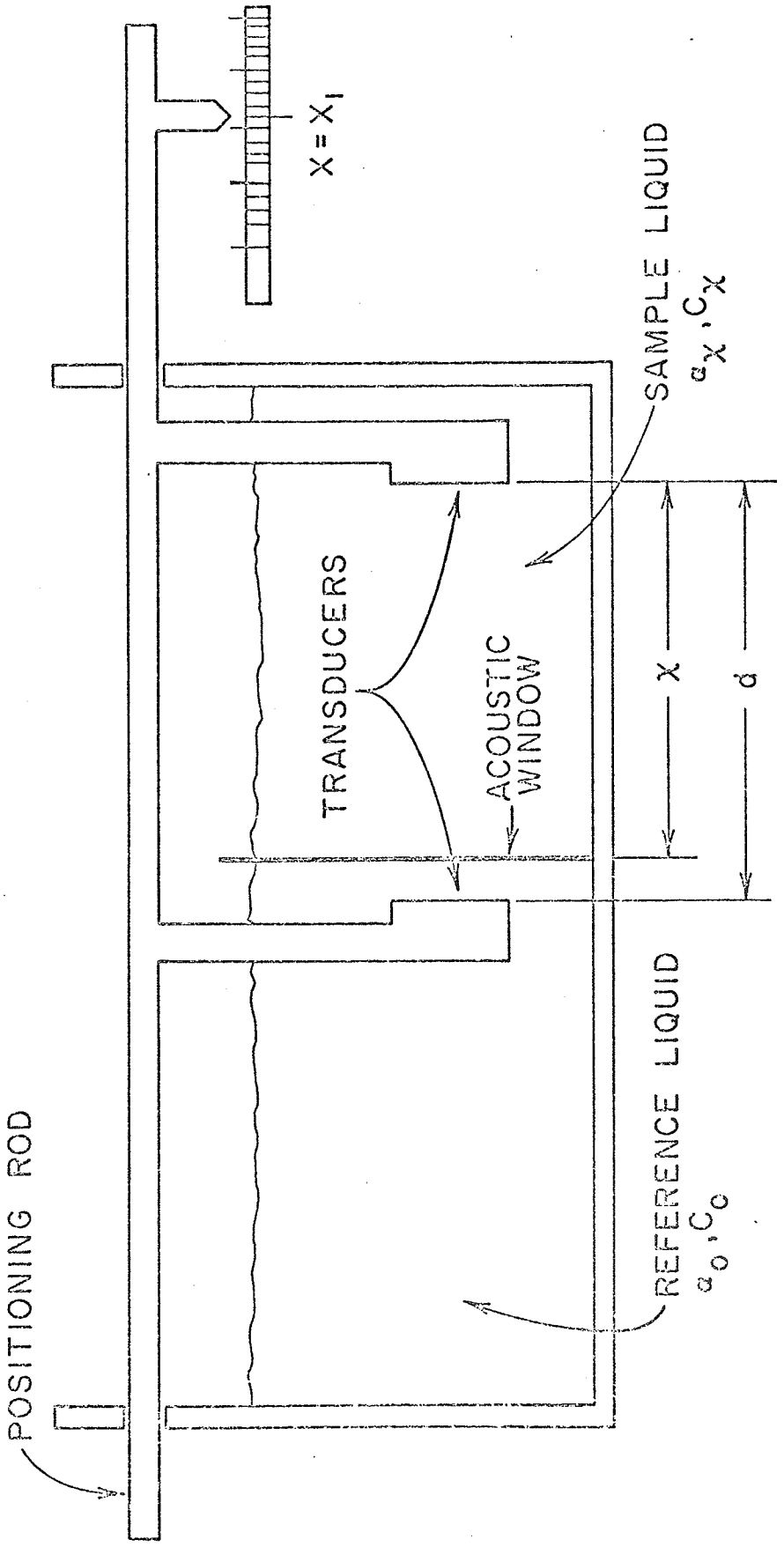

FIGURE 3-6

LOW FREQUENCY TECHNIQUE

TABLE 3-2. EXAMPLE OF DIFFRACTION CORRECTION FOR CARSTENSEN TECHNIQUE

		Sample Liquid	Reference Liquid
Intrinsic Absorption Coefficient α	cm^{-1}	$500\ f^2 x\ 10^{-17}$	$25\ f^2 x\ x10^{-17}$
Velocity of sound c	cm/sec	1.55×10^5	1.50×10^5
Radius of crystal a	cm	1.27	
Frequency of absorption measurement f	Hz	1.0×10^6	
Normalized radius of crystal* $ka = \frac{2\pi a}{\frac{1}{2}(\lambda_o + \lambda_x)}$		16.7π	
Displacement of transducer carriage Δx	cm	5.0	
Initial separation between transducers d	cm	5.0	
Normalized	$d\lambda_o/a^2$	0.465	
Final separation between transducer d	cm	5.0	
Normalized	d_1/a^2	0.480	
Attenuation due to intrinsic absorption $\Delta x(\alpha_x - \alpha_o)$	db	0.207	
Attenuation due to diffraction effects from table (Del Grosso, 1964)	db	0.0068	
Total observed attenuation	db	0.214	

*Subscript o refers to reference liquid; subscript x refers to sample liquid.

The electronic system associated with the low frequency instrument is the same as in Fig. 3-4 with the exception that the Matec receiver and Hewlett Packard isolation amplifier are replaced by a combination Arenberg PA620-L preamplifier and Arenberg Model WA 600 wideband amplifier which are more appropriate for the frequencies of interest below 1 MHz. Absorption measurements are thus made in the same manner as described for the high frequency system.

In order to measure the velocity of sound in the sample liquid, the phase of the first received pulse is compared to that of the reference signal, and the change in the total number of acoustic wavelengths between the transmitting and receiving transducers is observed as the transducers are displaced to a new position. From Fig. 3-6, if n is the total number of wavelengths at position $x = x_1$, then

$$n = \frac{d - x_1}{\lambda_o} + \frac{x_1}{\lambda_x} \tag{3-11}$$

If the transducers are displaced to position x_2 such that the total number of wavelengths has changed by an integral number m, then

$$n \pm m = \frac{d - (x_1 + \Delta x)}{\lambda_o} + \frac{x_1 + \Delta x}{\lambda_x} \tag{3-12}$$

If (3-11) and (3-12) are combined, the velocity c_x is found to be

$$c_x = \frac{c_o}{1 \pm \frac{mc_o}{\Delta xf}} \tag{3-13}$$

Since, for the solutions used in the present investigation $c_x \approx c_o$, then $mc_o/\Delta xf << 1$, and therefore (3-13) can be approximated by the first two terms of the Taylor series expansion, i.e.,

(3-14) $$(c_x - c_o) = \mp \frac{mc_o}{\Delta xf}$$

The advantage of determining c_x with this method over the high frequency pulsed interferometer method described above, is best seen by example. Suppose that $mc_o/\Delta xf$ can be determined with a precision of ± 1% and $c_x - c_o$ = 15 m/sec. If c_o is 1,500.00 m/sec then c_x has been determined to ± 0.01%. On the other hand, with the high frequency technique, if λ_s can be determined to only ± 1%, c_x also has the same uncertainty. In the present investigation, Δx is measured manually with a Gaertner model M303 micrometer slide with a traveling microscope which reads directly to 10^{-5} m.

B. Mechanical Description

1. Low Frequency Apparatus

The mechanical construction of the low frequency system is shown schematically in Fig. 3-7, and photographs of the assembled system appear in Figs. 3-8 and 3-9. A rigid frame made of 3/4 in. brass plate is reinforced with 2 x 2 in. horizontal bars. The frame supports the double chamber absorption tank, the tracking rods, and the frame maintains the plane of the acoustic window perpendicular to the tracking rods. A table mounted on one side of the frame is used to support a motor driven linear actuator which varies the position of the transducer carriage.

a. Absorption Tank

The low frequency system was designed to minimize the effects on the apparent absorption coefficient due to diffraction of the sound beam and the propagation of guided modes. Although these effects are inherently at least an order of magnitude smaller with this technique than with the

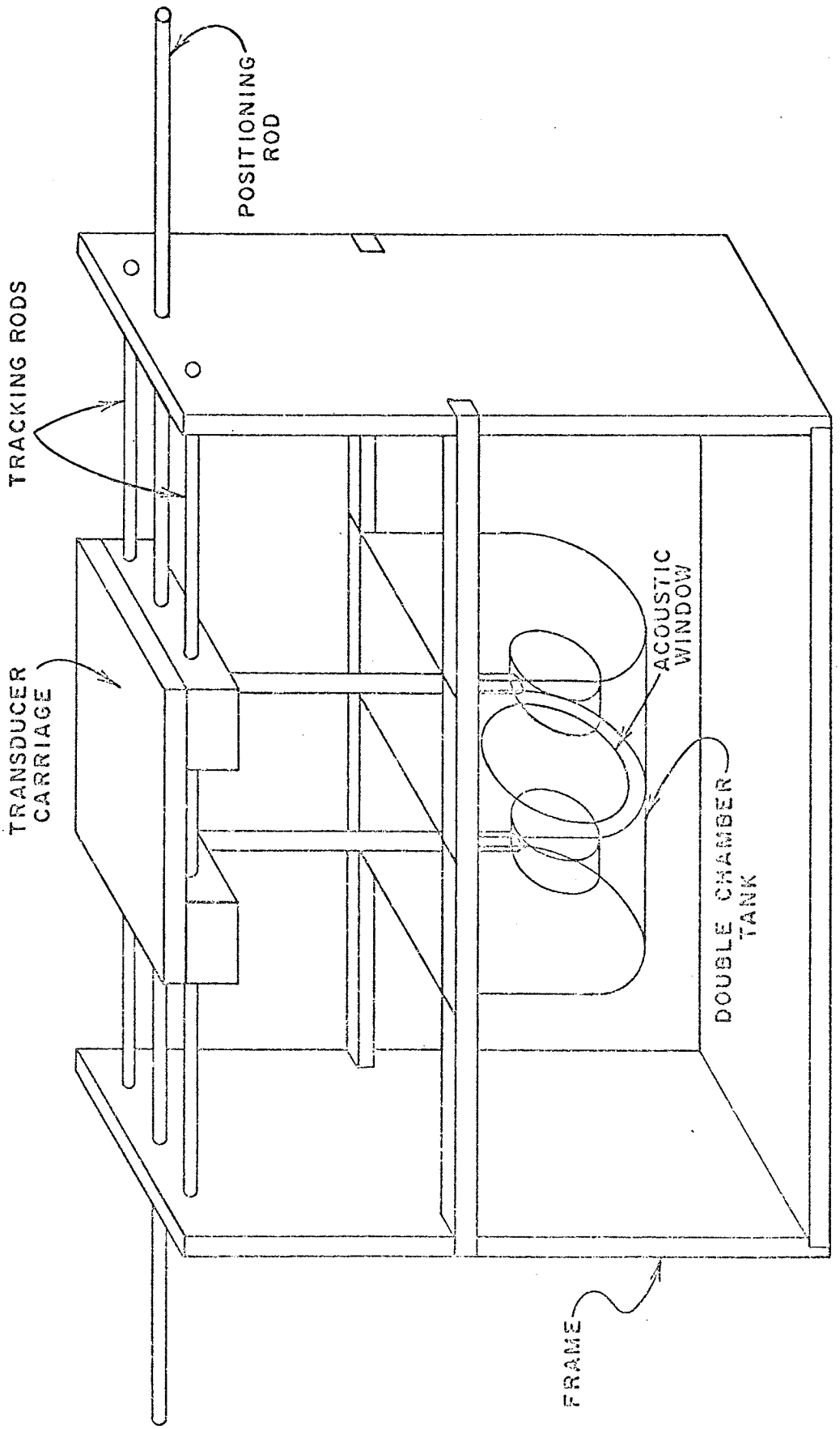

FIGURE 3-7

SCHEMATIC DIAGRAM OF LOW FREQUENCY INSTRUMENT

FIGURE 3-8

PHOTOGRAPH OF LOW FREQUENCY INSTRUMENT

FIGURE 3-9

PHOTOGRAPH OF LOW FREQUENCY ABSORPTION CHAMBER WITH TOP PLATE REMOVED

high frequency technique, when investigating liquids which have absorption coefficients close to that of the reference liquid and which have a speed of sound which differs from that of the reference liquid by 10% or more, diffraction effects may become more significant than was indicated in Table 3-2.

When the diameter of the transducers approaches the lateral dimension of the tank, acoustic energy is guided along the boundaries of the tank. In order to minimize these effects, the lateral boundary must be large compared to the transducer diameter. A minimum of twice as large is suggested by Del Grosso (1965) and this figure is a reasonable compromise between minimization of guided mode effects and minimization of the volume required to fill the tank. The transducers employed in this investigation are 3 in. diameter, the lateral dimension of the tank is 6 in. and the volume of each chamber is 4 ℓ. The absorption chamber is fabricated in two halves from type 304 stainless steel and is heli-arc welded on the outside edges. The inside corners are filled with epoxy resin (Emerson Cummings Type 2850 FT) to prevent traces of rust from forming due to minute quantities of impurities in the metal in the immediate area of the weld. The top of the tank is left open to permit entry of the transducers, which are attached to a carriage on the tracking rods. A plexiglass dust cover is suspended from hangers on the positioning rod in order to minimize contamination of the solutions from the air and to reduce evaporation.

Two drains are placed in each chamber to facilitate withdrawal of the liquid and to allow circulation of the fluid by means of submersible pumps. Circulation of the fluid provides a convenient way to eliminate concentration gradients which may form, for example, when minute amounts of water which remain in the tank from previous cleaning operations do

not thoroughly mix with the sample solution. Further, since the sample chamber is not completely surrounded by the temperature control bath, temperature gradients may produce refraction of the sound beam. These effects are especially troublesome at solution temperatures remote from the ambient temperature. Circulation, in this case, is necessary in order to measure the absorption coefficient with the degree of accuracy required (Pinkerton, 1949b). Two difficulties may arise however. First, the circulation pumps may produce bubbles which, in liquids of high viscosity do not dissipate immediately resulting in a distribution of scattering structures which appreciably affect the absorption measurements. Second, the circulating pump is itself an acoustic generator and the noise it produces is superimposed on the sound beam causing difficulties during all velocity measurements and during the high frequency absorption measurements, i.e., > 10MHz.

b. Acoustic Window

The acoustic window is the most important single structure of the acousticchamber. It is 5-1/2 in. in diameter and it is sealed between the two halves of the absorption chamber with neoprene gaskets. Two materials, 0.0006 in. thick Saran, manufactured by Dow Chemical Co. and 0.003 in. thick polyethelyne sheet have been employed successfully as acoustically transparent membranes. The choice of material was based on acoustic impedance, chemical inertness and the ability to form a stiff planar membrane when stretched. The acoustic impedance of both materials differs from that of water, and all other aqueous solutions used in these experiments by a factor of approximately two and therefore some reflection of the acoustic pulse at this boundary is inevitable. Since the impedance

mismatch at the boundary is only a factor of two and since maximum power transfer is not an important factor, the only restrictions on the window thickness are those associated with the receiver sensitivity and signal to noise ratio necessary to resolve the signal transmitted through the window.

Vibration which may be imparted to the low frequency instrument results in movement of the acoustic window. Stiffening of the window minimizes the movement, however, two important effects are seen. First, as the window moves the relative amounts of sample and reference liquids in the acoustic path change and if the absorption coefficient for each liquid is different, a corresponding amplitude fluctuation of the acoustic energy arriving at the receiver will occur. For the case of different velocities of propagation of the two liquids, there will occur corresponding fluctuations in the acoustic path length and the resulting phase jitter will limit the precision of the velocity measurements.

c. Transducer Assembly

The transducer carriage is fabricated from metal blocks mounted a fixed distance apart by a top plate. Each block contains two linear motion ball bushings which are precision fitted onto the tracking rods. The carriage attaches to a third rod located midway between the two tracks and is used for positioning the transducer carriage. The positioning rod is attached to a linear actuator which, when driven by a synchronous reversible motor and a multi-ratio speed reducer moves with a constant speed in either direction selected. By proper selection of the gear ratio, the speed of the transducers can be varied from 0.001905 cm/sec to 0.381 cm/sec. Two cams located along the positioning rod automatically

reverse the direction of travel when each contacts a microswitch. In this way, the transducers can be cycled back and forth automatically between any set displacement limits.

Each transducer is attached to the carriage through an adjustable mechanism which is employed to center it on the axis of the acoustic window and to position it parallel to the other transducer (Fig. 3-10). This mechanism was modified from a military surplus "astro compass" and obtained from Edmond Scientific Co., Burrington, N.J. A locking mechanism is also provided so that after adjustments are made, the transducer assembly remains rigid.

A matched set of two 3 in. diameter lead zirconate-lead titinate ceramic discs having a fundamental thickness mode frequency of 0.35 MHz was employed for most of the experiments. In the earlier phases of the experimental work, a pair of 2 in. diameter 0.50 MHz quartz discs and another pair of 2 in. diameter 1.0 MHz quartz discs were employed. Each transducer is edge mounted in a waterproof stainless steel housing in such a way that its front face is in contact with the liquid and the back face is exposed to an air cavity in the housing. Since the ratio of the acoustic impedance of most aqueous solutions to that of air is about 3.6×10^4 to 1 (Kinsler and Frey, 1962), essentially all of the acoustic energy is coupled to the liquid. Each transducer has a thin layer of gold on nickel vacuum deposited on both major surfaces as chemically inert electrodes. The front radiating face is at ground potential and the rf voltage is applied to the rear face. Fig. 3-11 is a schematic diagram of the transducer housing.

FIGURE 3-10

PHOTOGRAPH OF LOW FREQUENCY TRANSDUCERS AND POSITIONING MECHANISM

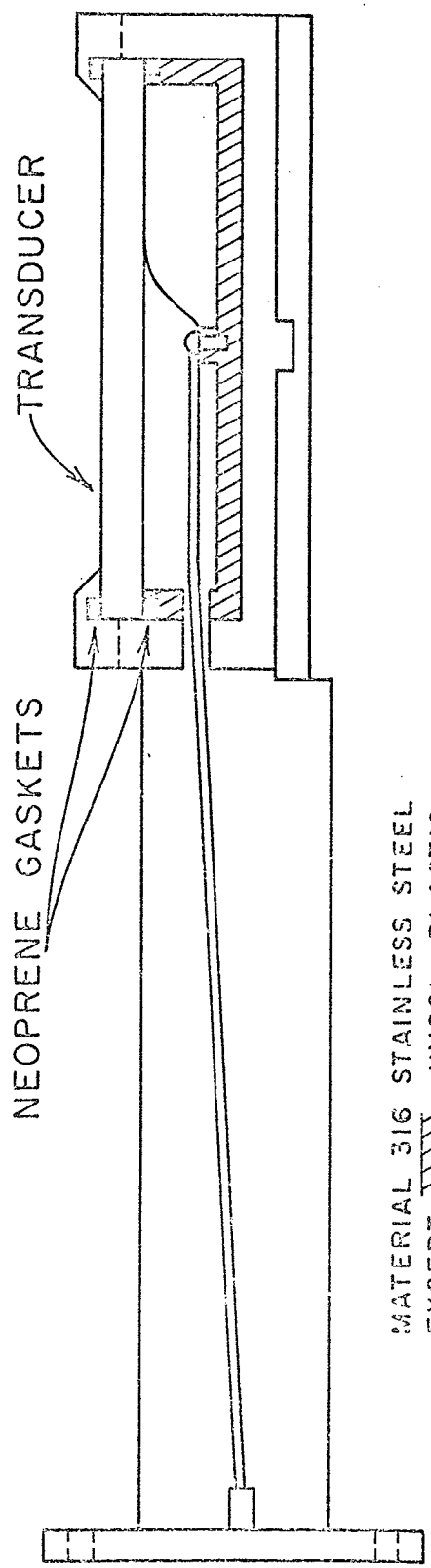

FIGURE 3-11

SCHEMATIC DIAGRAM OF TRANSDUCER HOUSING

2. High Frequency Apparatus

The high frequency absorption chamber was designed and fabricated by Hawley (1966) and aside from a few modifications a detailed description can be found in there. Fig. 3-5 shows a schematic drawing of the high frequency instrument. A movable piston, with the front face of a transducer mounted flush with its front surface, can be positioned within the cyclindrical absorption chamber utilizing the chamber wall as the guiding surface. A second transducer, acoustically matched to the first, is mounted on the bottom of the chamber in a ball and socket arrangement which can be positioned to parallel the two transducers and to arrange them coaxially. One set of matched transducers fabricated from X-cut quartz has a fundamental thickness mode frequency of 3.0 MHz and is usable to about 57 MHz where they become inefficient. Above this frequency a matched pair of 15 MHz quartz plates, mounted on fused quartz delay rods are employed and are usable to about 165 MHz where dynamic misalignment during piston translation becomes the limiting factor.

3. Temperature Control System

A temperature regulated water jacket surrounds the low frequency double chamber absorption tank and maintains the temperature constant to within ± 0.02°C over a range from 1°C to 50°C. The temperature of the bath is controlled by a reservoir tank whose liquid is maintained at a constant temperature, and is then circulated through the heat exchange coils in the water bath. A Yellow Spring Model 71 "on-off" type temperature controller with a fast acting thermistor probe activates alternately a 450 W heater and a Tecumsah model F34-2JG refrigerator unit to control the reservoir temperature. The temperature control instrumentation for

the high frequency system is similar to that described above except that a Yellow Spring Model 72 "proportional" temperature controller is used. This device supplies only the amount of power to a heater that is necessary to maintain the temperature at a preset level and is capable of maintaining the temperature to ± 0.0 1°C. All temperatures are measured with a thermometer checked against a NBS calibrated thermometer and were found to be within ± .05°C.

C. Methods

1. Low Frequency Measurements

In order to prepare the double chamber tank for acoustic measurements, it is necessary to insure that the acoustic window is as taut as possible without rupturing. The window material is stretched over a plexiglass frame and is secured in place with masking tape. It is then treated with hot running water and is stretched further. This process is repeated several times until the window no longer slackens when the hot water is applied. The plexiglass frame is then placed over the window port on one half of the double chamber tank, and the other half of the tank is positioned. When the two halves are assembled, the tank is installed in the temperature control bath. In order to fill the tank, equal amounts of liquid are introduced into each chamber simultaneously to prevent differential forces which would tend to stretch the window. Before employing a new liquid, the tank is thoroughly cleansed and, if necessary, the window is replaced.

After the transducers have been installed and temperature equilibrium has been reached, the transducers are set parallel to each other and to the acoustic window. Using the single crystal pulse echo technique

provided by the Matec Model PR201 Ultrasonic Comparator, one transducer is positioned so that the largest amplitude reflection is received from the acoustic window. Because the transducer has its greatest sensitivity along the axis parallel to its thickness direction, a maximum output voltage will be obtained when the reflecting surface and transducer are parallel. The other transducer is then positioned so that it also becomes a parallel reflector. The above procedure is carried out at the highest frequency to be used in the experiments since the directivity of the transducer increases with frequency and the adjustment is more sensitive.

If the absorption coefficient of a sample liquid is 0.03 cm^{-1} greater than that of the reference liquid, the amplitude changes which occur to the first received pulse are recorded as the transducer carriage is displaced. However, when the difference of the absorption coefficients of the two liquids is less than 0.03 cm^{-1} such as would occur at the lower frequencies, and the attenuation over the entire acoustic path is such that the amplitude of the second received pulse is within 10 db of the first received pulse, the amplitude of the second pulse is recorded. The amplitude change which occurs to the second pulse is three times greater than that of the first pulse due to the increased acoustic path length. Similarly, when the total amplitude change occurring to the second pulse is less than about 2 db and the amplitude of the third received pulse is within a few db of the second pulse, a recording can be made from the third pulse.

When recording the amplitude of a pulse other than the first, reflections from the window become important. If the absorption coefficients for both the sample and reference liquids are not sufficiently high, reflections from the window will not die out rapidly and will bounce

back and forth in such a manner as to arrive at the receiving transducer simultaneously with the second received pulse. This occurs only when the window is in the region near the center of the path between the two transducers. Since the transducer carriage is in motion, the phase of the received pulse is continually changing with respect to the reflection from the window and the resulting signal, the algebraic sum of all signals arriving at the receiving crystal, is oscillatory in nature and appears so on the recording. An additional complication arises due to the nature of the pulse height detector which has a time constant of about 1 sec and responds only to the peaks of an input waveform. Since the oscillations are more rapid than the pulse height detector can follow exactly, the resulting amplitude variations are not averaged out and the recording shows the resulting shift upwards of the DC level. However, when the transducers are positioned away from this critical region, the linear recording is restored. The situation is even more complex when recording the amplitude of the third pulse since there is an opportunity for many more reflections from the window to interfere. These regions are ignored when measuring the absorption coefficient since the slope of the linear portion of the recording is unaffected by these oscillations.

2. High Frequency Measurements

When employing the high frequency technique about 10 MHz, the requirement of parallelism is of even greater importance. First, since the wavelength is smaller at these frequencies, the change in amplitude of the received signal per unit degree of rotation of the reflector is increased and the mechanical adjustment of the parallelism is very critical. Second, since one of the transducers is mounted in a moveable

piston, parallelism must be maintained for all possible piston positions that will be encountered during a set of measurements. The parallelism is adjusted after the sample chamber is filled with the liquid to be measured and temperature equilibrium is established. The adjustable transducer is positioned so that the maximum signal is received. Before actual measurements are made, the parallel alignment of the two crystals is checked as a function of piston position in the following way. The absorption coefficient is measured along four adjacent positions of transducer separation. With the proper combination of the frequency and the absorption coefficient of the liquid, it is possible to examine the alignment of the transducers over a total separation of about 5 cm. For example, when the transducers are properly aligned the observed absorption coefficient in water at 50 MHz over all the positions does not vary by more than ± 1.5%.

This measurement also demonstrates the absence of finite amplitude effects at the intensities used (less than 0.01 watts/cm^2). If the receiver gain is maintained constant, and the attenuation of the rf signal due to absorption by the liquid is compensated for by increasing the amplitude of the rf signal, the four absorption coefficient measurements will each be at a different intensity level. For the example of water at 50 MHz, a total amplitude range of 52 db resulted with no detectable change in the observed absorption coefficient. If finite amplitude effects were present, the observed absorption coefficient would increase with amplitude (Fox and Wallace, 1954).

3. Preparation of Polyethelene Glycol Solutions

Polyethylene glycol (PEG) samples were obtained in powder form in narrow distributions of molecular weight through the courtesy of Dow

Chemical Company, Midland, Michigan. Lot E23, average molecular weight 20,000 and Lot E77 average molecular weight 4,500, were used in this study. The other molecular weight polymers, i.e., 1,450, 400, 140, and 62 were obtained from Matheson Coleman and Bell, Cincinnati, Ohio. Stock solutions of about 0.2 gm/cc and 0.1 gm/cc were prepared by dissolving the polymer in singly distilled water obtained from the laboratory still and then filtered twice through Type A glass fiber filters (Gellman Inst. Co., Ann Arbor, Michigan) in order to remove foreign particles larger than 0.3μ diameter. The stock solutions were refrigerated at 6°C until acoustic measurements were made. The concentration of each sample was determined at 20.0°C to ± 0.5% by evaporating a known volume in a vacuum dessicator. The determination was carried out on each solution after its withdrawal from the acoustic chamber in order to avoid errors in the concentration of the stock solutions due to evaporation and dilution.

4. Preparation of Bovine Serum Albumin Solutions

Bovine serum albumin (BSA) Fraction V powder was obtained from General Biochemicals, Chagrin Falls, Ohio from Lot 82268, and was kept at -7°C until used. The solutions were prepared by placing enough powder on top of a quantity of singly distilled water in a flask to prepare a solution of the proper concentrations. Since BSA is not immediately soluble in water, the flask was placed in the refrigerator until mixing of the two components was complete, usually accomplished overnight. The solution was filtered in the same manner as the polyethylene glycol and after filtration was returned to the refrigerator until used. Generally the acoustic experiments were started within a few hours after the solutions were prepared.

The concentration of the protein solution was determined with a Beckman Model DU spectrophotometer after the acoustic measurements were made. The spectrophotometer measures the decrease in the intensity of light of a known wavelength as it passes through a fixed length of a sample of liquid. For BSA it has been determined that the absorbance for ultraviolet light of wavelength 280 mμ passing through 1 cm of solution of concentration 0.01 gm/cc would be 6.6. For any other sample of BSA, the following relation (Beer's Law) holds:

$$A = 6.6\ Lc \tag{3-15}$$

where A is the measured absorbance, L is the optical path length through the sample in centimeters, and c is the concentration of the solution in grams per 100 cm^3.

The pH of the BSA solutions was changed in steps ranging from 0.2 pH to 0.5 pH by the addition of known quantities of 1 Molar standard volumetric solutions of HCl and KOH. During this procedure, the solutions were gently stirred to minimize pH gradients. Measurements of pH were made to ± 0.1 pH unit with a Beckman model H-2 Glass Electrode pH meter standardized with accurate buffer solutions at pH 4, 7, and 9. All pH measurements were made at room temperature which fluctuated between 19°C and 23°C. Ultrasonic absorption and velocity measurements were not begun on the BSA solutions until at least 15 min after a pH change was made. This allowed enough time for the temperature to return to its equilibrium value and also allowed the molecules to reach configurational equilibrium (Tanford et al., 1955). The pH values recorded were those obtained after the acoustic measurements were performed and were never different from the initial value by more than ± 0.1 pH. The pH was varied from about 2.3 to

about 11.8 and this was considered the maximum range allowable with respect to possible damage to the stainless steel absorption chambers and to the epoxy resin used in mounting the quartz crystals. For a particular set of experiments, the neutral solution was examined first. Then after the last experiment at either pH 2.3 or pH 11.8, the pH was returned to neutral and the solution was stored in the freezer for possible future use.

D. Discussion of Errors

Errors from many sources must be considered in order to estimate the accuracy with which the absorption coefficient and velocity of sound are determined in this investigation. The first arises from the use of pulses instead of continuous wave signals. It has been shown by Pellam and Galt (1946) that the small bandwidth associated with a pulse whose duration is 15 times that of the period of the fundamental frequency of the wave, produces a fractional error in the absorption coefficient in most liquids of roughly 1 part in 250. In addition, in a dispersionless medium, the phase velocity and group velocity are equal and no error arises from the pulse method. In this investigation, however, the velocity of aqueous solutions of bovine serum albumin exhibits a dispersion of less than 0.1 m/sec per megacycle. (See Fig. 4-14.) Since the bandwidth of the pulse described above is roughly 0.067 MHz, the maximum difference between phase and group velocity is 0.0067 m/sec which is beyond the resolution of the present technique and thus will be neglected.

Diffraction corrections, discussed earlier are based on the premise that the transducer behaves as a piston vibrator. In practice, however, the motion of the surface of the transducer is uneven (Bergmann, 1949) and the diffraction corrections cannot be evaluated accurately. With the

high frequency technique, the estimated uncertainty in the diffraction correction itself is about ± 60%, however, above 10 MHz the relative contribution of diffraction is small, and the resulting uncertainty in determining the absorption coefficient is less than 5% for liquids with high absorption coefficients such as aqueous solutions of BSA at 0.05 gm/cc. In the low frequency system, the diffraction corrections are even more uncertain due to the fact that only a small change of the acoustic path length occurs and a positive or negative correction to the observed absorption coefficient can result (see Figs. 3-1, 3-2, 3-3).

Periodically, throughout the course of the experiments, the absorption coefficient of distilled water was measured in the high frequency system in order to check the receiver linearity and the parallel alignment of the transducers. Between 14 MHz and 80 MHz the average value of α/f^2 over 4 trials was within 3.0% of the accepted value and the fractional standard deviation of the measurements was 2.5%. Above 100 MHz, the value of α/f^2 was within 5.5% of the accepted value with a fractional standard deviation of 7%. At the high frequencies, this greater error is due to the increased difficulty in maintaining the transducers parallel while the piston moves within the absorption chamber. It is felt that the figures presented above are representative of the uncertainties associated with absorption coefficients obtained on all the other liquids measured in the high frequency system.

Except for the receiver, both the low frequency instrument and the high frequency instrument share the same electronics and between 8 MHz and 15 MHz either can be used to determine the absorption coefficient of a liquid. For BSA solutions, the values of the absorption coefficients obtained in each system agreed to within ± 2%. With the present detection

system, the smallest change of amplitude that can be resolved is ± 0.05 db, however, 1.0 db is the smallest change of amplitude that can be detected with a ± 10% uncertainty due to system nonlinearities. This corresponds to a difference in absorption coefficients between sample and reference liquids of about 0.002 cm^{-1}. The system nonlinearity reduces to ± 1% above $\Delta\alpha$ = 0.02 cm^{-1} and so on. Since the uncertainty in the measured value of $\Delta\alpha$ depends on the magnitude of $\Delta\alpha$, the fractional standard deviations are tabulated in terms of $\Delta\alpha$ in Table 3-3.

TABLE 3-3. STATISTICAL VARIATION OF α, LOW FREQUENCY SYSTEM

$\Delta\alpha$ (cm^{-1})	Fractional Standard Deviation
$\alpha > 0.1$	± 2.1%
$.01 < \alpha < .099$	± 2.0%
$.005 < \alpha < .0099$	± 3.0%
$.002 < \alpha < .00499$	± 8.5%

In the high frequency pulsed interferometer, the velocity of sound was measured at 8.87 MHz over a selected region of the linear actuator. For distilled water, the velocity of sound was found to be within ± 1 m/sec of the accepted value (Greenspan and Tscheigg, 1959) with a standard deviation of 0.5 m/sec. The velocity of sound was also measured at other frequencies up to about 45 MHz, however, the standard deviation was much greater (± 2 m/sec at 45 MHz) due to short range nonlinearities in the linear actuator and the small degree of dynamic misalignment between the transducers. The velocity measurements reported in this thesis were obtained at 8.87 MHz.

Additional sources of error are listed below in Table 3-3 and are self-explanatory.

TABLE 3-3. ADDITIONAL SOURCES OF ERROR

Frequency stability during experimental measurement

a) > 5 MHz ± .001%

b) < 5 MHz ± 0.025%

Uncertainty in frequency measurement ± 0.001%

Temperature stability

a) Low frequency system ± .02°C

b) High frequency system ± .01°C

Uncertainty in temperature measurement ± .05°C

Resolution of Δx for low frequency system 5×10^{-6} meters

Stability of Δx measurement due to vibration, etc., 5×10^{-5} meters

Concentration of polyethelyne glycol solutions ± 0.5%

Concentration of bovine serum albumin solutions

a) relative ± 1%

b) absolute ± 5%

CHAPTER 4

RESULTS

A. Bovine Serum Albumin (BSA)

The absorption coefficients of aqueous solutions of BSA were measured as a function of pH at 8.87 MHz, 14.79 MHz, 26.65 MHz and 50.25 MHz in the high frequency system at 20.0°C. The procedure for examining the absorption coefficient and the velocity of sound as a function of the pH of the solution is referred to as an ultrasonic titration and the low frequency system was used for titrations at 2.39 MHz and 4.43 MHz at 19.9°C. At neutral pH, the absorption coefficient was measured over the frequency range from 0.3 MHz to 165 MHz, the range from 45 MHz to 163 MHz being examined with the delay rods employed in the high frequency system as discussed by Hawley (1966).

The commonly accepted method for presenting acoustic absorption data for solutions is to plot the excess frequency free absorption per unit concentration, A, as a function of frequency, pH, etc., where

$$A = \Delta\alpha/cf^2 \tag{4-1}$$

where c is the concentration of solute in grams per cubic centimeter of solution and $\Delta\alpha$ is the difference in the absorption coefficients of the solution and the solvent. This method for presenting the absorption data for solutions evolved as follows. For pure Stoke's liquids, i.e., those for which the only mechanism of absorption is due to shear viscosity, α/f^2 is a constant and therefore frequency free. Further, the absorption coefficient of a solution is generally greater in magnitude than that of the pure solvent, so that it is sensible to examine only that portion of

the absorption that is due to the presence of the solute by taking the difference between the values of α/f^2 of the solution and solvent. For water, α/f^2 is constant at all ultrasonic frequencies thusfar attained and is listed in Table 4-1 as a function of temperature.

TABLE 4-1. VALUES OF α/f^2 FOR DISTILLED WATER AS A FUNCTION OF TEMPERATURE (Pinkerton, 1949a)

TEMP (° C)	$\alpha/f^2 \times 10^{17}$ ($sec^2 cm^{-1}$)
0	56.9
5	44.1
10	35.8
15	29.8
20	25.3
30	19.1
40	14.61
50	11.99

The low frequency technique measures the excess absorption coefficient of a solution directly if the solvent is also used as the reference liquid. On the other hand, the solvent contribution must be subtracted from the measured absorption coefficient when the high frequency technique is employed. The values of α/f^2 for water interpolated from Table 4-1 were used for this purpose.

In aqueous solutions of BSA, the excess absorption has been shown to increase linearly with concentration at least to about 0.1 gm/cc in the pH region where expansion of the molecule is known not to occur (Hawley, 1966) Fig. 4-1. This implies that contributions to the absorption arising

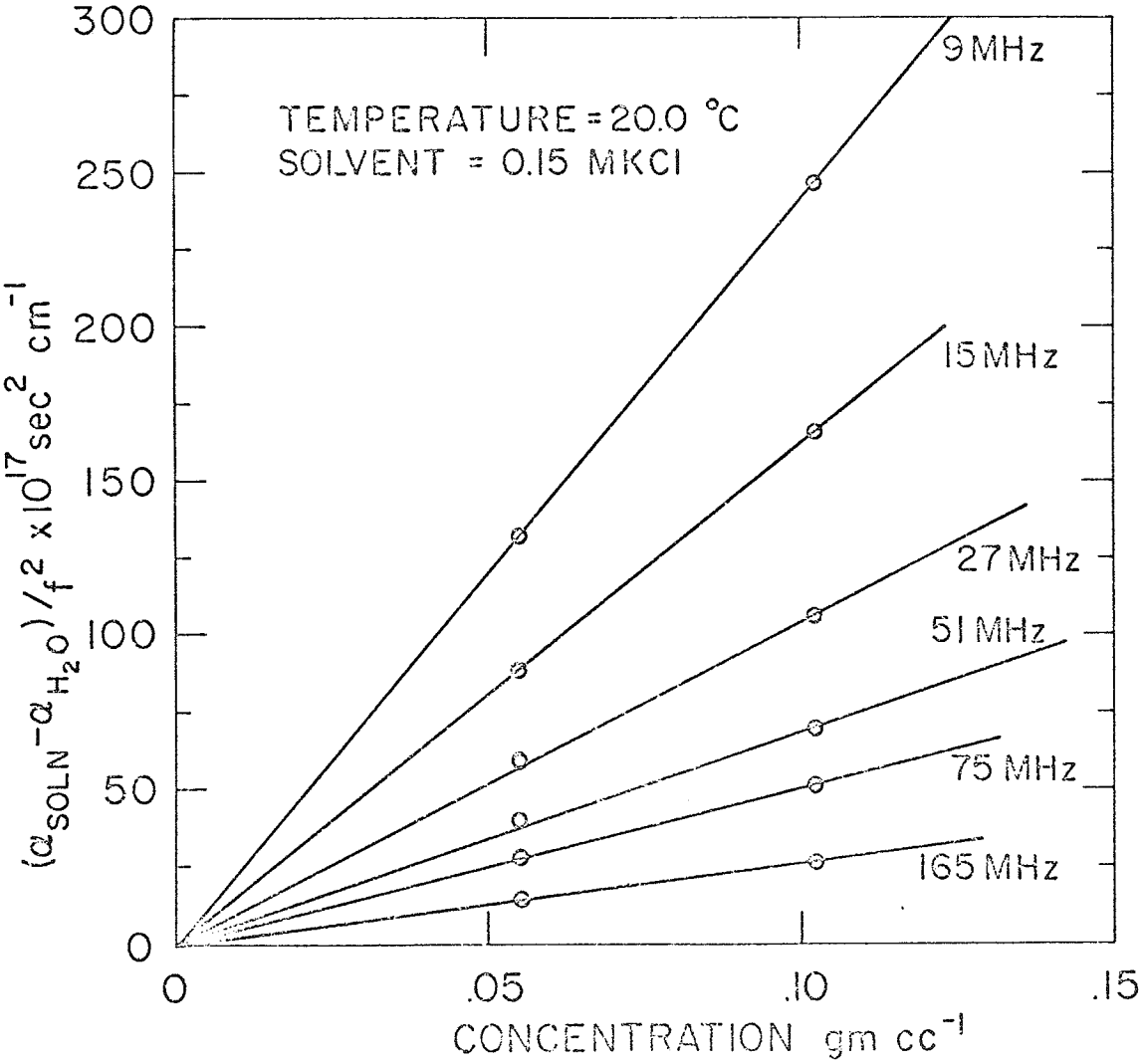

FIGURE 4-1

CONCENTRATION DEPENDENCE OF ABSORPTION--BSA (Hawley, 1966)

from intermolecular interactions are not important, and is equivalent to employing an infinitely dilute solution. In the pH regions where expansion occurs, the question of absolute linearity has not been investigated although this investigation indicates that the absorption coefficient is linear over the range of concentrations from 0.0436 gm/cc to 0.0531 gm/cc.

The excess frequency free absorption parameter is plotted as a function of pH for the acid titration of aqueous BSA solutions in Figs. 4-2, 4-3 and 4-4. The concentration of the BSA solutions employed in the high frequency system were 0.0436 gm/cc and 0.0531 gm/cc for the two trials reported, and the concentration of the solution employed in the low frequency system was 0.0918 gm/cc. The reversibility of the absorption coefficient was investigated by titrating the BSA solution back to the neutral pH. In the figures, the crosses represent the back titration values of A, and it is clear that within the experimental error, the ultrasonic absorption coefficient goes through reversible changes with pH. Other parameters such as the hydrodynamic properties and optical rotation, which are used to characterize molecular configuration, have also been shown to be completely reversible (Foster, 1960) within the pH range investigated in this study.

When the acid titration is reversed by addition of an alkaline solution, a salt forms and an experiment was performed to measure the effect of the presence of salt on the absorption coefficient in aqueous BSA solutions. Potassium chloride was used since it is the salt that forms when hydrochloric acid is neutralized with potassium hydroxide. A 2.0 Molar KCl solution was prepared and known volumes were added to the BSA solution in the absorption chamber. The results, indicated in Fig. 4-5, show that the variation in A for the solution decreases by less than 1% as the salt

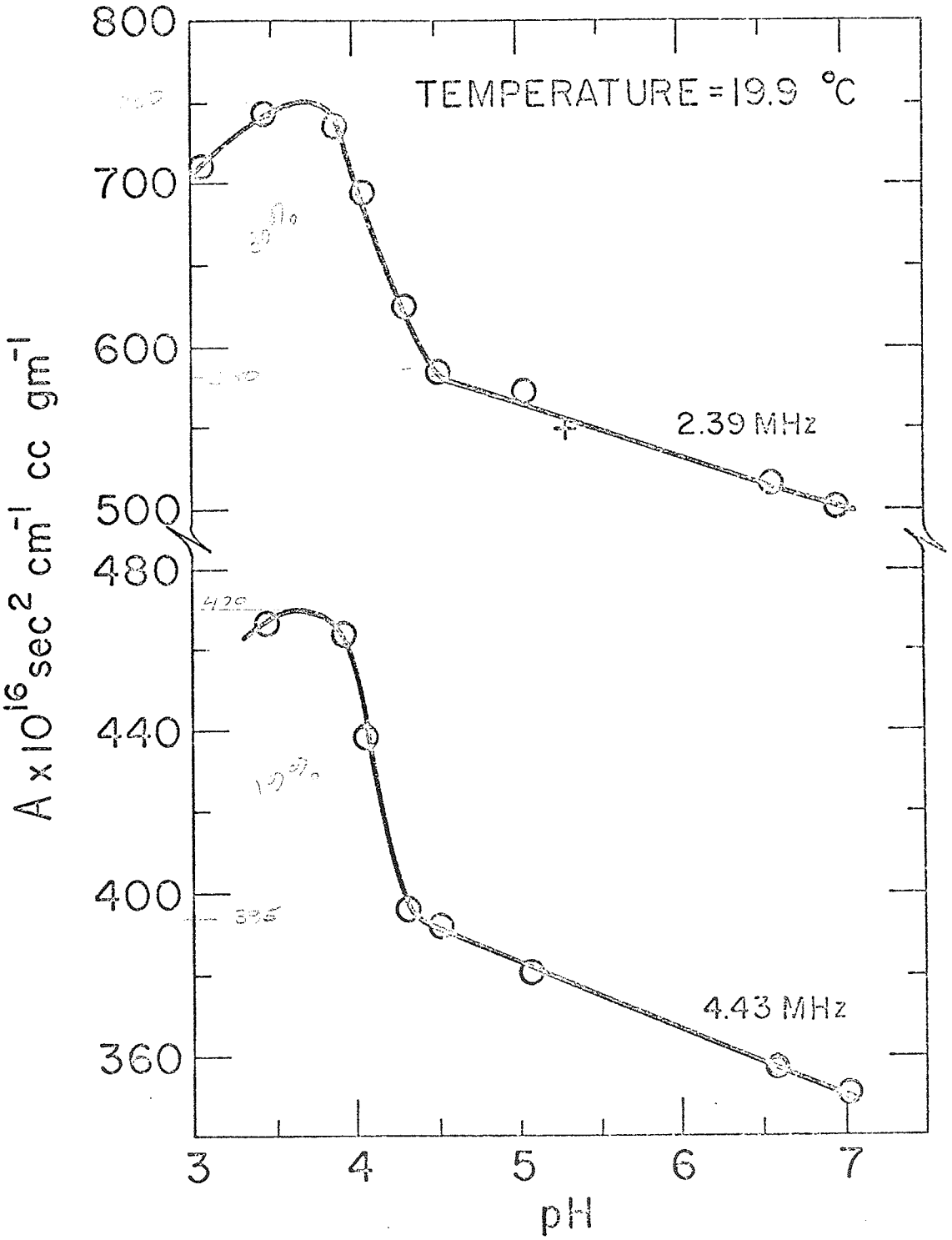

FIGURE 4-2

ULTRASONIC ABSORPTION TITRATION--BSA

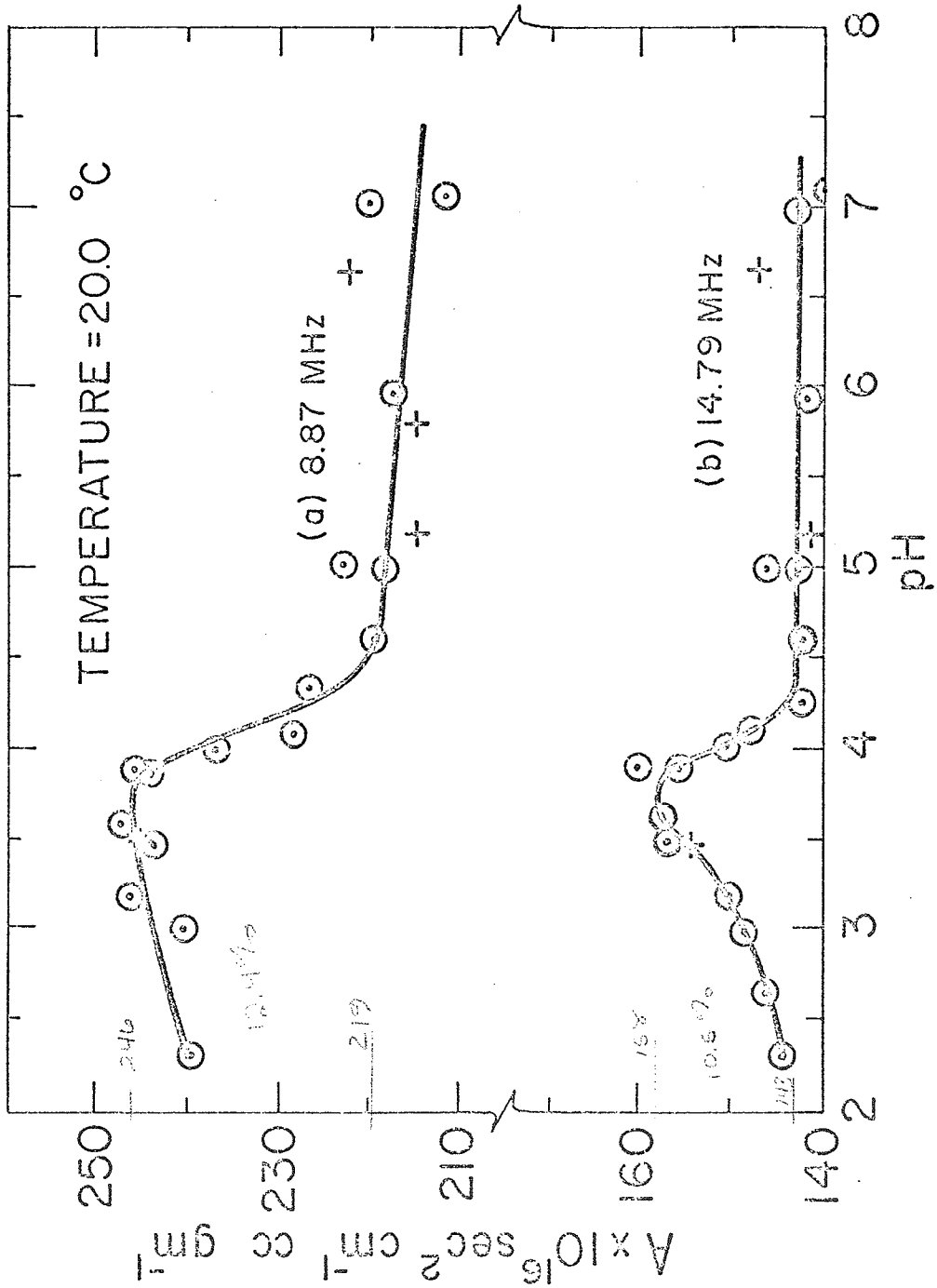

FIGURE 4-3

ULTRASONIC ABSORPTION TITRATION--BSA

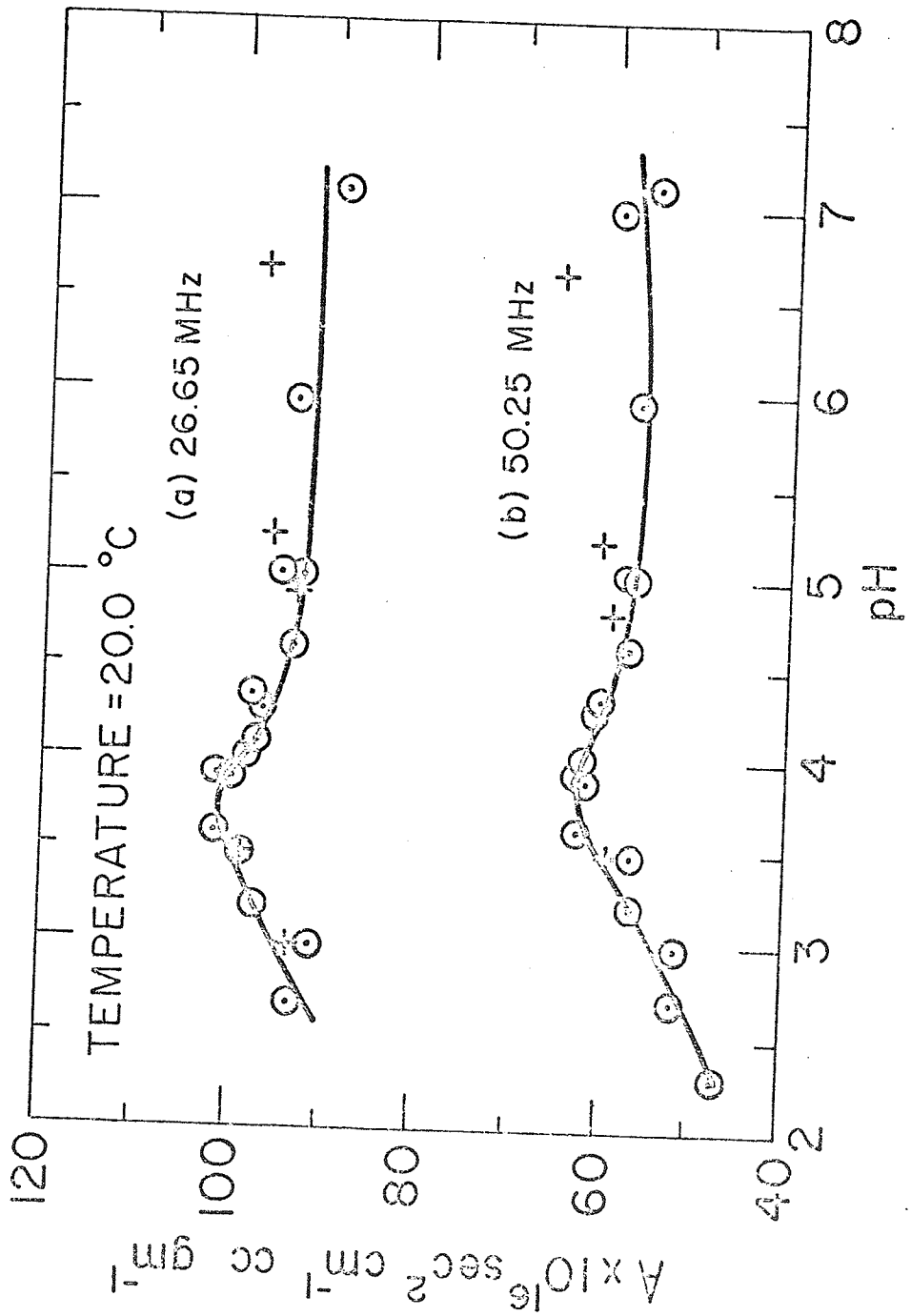

FIGURE 4-4

ULTRASONIC ABSORPTION TITRATION--BSA

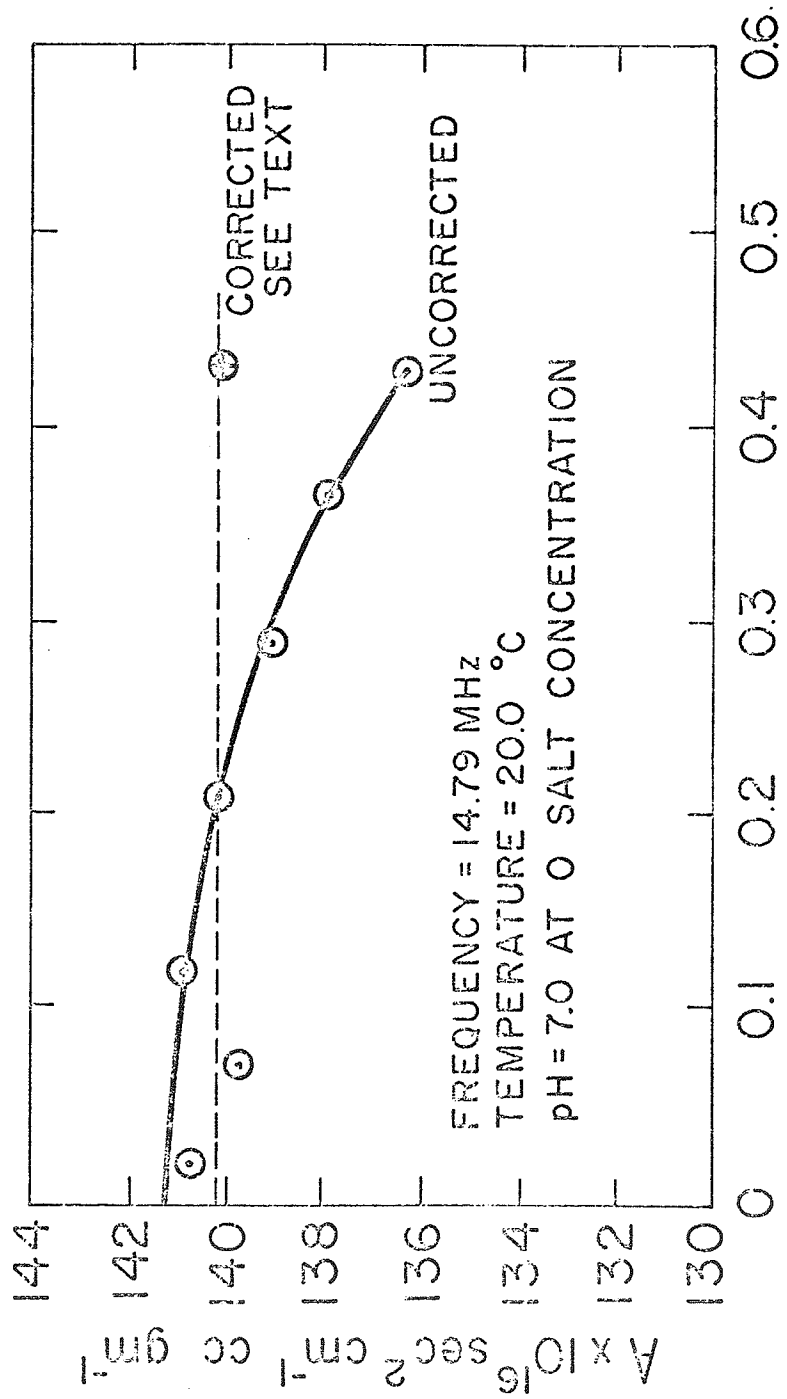

FIGURE 4-5

DEPENDENCE OF ABSORPTION IN BSA SOLUTIONS ON THE PRESENCE OF KCl

concentration is increased from 0 to 0.1 Molar, the maximum amount of salt present after a typical back titration. However, when salt is added to water alone, the absorption coefficient also decreases as shown in Fig. 4-6. If now, instead of considering the solvent for the BSA to be water, the salt solution is considered as the solvent, the value of α/f^2 of the solvent can be determined from Fig. 4-6 and the value of A can be corrected for the new solvent. When this is done, there is no longer any difficulty in interpreting the effect of the presence of salt on the excess absorption coefficient of BSA solutions, and the apparent effect is seen to be entirely due to the action of the salt on the solvent. Fig. 4-5 also shows the corrected curve. Since the effect is small, however, the values of A for the back titrated solutions will not include the effect of the salt on the water. This result is consistent with the results of Carstensen and Schwan (1959b) who found no salt effect on the absorption in aqueous solutions of hemoglobin, a similar globular protein, in this pH region.

As the BSA solution is made acidic, the absorption increases by a small amount until the pH reaches about 4.3. At this point, there is an abrupt increase in the absorption coefficient which for 2.39 MHz is 50% larger at pH 3.65 than at pH 7.0 while at 50.25 MHz, the increase is only 6.9%. Below pH 3.6, the absorption coefficient decreases slowly and only at 50.25 MHz does it go substantially below its value at neutral pH. In an early experiment, a BSA solution was prepared using 0.15 M KCL instead of pure water and it was found that the variation of the absorption coefficient with changes in pH was essentially the same as that presented in Figs. 4-3 and 4-4.

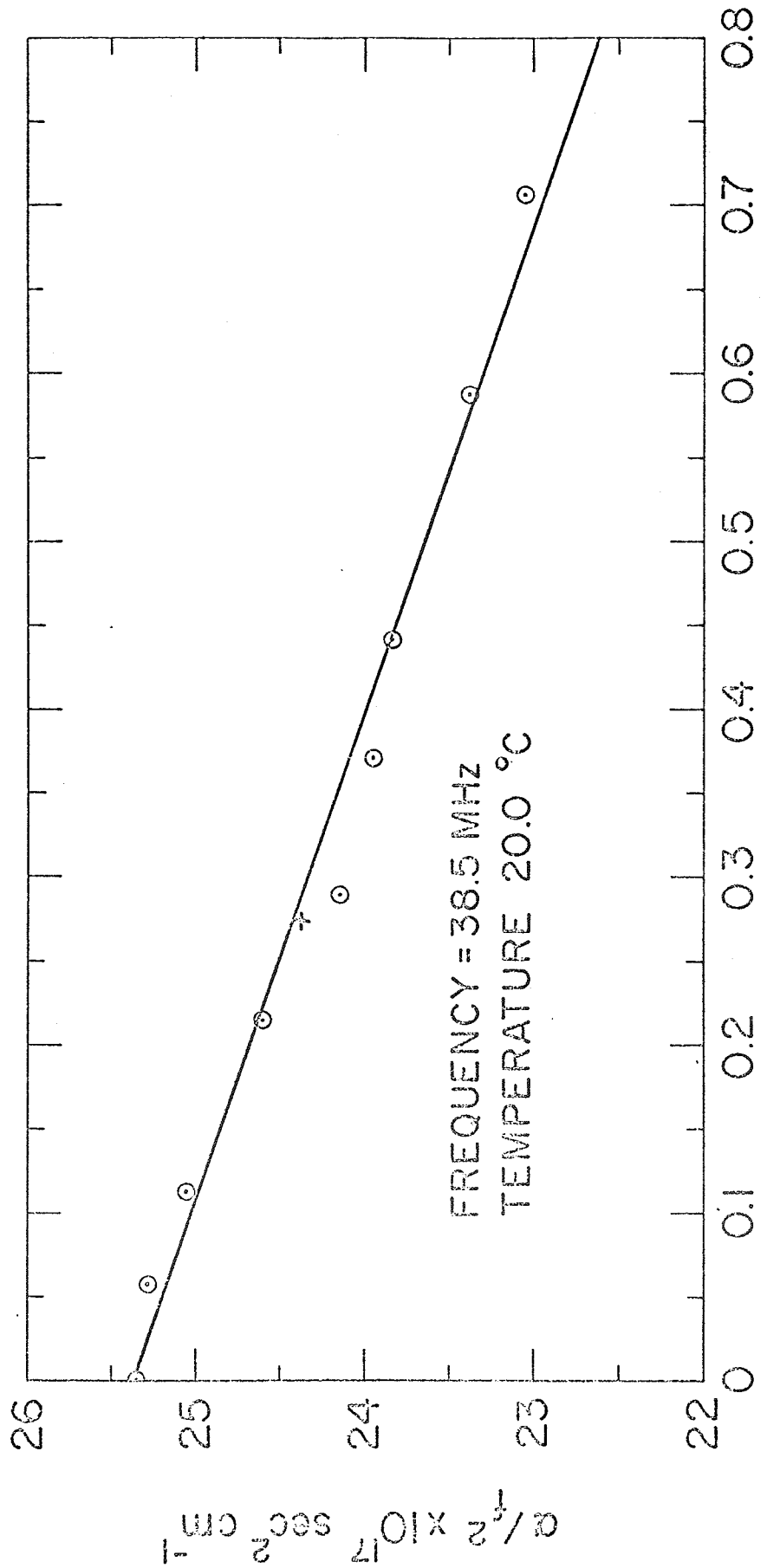

FIGURE 4-6

DEPENDENCE OF ABSORPTION IN DISTILLED WATER ON THE PRESENCE OF KCl

The velocity of sound was also measured as a function of pH at 2.39 MHz. Since the difference between the velocity in the BSA solution and the velocity in water, the reference liquid, amounts to approximately 25 m/sec, and the BSA concentration changes as a function of pH, a reduced velocity parameter, normalized for concentration, is more easily interpreted than comparing velocities at different concentrations. The assumption is made that the velocity varies linearly with concentration which appears reasonable from the results for polyethylene glycol presented in Fig. 4-24 and the theoretical considerations of Barthel (1954), who demonstrated that in most dilute aqueous solutions the velocity of sound should vary linearly with concentration. Fig. 4-7 shows the result of the velocity titration. The reduced velocity exhibits a minimum at about pH 4.1 which is the approximate midpoint of the abrupt increase of the absorption coefficient.

Ultrasonic titration of BSA on the alkaline side of neutral shows an even greater increase in the absorption coefficient than at low pH as shown in Figs. 4-8, 4-9, and 4-10. As the alkalinity of the solution is increased from pH 7, the variation of A with pH is small up to about pH 10 where the increase in A becomes greater per unit change in pH. At pH 10.5, the absorption increases sharply and at 8.8 MHz, the absorption at pH 11.6 is about 140% greater than that at pH 7.0. The alkaline effect is also shown to be reversible over the pH range covered. The velocity of sound was measured as a function of pH simultaneously with the absorption measurements in the high frequency system and the results presented in Fig. 4-11, indicate that the velocity and absorption behave similarly as a function of pH. This is in contrast to the absence of such a correlation for the acid titration. The magnitude of the reduced velocity at

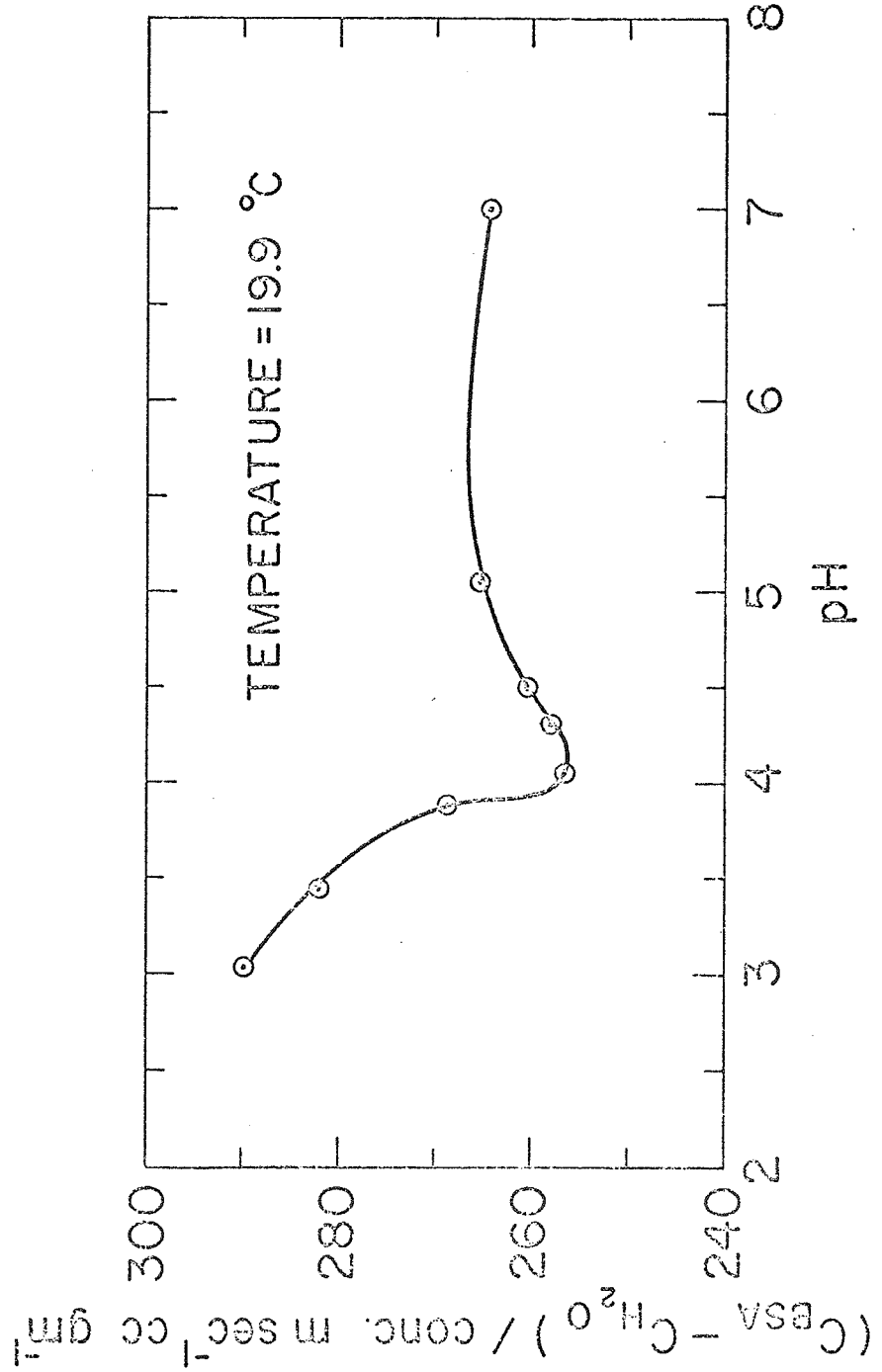

FIGURE 4-7

ULTRASONIC VELOCITY TITRATION--BSA

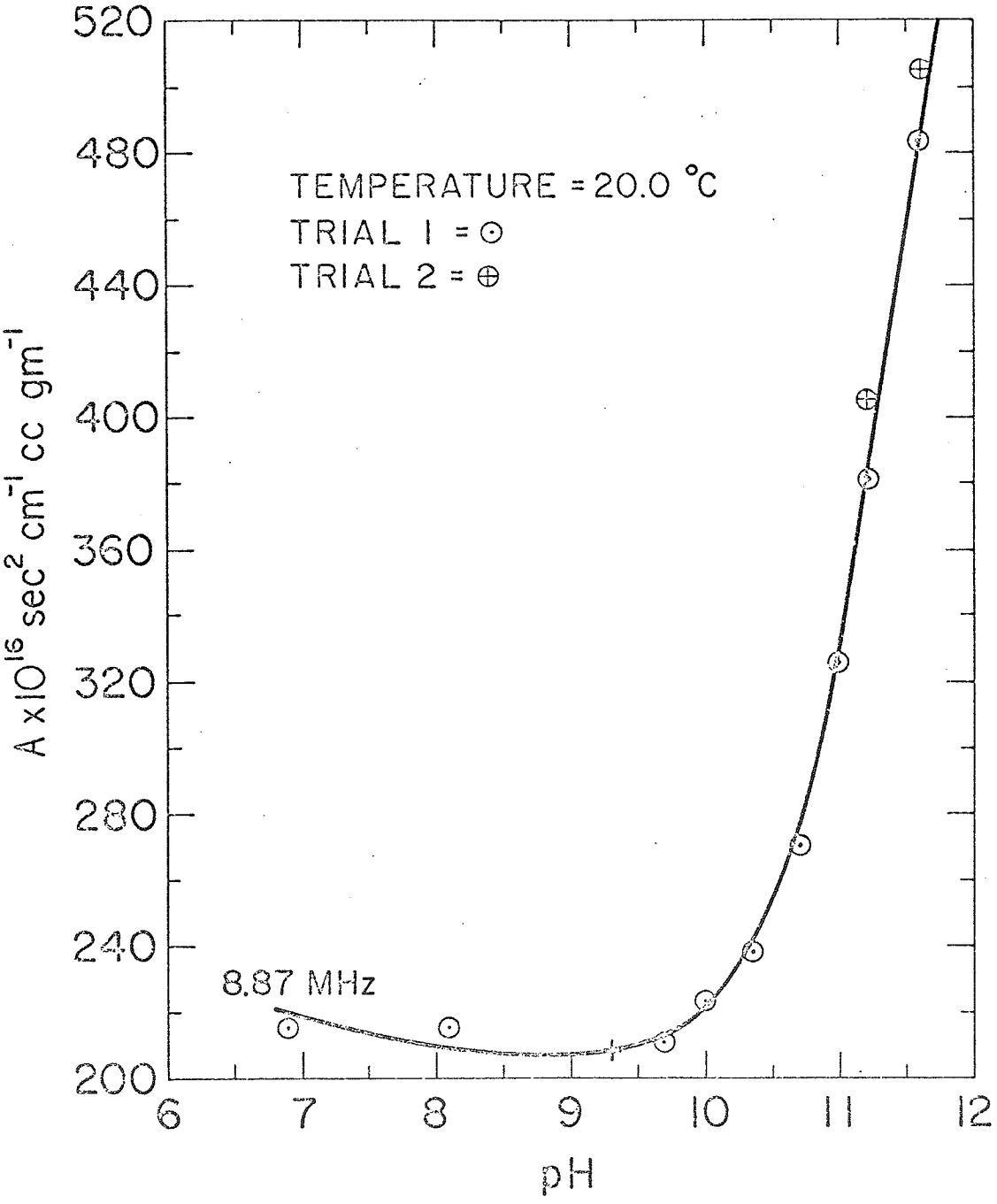

FIGURE 4-8

ULTRASONIC ABSORPTION TITRATION---BSA

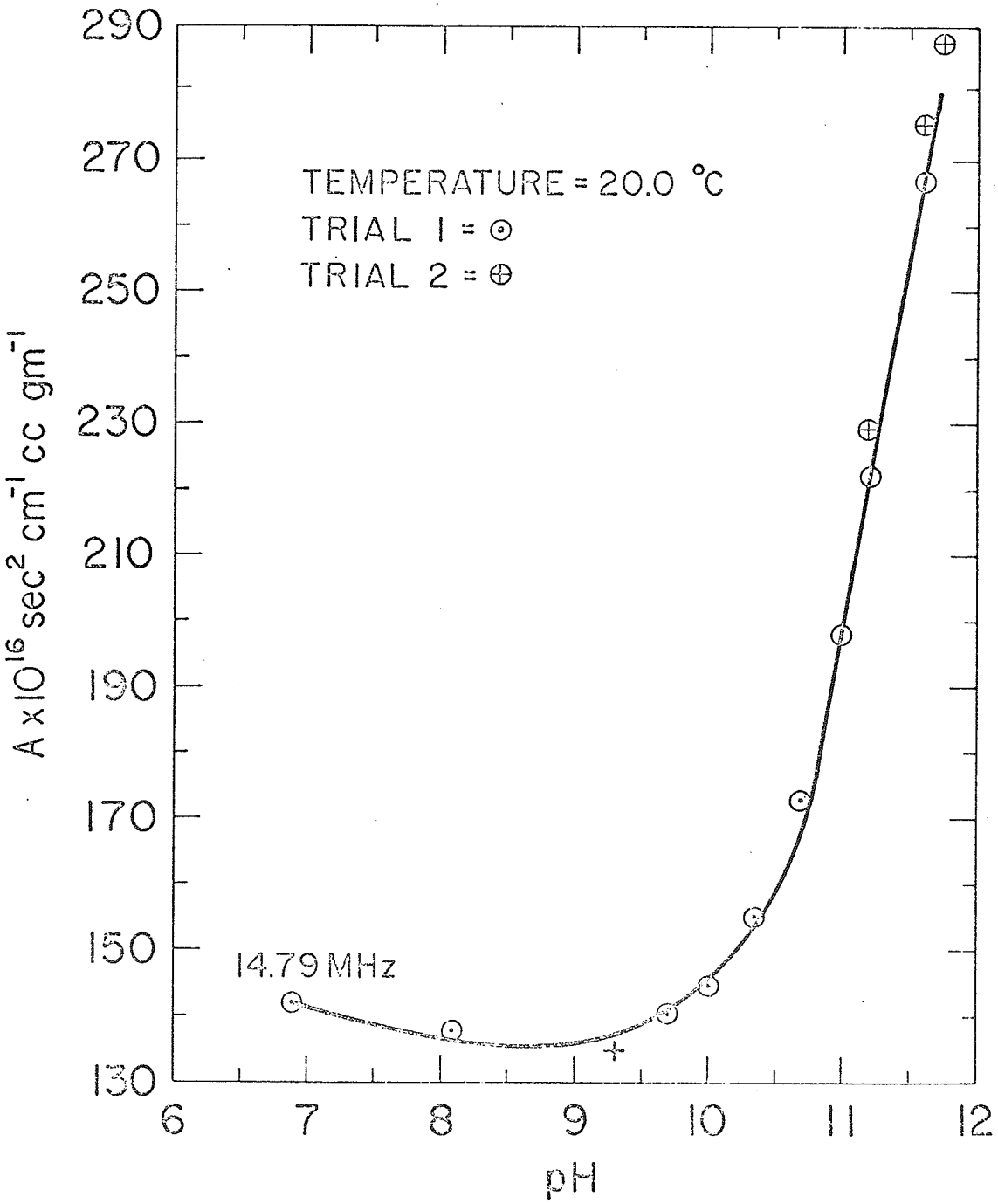

FIGURE 4-9

ULTRASONIC ABSORPTION TITRATION--BSA

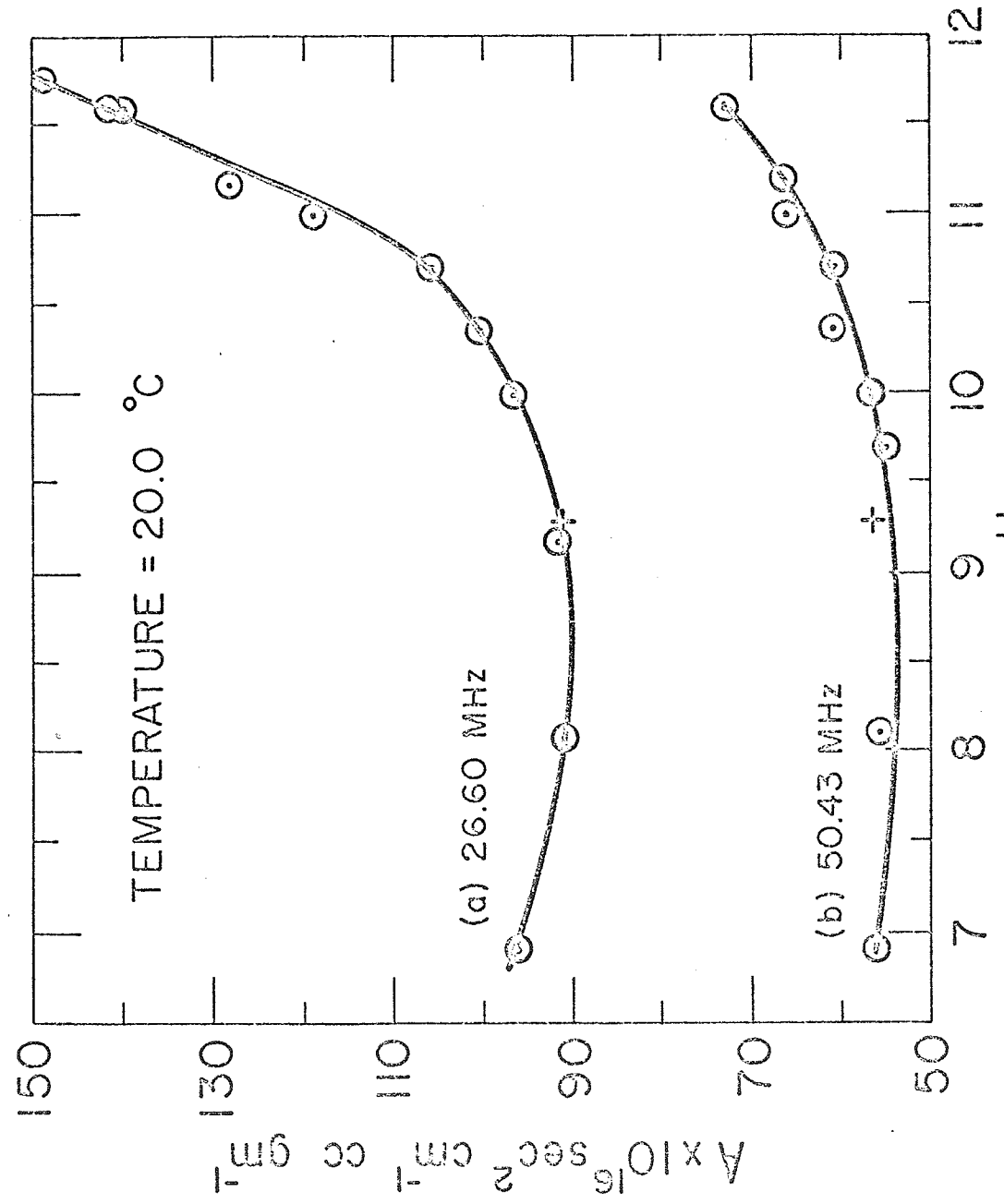

FIGURE 4-10

ULTRASONIC ABSORPTION TITRATION--BSA

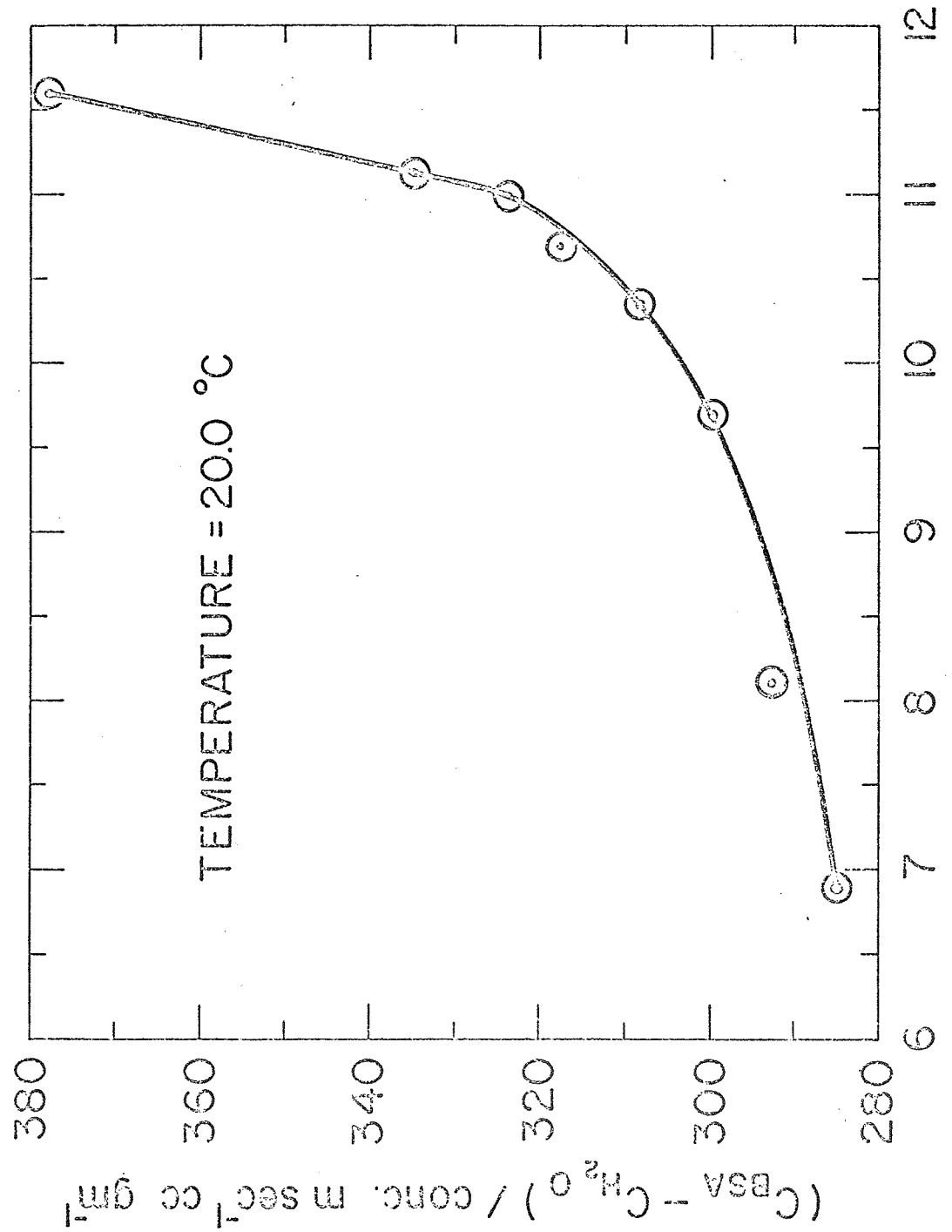

FIGURE 4-11

ULTRASONIC VELOCITY TITRATION--BSA (HIGH FREQUENCY PULSED INTERFEROMETER)

pH 7 is 284.5 for the alkaline titration (Fig. 4-11) and 264.3 for the acid titration (Fig. 4-7) and the apparent discrepancy is within the uncertainties of velocity measurements with the pulsed interferometer, i.e., ± 1.0 m/sec, and the uncertainties in the concentrations of BSA.

Before considering the mechanism or mechanisms responsible for the abrupt changes in the absorption coefficients, the origin of the excess absorption in the neutral region will be examined. The frequency dependence of A was measured in three overlapping frequency ranges, and a composite of all the data at neutral pH is shown in Fig. 4-12. Fig. 4-13 shows the data plotted as a function of frequency for pH 7, 11.5, and 3.0. Between 3 MHz and 25 MHz, the agreement between this investigation and that of Hawley (1966) on BSA in 0.1 M KCl is excellent. However, beyond 25 MHz, the value of A is systematically lower than that of Hawley's and this is accounted for in the following manner. In the present investigation, the concentration of the BSA solution used in the highest frequency range was 0.0353 gm/cc. At 165 MHz, the observed value of α/f^2 was found to be 33.3×10^{-17} $sec^2 cm^{-1}$ with an estimated uncertainty of ± 5.5% and the contribution of the solvent was 25.3×10^{-17} $sec^2 cm^{-1}$. Assuming that the contribution of the solvent is known accurately, the uncertainty in the difference becomes ± 23%.

It is evident from Fig. 4-12 that over the frequency range covered, a broad distribution of relaxation times are necessary to characterize the absorption coefficient. Further evidence of the presence of relaxation phenomena is the presence of velocity dispersion shown in Fig. 4-14. In order to detect the small amount of dispersion, the low frequency system was employed, and consequently, meaningful data could be obtained only at frequencies less than 13.4 MHz.

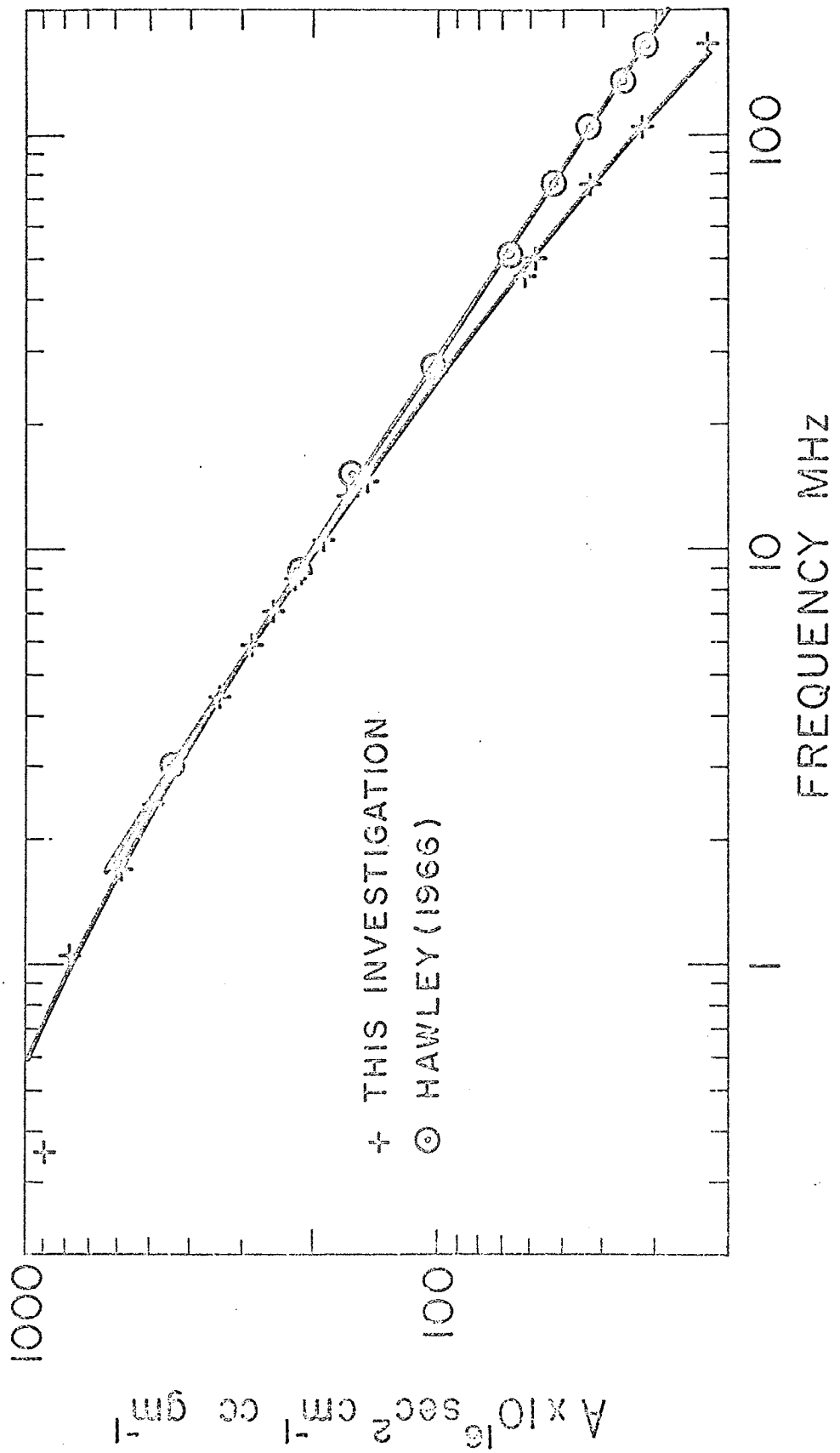

FIGURE 4-12

ULTRASONIC SPECTROGRAM--BSA

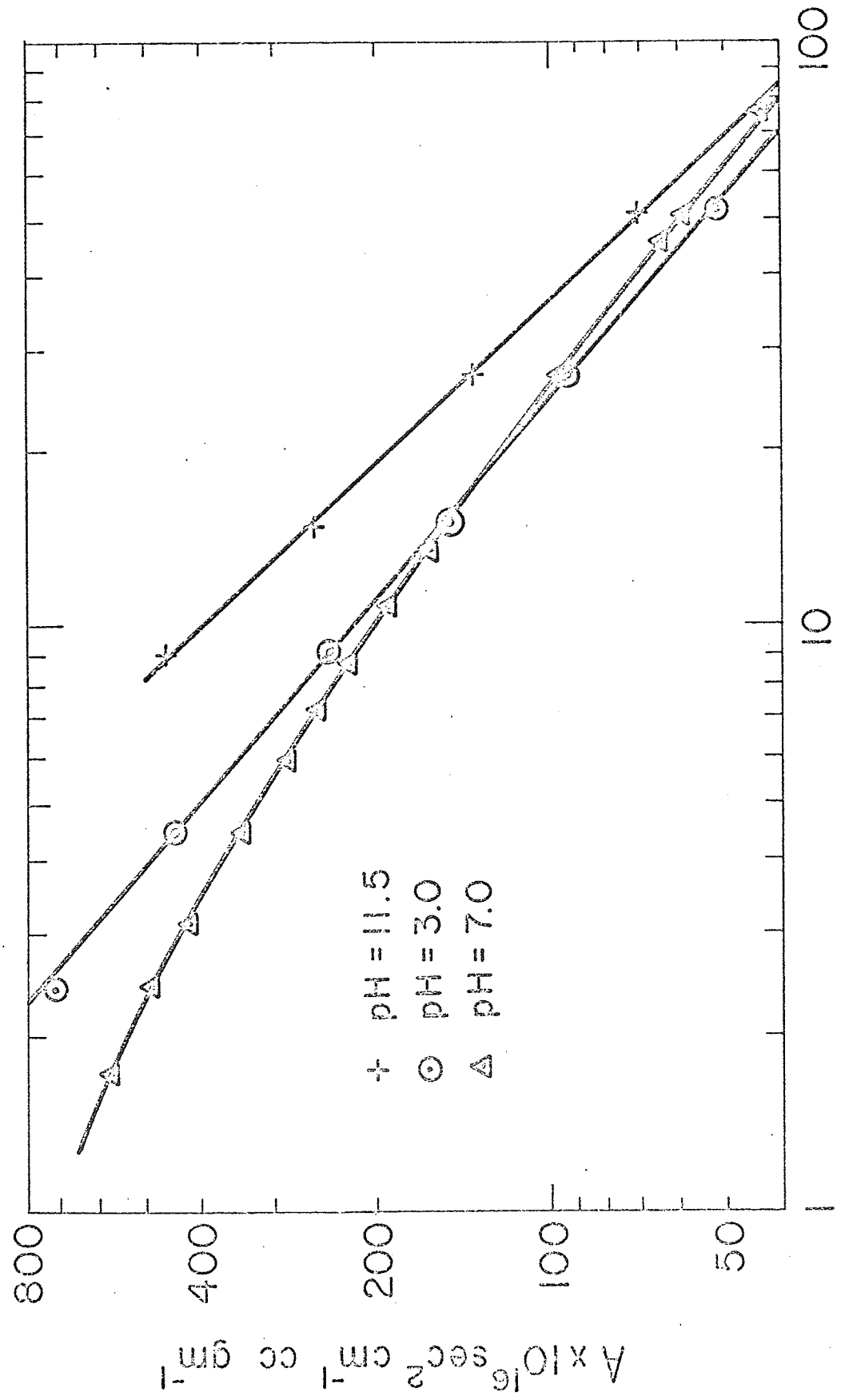

FIGURE 4-13

ULTRASONIC SPECTROGRAM--BSA

LWK'S FIG 4-13

• pH 7.0 T = 20.0°C $m(Hi) = \frac{4.56}{6.0} = 0.76$ $m(Lo) = \frac{3.504}{6.0} = 0.60$

+ pH 3.0 T 20.0°C

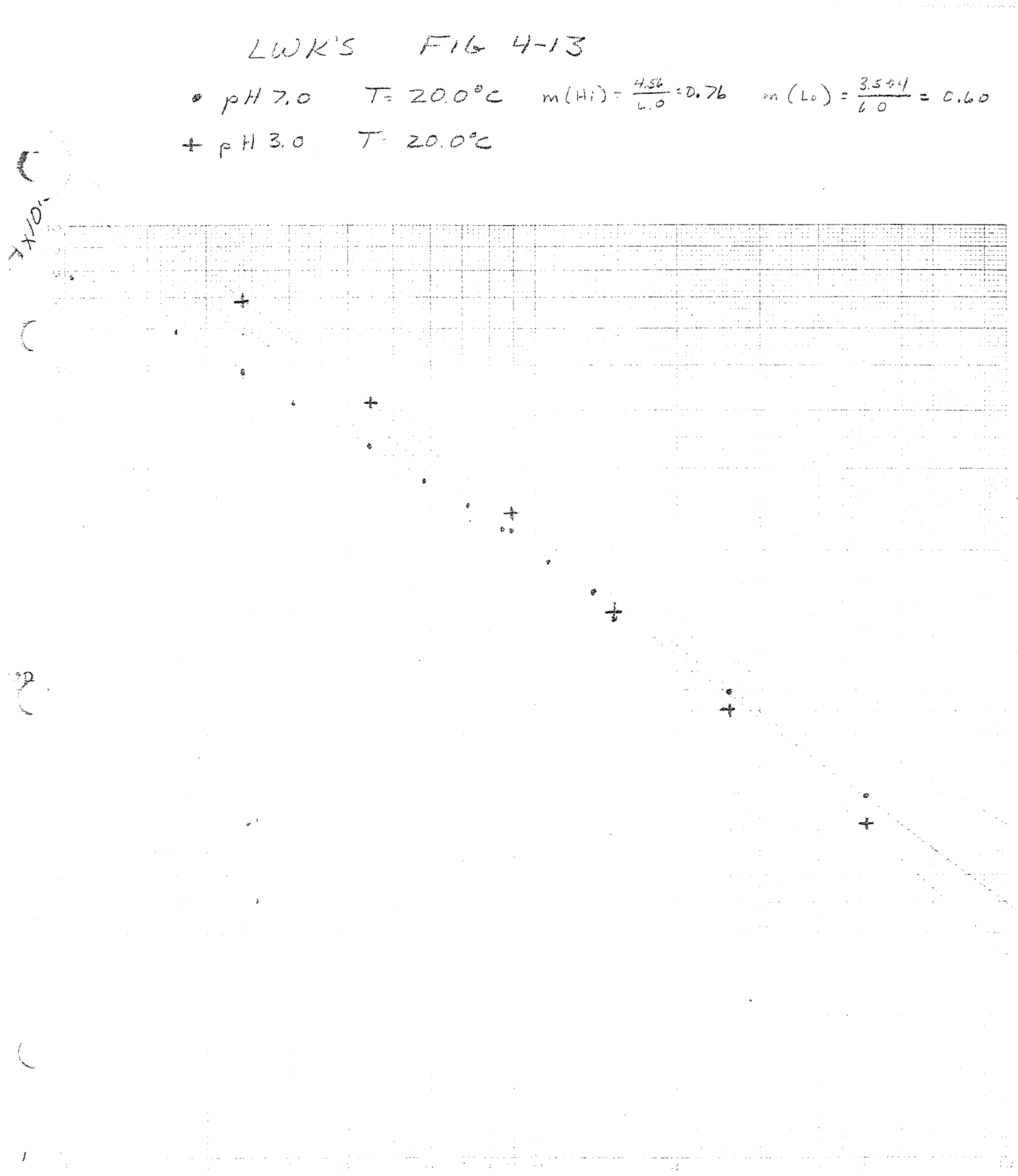

FREQ (MHz)

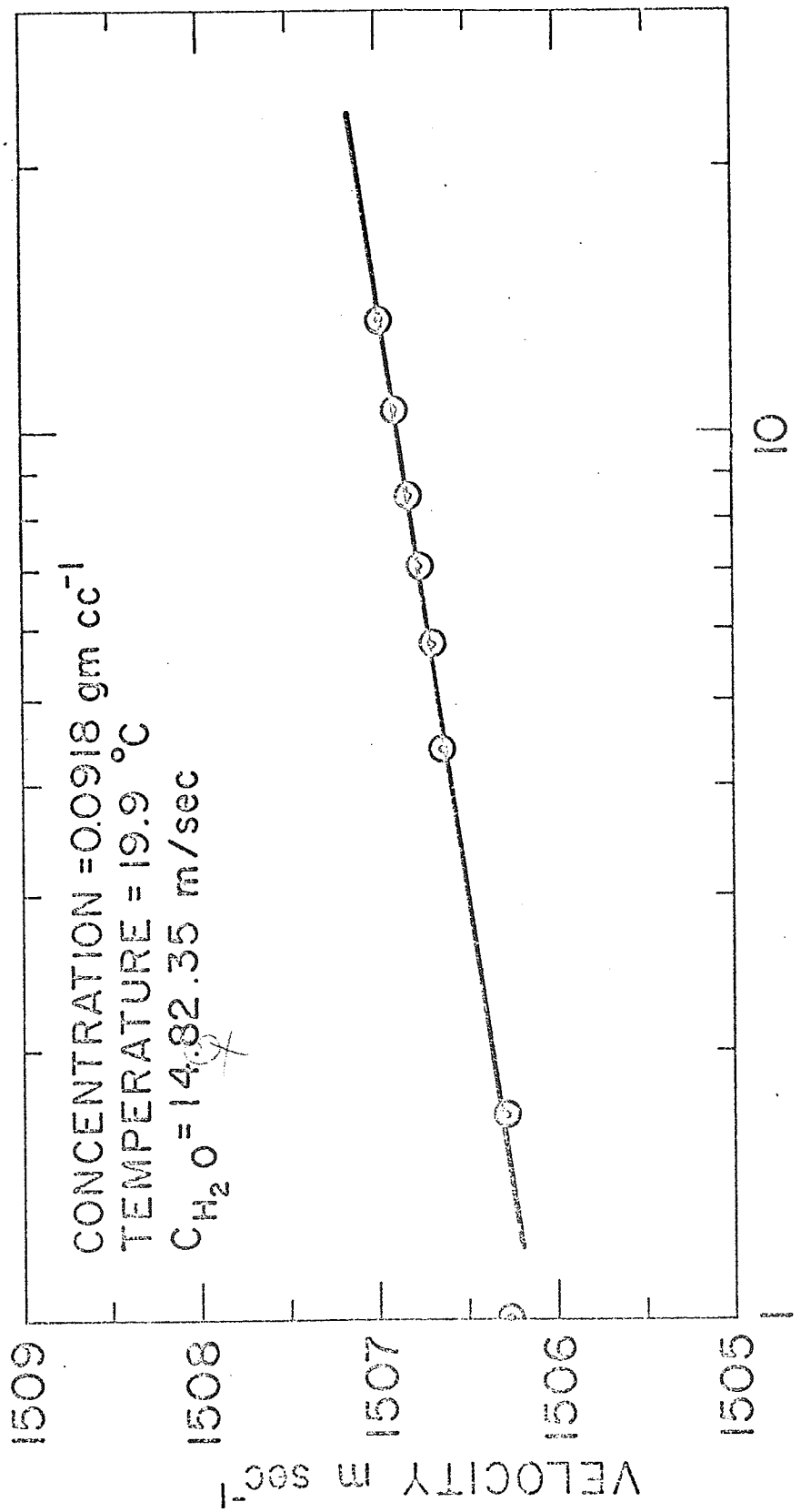

FIGURE 4-14

VELOCITY DISPERSION IN AN AQUEOUS SOLUTION OF BSA

In order to assess the importance of the known mechanisms of absorption in aqueous solutions of BSA (as discussed in Chapter 2) the absorption due to the dynamic shear viscosity as predicted by the Cerf-Scheraga theory will be evaluated first. If (2-36) and (2-37) are combined with (4-2), viz.,

$$(4\text{-}2) \qquad A_s = \frac{\Delta\alpha_s}{cf^2} = \frac{8\pi^2}{3\rho_o c_o^3}\left[\frac{n^* - n_s}{c}\right]$$

where A_s is the excess frequency free absorption per unit concentration for shear viscosity alone. Using the physical parameters of BSA listed in Table 4-2, A_s reduces to

$$(4\text{-}3) \qquad A_s = 8.88 \times 10^{-17}\left(3.434 + \frac{2.372}{1 + 165 \times 10^{-9}\,\omega^2}\right)$$

The physical properties of BSA are not all known precisely and various values are found in the literature, a few of which have been included in Table 4-2. However substitution of any of the alternate parameters does not change the significance of the result. From Fig. 4-15A, it can be seen that the dynamic shear viscosity contributes only a small fraction of the observed absorption coefficient.

In order to determine the fraction of the longitudinal acoustic wave that is dissipated as transverse energy and the amount of the loss associated with relative motion between the solute and solvent molecules (2-40) has been evaluated and plotted in Fig. 4-15B. The ordinate of the graph in this case is α/f^2 and represents the total absorption that would be observed if this process were the only one responsible. For the purpose of this analysis, the molecules have been considered to be spherical. Although this is only an approximation, the results should be of the

TABLE 4-2. PROPERTIES OF BSA SOLUTIONS NECESSARY FOR EVALUATION OF THE CONTRIBUTION OF DYNAMIC SHEAR VISCOSITY TO THE ABSORPTION COEFFICIENT

η_s = 0.01 gm/(cm sec)

Mw = 68,000 (Cal Biochem. Co.)

$c_o = 1.5 \times 10^6$ cm/sec

$\rho_o \cong 1.0$ gm/cm^3

$N_a = 6.02 \times 10^{23}$ mole^{-1}

p = 5 (Allis and Ferry, 1965)

$2a = 170 \times 10^{-8}$ cm (Allis and Ferry, 1965)

$V_s = 4/3\pi ab^2 = 1.03 \times 10^{-19}$ cm^3

ν_A = 3.434 (Scheraga, 1955)

ν_B = 2.372 (Scheraga, 1955)

$\tau = 165 \times 10^{-9}$ sec (Allis and Ferry, 1965)

Alternate values of parameters that have been used without significantly altering the result

Mw = 67,000 (Tanford, 1961)

$\tau = 198 \times 10^{-9}$ sec (Tanford, 1961)

$V_s = 1.36 \times 10^{-19}$ cm^3 (Bloomfield, 1966)

p = 3.3 (Tanford, 1961)

$2a = 190 \times 10^{-8}$ cm (Bloomfield, 1966)

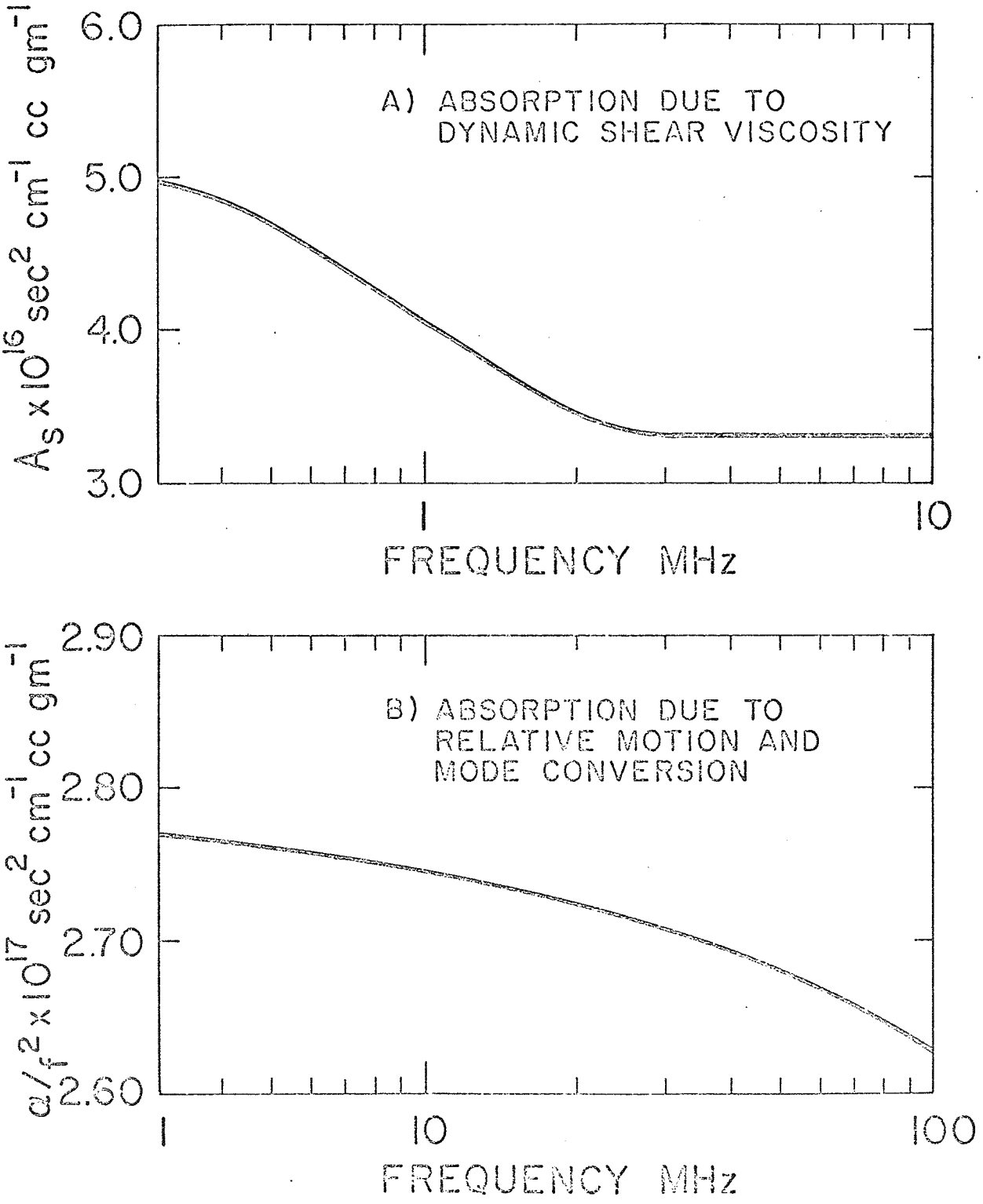
A) ABSORPTION DUE TO
DYNAMIC SHEAR VISCOSITY
$A_s \times 10^{16}$ sec^2 cm^{-1} cc gm^{-1}
6.0
5.0
4.0
3.0
1
10
FREQUENCY MHz
B) ABSORPTION DUE TO
RELATIVE MOTION AND
MODE CONVERSION
$\alpha/f^2 \times 10^{17}$ sec^2 cm^{-1} cc gm^{-1}
2.90
2.80
2.70
2.60
1
10
100
FREQUENCY MHz

FIGURE 4-15

correct order of magnitude. The mass density of the molecule is taken as 1.33 gm/cm^3 (Andregg, et al., 1955) and the radius, R, of the equivalent sphere was evaluated from the intrinsic viscosity data of Tanford et al. (1955) and the Einstein (1920) relationship for the intrinsic viscosity of a dilute solution of rigid spherical particles.

$$[\eta] = \frac{10\pi N_a R^3}{3M_w} \tag{4-4}$$

and found to be about 34×10^{-8} cm. It is observed, however, that these effects contribute only a small proportion of the observed absorption. Thus, as has been shown, shear processes can be expected to play only a minor role in explaining the magnitude of the observed absorption coefficient. However, it is not possible to investigate the complete behavior of these solutions with longitudinal sound waves only and a study has been performed by Allis and Ferry (1965) on the dynamic shear viscoelastic properties of paramyosin and BSA solutions in the frequency range from 0.04 Hz to 400 Hz. In order to observe rotational relaxation of the molecules at these low frequencies, η_s must be made large, as required by (2-37). A mixture of glycerol and water was employed to achieve the necessary η_s and it is not known what effect the glycerol may have on the properties of the BSA molecules compared with the case where pure water is employed as the solvent. The results obtained for paramyosin conform rather well with predictions of the Cerf-Scheraga theory, however, the results for BSA do not. It is suggested by the authors that the origin of the viscoelasticity in BSA does not arise from orientation of the molecule by the shear stresses but primarily from an intramolecular flexibility not observed by other investigators. However, a re-examination of the contribution of shear viscosity predicted by the Cerf-Scheraga theory, taking

into account the discrepancy reported by Allis and Foster, does not significantly alter the result presented here.

For absorption due to a viscous process, whether shear or structural, the temperature dependence of the absorption coefficient is that of the viscosity, as long as the period of the wave is not in the neighborhood of any relaxation processes. For this case, the temperature dependence is given by Eyring (1936) as

$$\alpha = \frac{8\pi^2 f^2}{3\rho_o c_o^3} [\eta_o e^{\Delta F/RT}] \tag{4-5}$$

where the bracketed term is the temperature dependent viscosity of the liquid, ΔF is the activation energy or potential energy barrier which, for example, hinders the free exchange of molecules from a high energy state to lower energy state. The velocity of propagation, c_o, is temperature dependent and the dependence of the density, ρ_o, is ignored for the present purpose since it is known to be small. In the presence of relaxation processes (4-5) does not describe the temperature dependence of α since the parameters that describe the relaxation process are also strongly temperature dependent (Lamb, 1965). The absorption coefficient was determined as a function of temperature from 15°C to 38°C and at two pH values, viz., 7.0 and 2.9. Higher temperatures were avoided since above 40°C irreversible denaturation of the molecule occurs (Foster and Yang, 1955). These data are shown in Fig. 4-16 in the manner most convenient for directly determining the activation energy, i.e., an Arrhenius plot. If (4-5) adequately describes the processes being observed, then a plot of $\log \frac{\alpha c_o^3}{f^2}$, where α is the total absorption observed, as a function of $\frac{1}{T}$ is linear and independent of frequency.

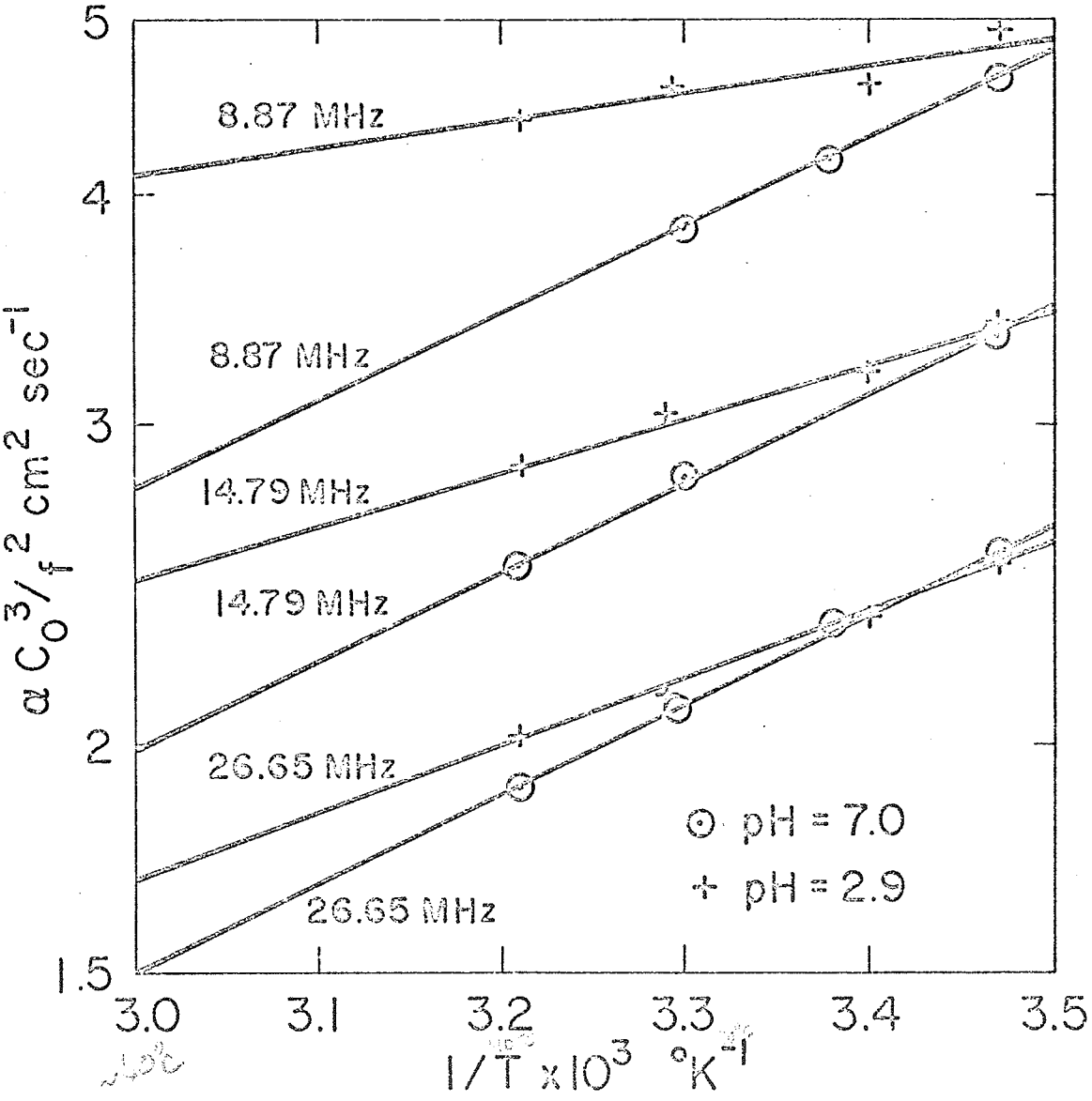

FIGURE 4-16

ARRHENIUS PLOT OF AN AQUEOUS SOLUTION OF BSA (0.05 gm/cc)

Fig. 4-16 shows this to be the case for pH 7. Table 4-3 lists the apparent activation energies determined for concentrations of 0.05 gm/cc of BSA in water. The velocity as a function of temperature was obtained from Fig. 4-17.

TABLE 4-3. ACTIVATION ENERGIES OF AQUEOUS BSA SOLUTION CONCENTRATION 0.05 gm/cc

pH	FREQ (MHz)	ΔF k cal/mole
7.0	8.87	2.19
7.0	14.79	2.23
7.0	26.65	2.26
2.9	8.87	0.671
2.9	14.79	1.35
2.9	26.65	1.70
water	all	4.23

In all cases, the apparent activation energy is less than that for pure water. At pH 7.0, the activation energy is independent of frequency, within the experimental error, as it is for water. However at pH 2.9, ΔF is a strong function of frequency indicating the presence of an additional relaxation mechanism, possibly related to the actual expansion of the BSA molecule which occurs in this pH region (see Chapter 5).

B. Polyethylene Glycol

The ultrasonic absorption coefficient was determined in aqueous solutions of several molecular weight fractions of polyethylene glycol (PEG) over a frequency range from 2 MHz to 163 MHz in the temperature range from 4.2°C to 32.2°C. Each molecular weight fraction consists of a narrow

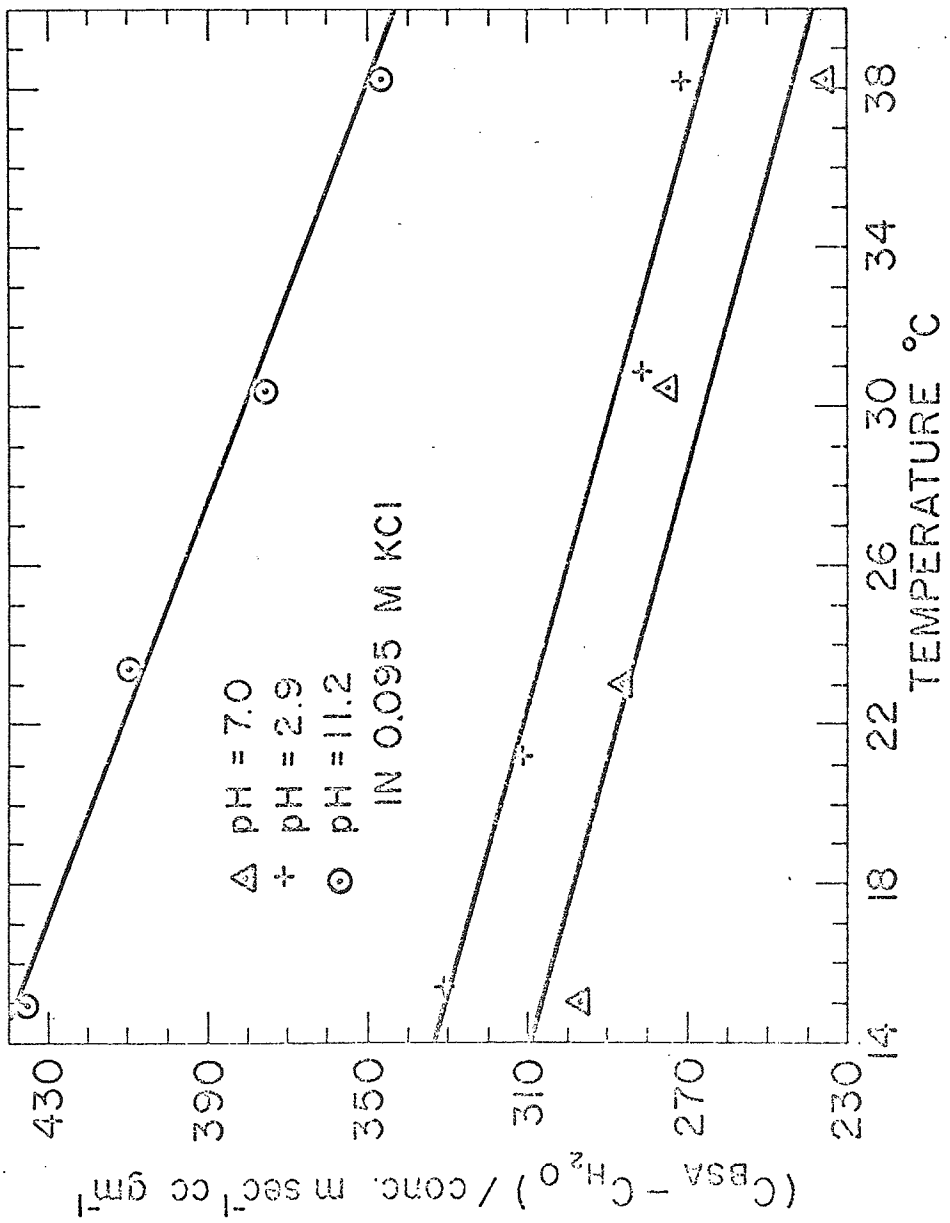

FIGURE 4-17

DEPENDENCE OF REDUCED VELOCITY OF SOUND ON TEMPERATURE

distribution of different size polymer molecules. The "weight average" molecular weight which characterizes the particular fraction is defined as

$$M_w = \frac{\sum_{i=1}^{\infty} g_i M_i}{\sum_{i=1}^{\infty} g_i} \qquad (4\text{-}6)$$

where g_i is the number of grams of molecules having molecular weight M_i in a given sample. This investigation was concerned with the following molecular weights: 20,000, 4,500, 1,450, 400, 150, and 62. The lowest molecular weight of the series corresponds to the monomer, i.e., the single molecular unit repeated along the polymer chain. Due to the low observed value of the excess absorption coefficient in aqueous PEG solutions, it was necessary to utilize concentrated solutions of polymer in the low frequency system. Fig. 4-18 demonstrates the linear relationship between α and concentration up to about 0.21 gm/cc. Non-linearity was detected at 0.25 gm/cc, and therefore all measurements were performed well within the linear range.

At 20.7°C repeated investigations failed to reveal any difference in the ultrasonic absorption coefficient between solutions of Mw 20,000 and Mw 4,500 over the entire frequency range and therefore these data were combined and averaged at each frequency. The excess absorption parameter A is shown in Fig. 4-19 as a function of frequency for all molecular weights investigated at 20.7°C. Evidence of relaxation is prominent in the molecular weight fractions above and including Mw 1,450; and may also be present for fractions between Mw 400 and Mw 1,450. The degree of polymerization appears to determine whether relaxation phenomena occur in this frequency range. Fig. 4-20 shows A as a function of frequency for

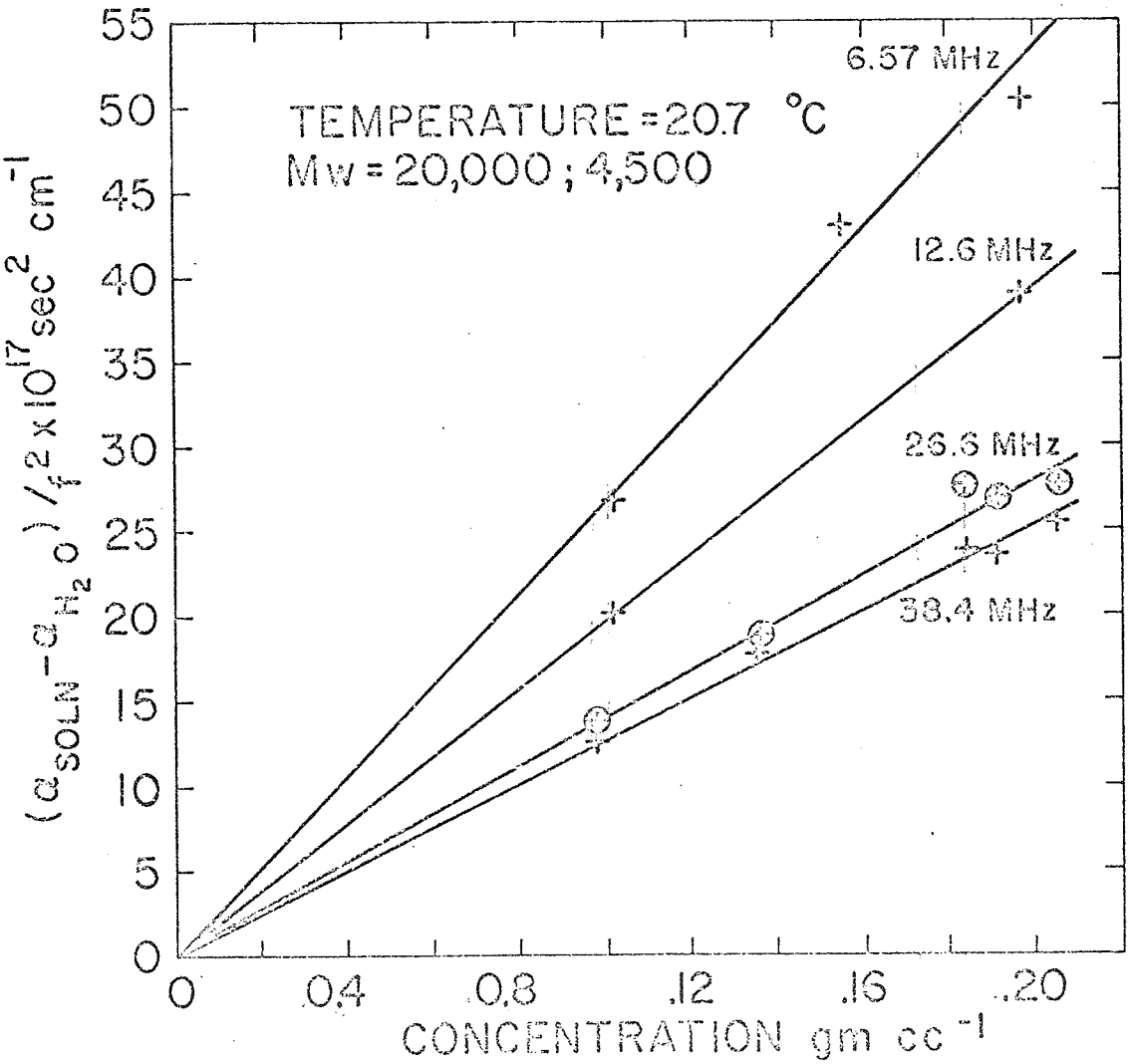

FIGURE 4-18

CONCENTRATION DEPENDENCE OF ABSORPTION--PEG

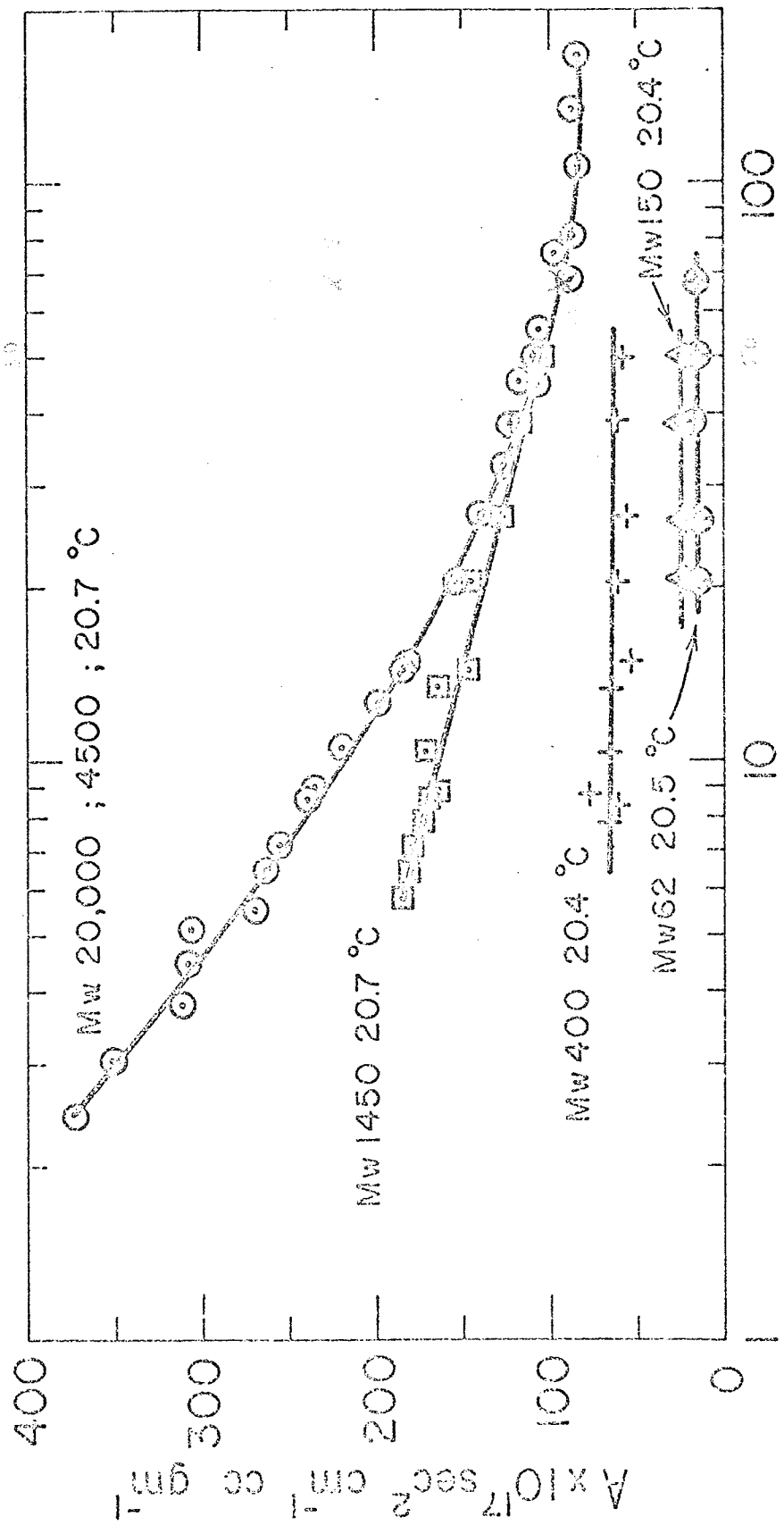

FIGURE 4-19

ULTRASONIC SPECTROGRAM--PEG

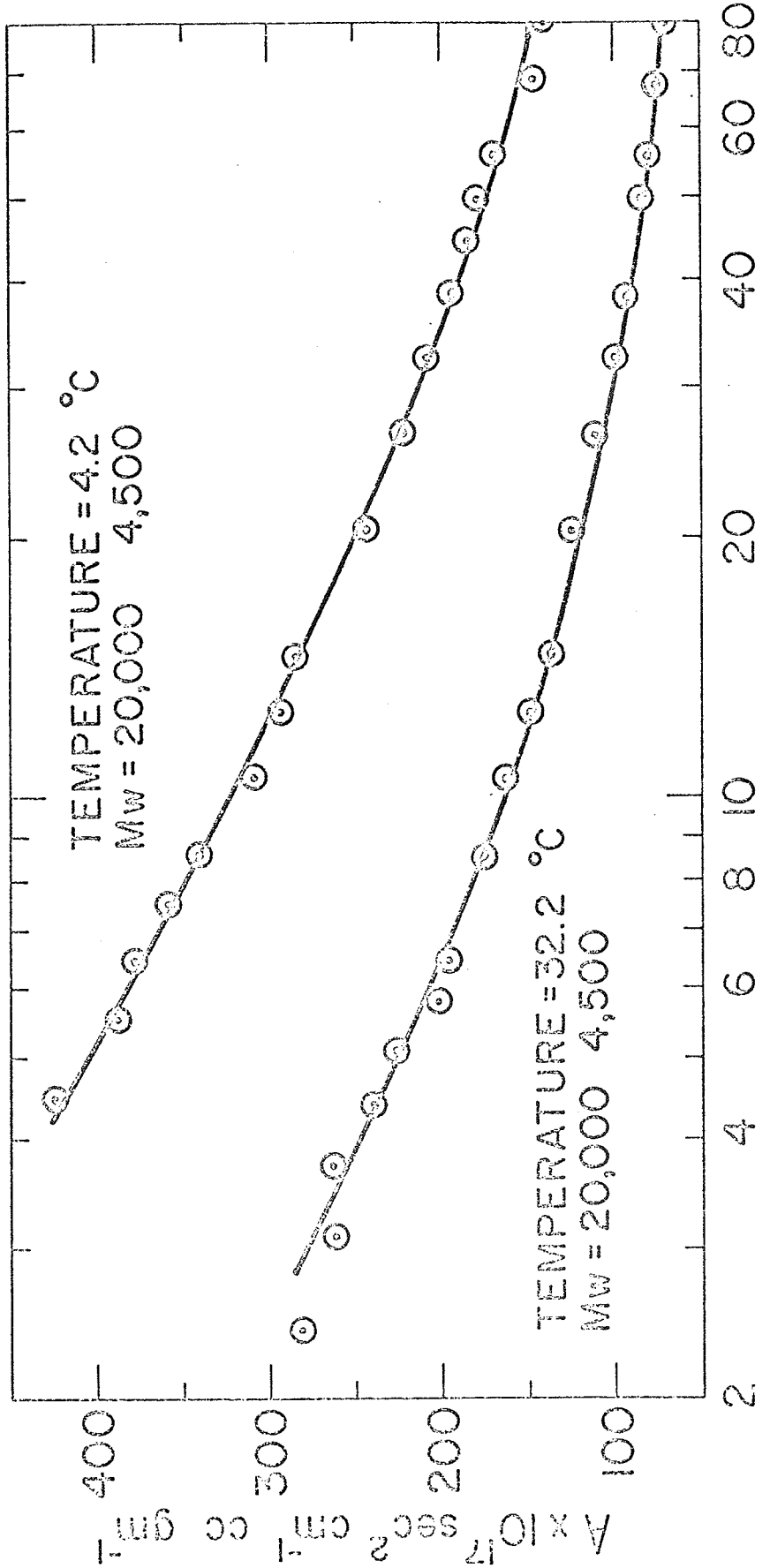

FIGURE 4-20

ULTRASONIC SPECTROGRAM--PEG

the two highest molecular weight fractions at temperatures of 4.2°C and 32.2°C. In order to compare the magnitudes of the absorption coefficients obtained in this study with previously reported investigations for Mw 20,000 and Mw 7,500 (Lewis, 1965; Hammes and Lewis, 1966). A is shown as a function of temperature in Fig. 4-21 at 10.0 MHz. The somewhat low values of A of the previous investigation are within the limits of experimental error since lower concentrations were employed. Arrhenius plots, Fig. 4-22, for a solution of Mw 20,000 and Mw 4,500 at 0.2 gm/cc and at two frequencies results in the activation energies shown in Table 4-4.

TABLE 4-4. APPARENT ACTIVATION ENERGIES FOR AQUEOUS SOLUTIONS OF PEG CONCENTRATION 0.2 gm/cc

Mw	Frequency MHz	ΔF k cal/mole
20,000	10.0	4.25
4,000		
20,000	50.0	4.70
4,000		
water	all	4.23

The velocity of sound was determined as a function of temperature for the PEG solutions using the high frequency pulsed interferometer and Fig. 4-23 shows the velocities for several solutions. With the exception of the monomer, the reduced velocity is independent of molecular weight and concentration. The reduced velocity data are shown in Fig. 4-24.

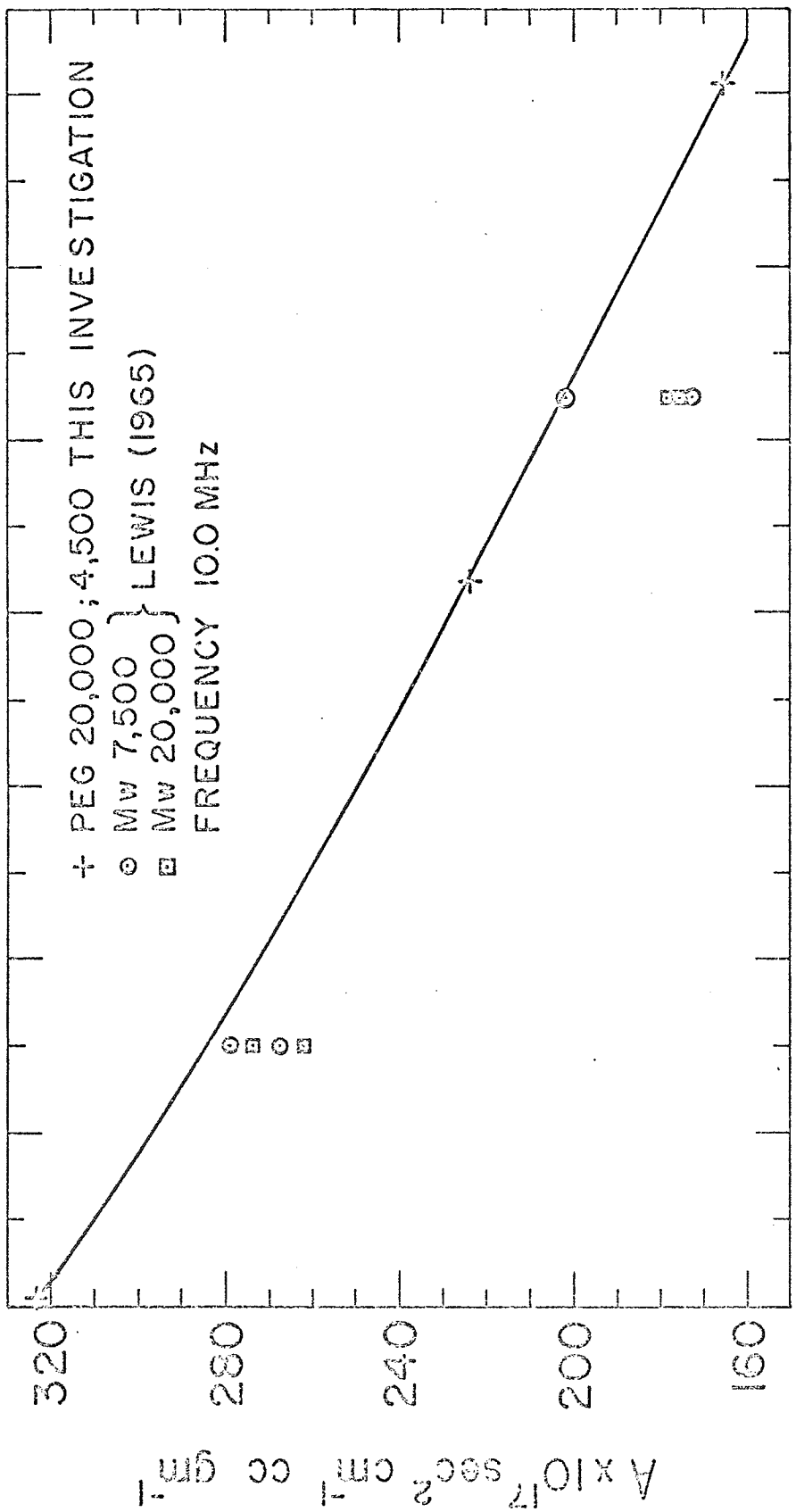

FIGURE 4-21

TEMPERATURE DEPENDENCE OF ABSORPTION--PEG

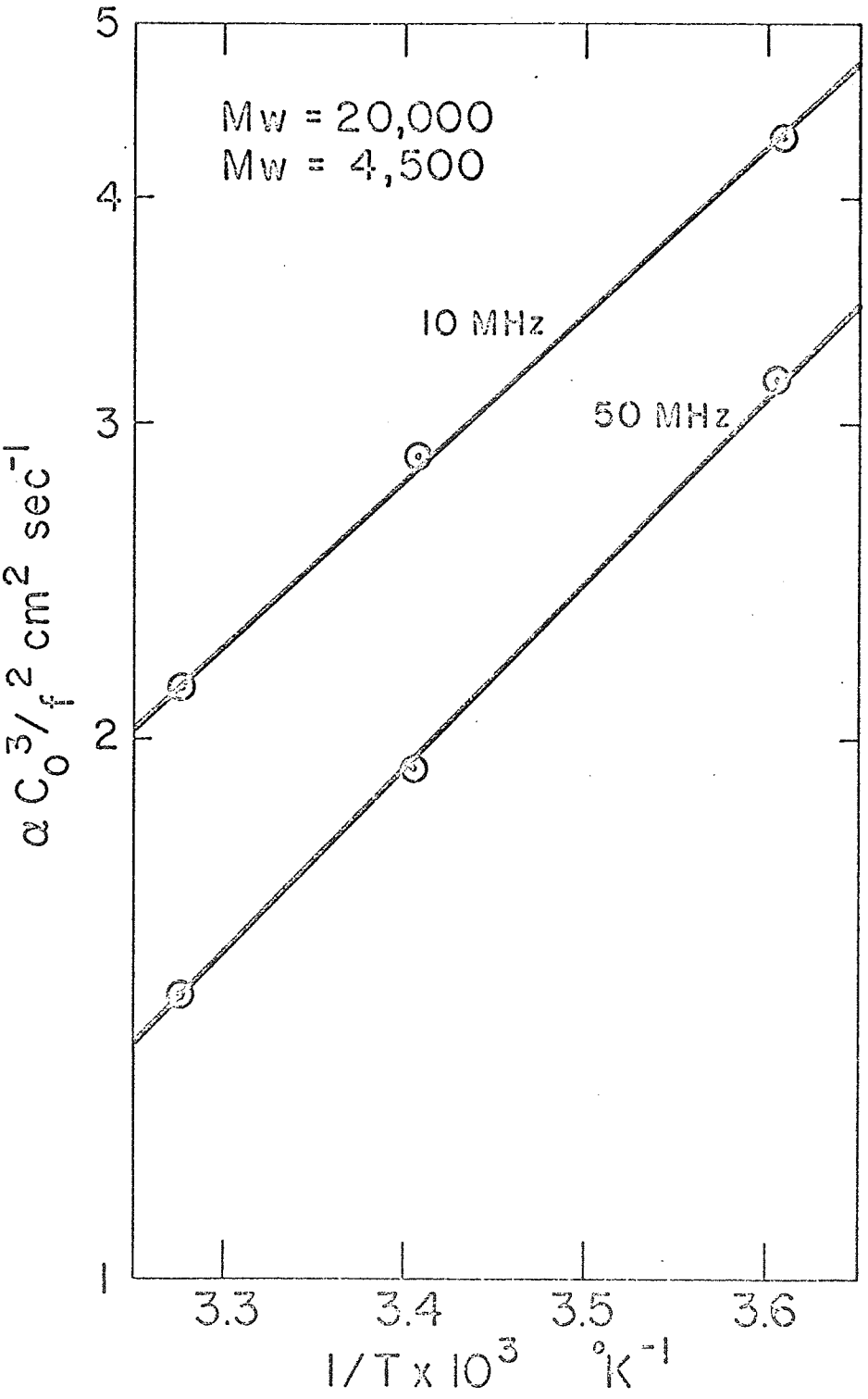

FIGURE 4-22

ARRHENIUS PLOT OF AN AQUEOUS SOLUTION OF PEG (0.20 gm/cc)

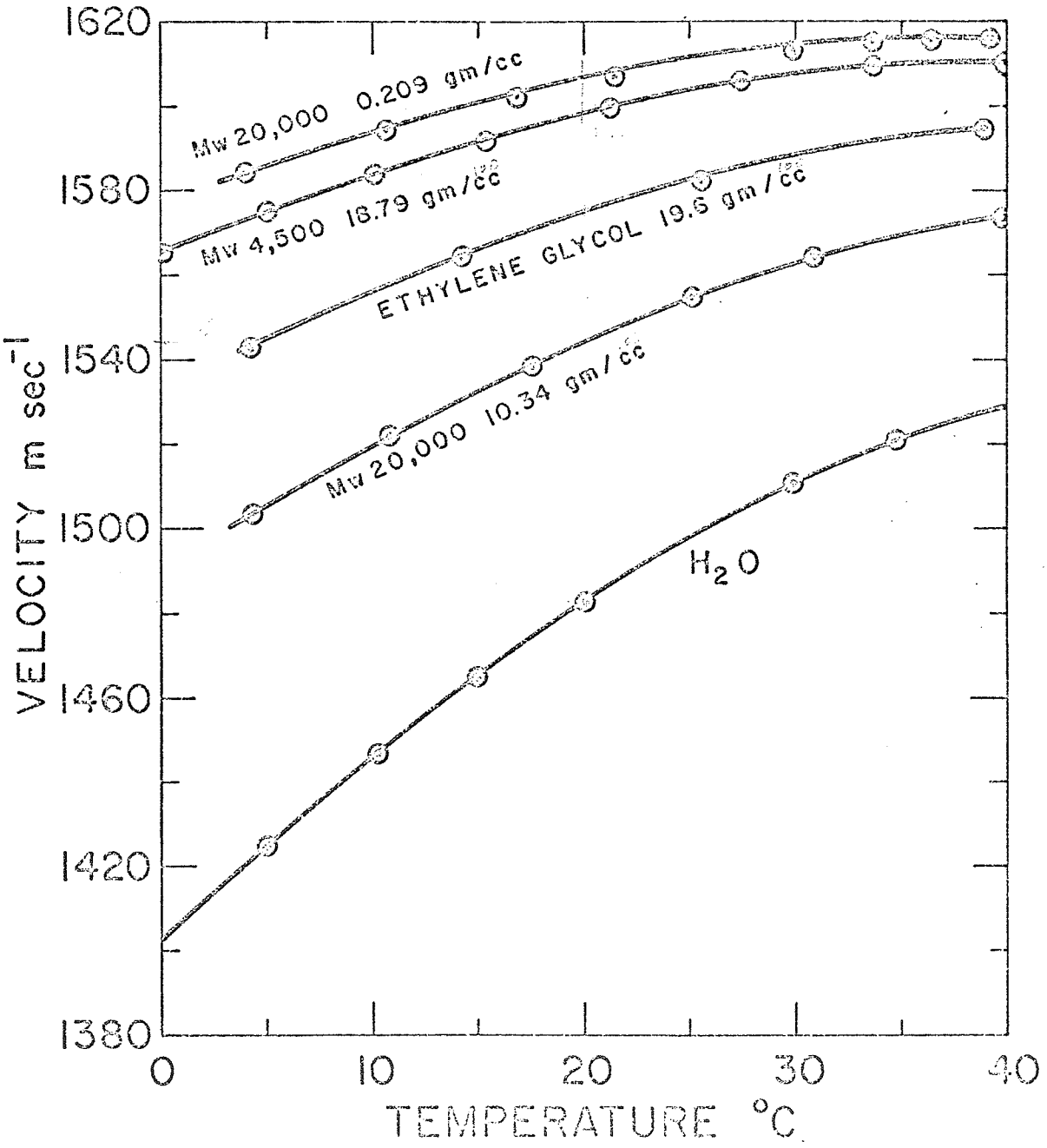

FIGURE 4-23

DEPENDENCE OF VELOCITY ON TEMPERATURE--PEG

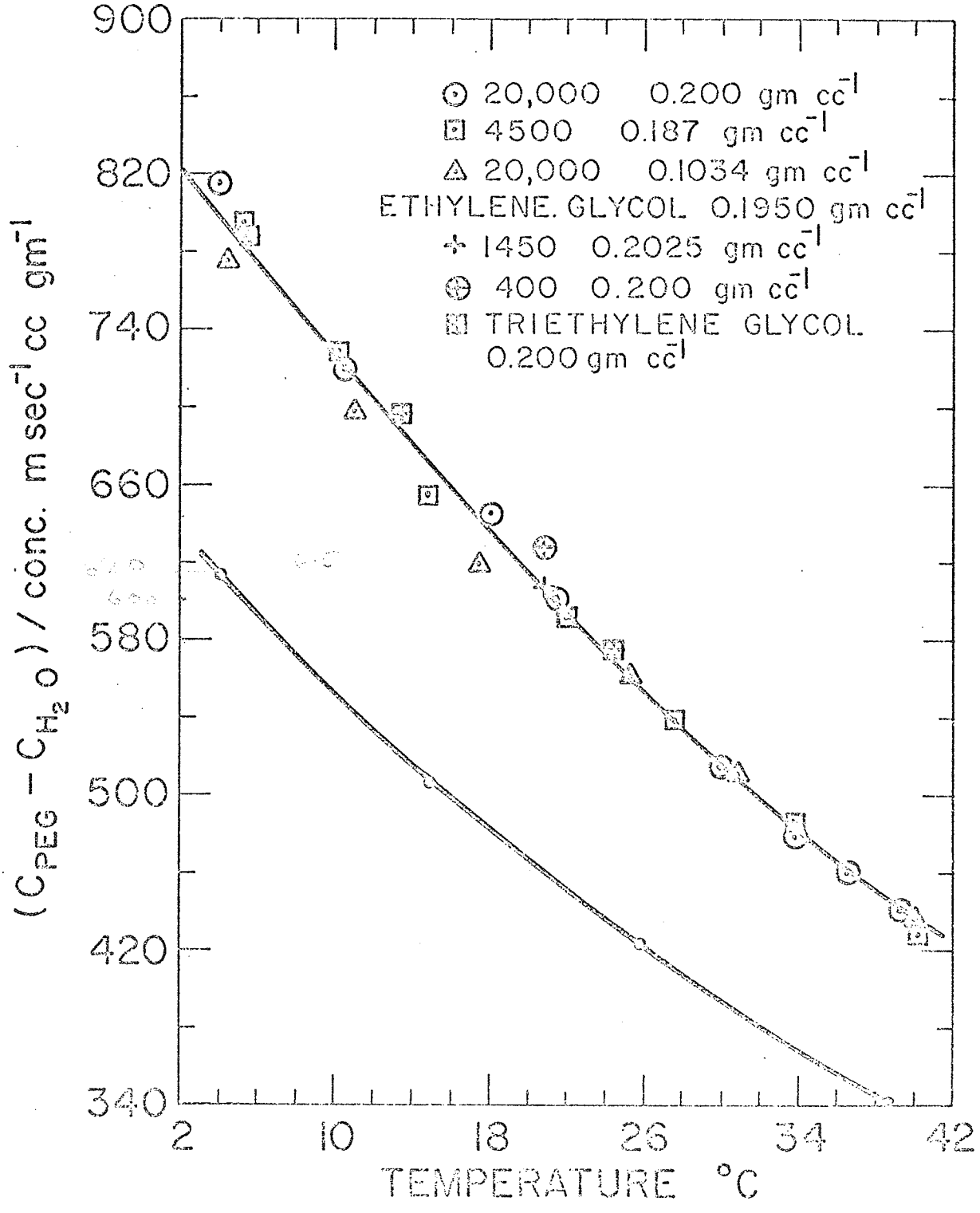

FIGURE 4-24

DEPENDENCE OF REDUCED VELOCITY OF AQUEOUS SOLUTIONS OF PEG ON TEMPERATURE

CHAPTER 5

DISCUSSION

A. Bovine Serum Albumin

The results of this investigation lead to the suggestion that the excess absorption is due to the bulk viscosity associated with either the BSA molecule or the hydration layer surrounding it. The distribution of relaxation times and the velocity dispersion are indicative of structural relaxation (Litovitz and Davis, 1965) and this mechanism has been thought to be responsible for the excess absorption observed in aqueous solutions of other biomacromolecules, viz., hemoglobin (Carstensen and Schwan, 1959b) and dextran (Hawley, 1966; Hawley et al., 1965).

In order to understand the observed changes of the ultrasonic absorption coefficient that occur with changes in pH, a brief resume of the physical-chemical properties of BSA in aqueous solution is presented. It has been generally recognized that serum albumin molecules undergo marked reversible structural changes as the pH of the environment is altered, although the exact nature of these changes remains unclear (Foster, 1960). Within the range $4.3 < pH < 10.5$, the molecule behaves as an undeformable solid particle approximated by a prolate ellipsoid. Outside this range, however, it was originally thought that a simple swelling of the compact globular structure occurred and was responsible for the observed increase in optical rotation (Jingensons, 1952), in viscosity (Yang and Foster, 1954), and other physical parameters. A review article by Foster (1960) contains a complete account of the experimental work up to 1960. The swelling was thought to occur in an all or none fashion until Tanford et al. (1955) discovered a distinct

stepwise change in the intrinsic viscosity as the pH was varied from 4.3 to 3.6 (Fig. 5-1). Specifically, between pH 4.3 and 4.0 [η] increases sharply from 3.7 cc/gm characteristic of the compact form to 4.5 cc/gm, an increase of 22%. No significant change occurs in [η] until about pH 3.5 where a much greater step increase of [η] to 8.3 cc/gm occurs, an increase of 84%. This two step change was observed when the BSA was suspended in 0.15 M KCl and was not observed at low salt concentrations. It should be noted here that the abrupt changes in the ultrasonic absorption coefficient are unaffected by the addition of 0.15 M KCl. Furthermore, in nearly the same pH region as the 22% increase in [η], the ultrasonic absorption coefficient at 2.39 MHz increases by 30% between pH 4.4 and pH 3.8, though at the higher frequencies the increase in A is less. It is interesting that there is no change in A corresponding to the 84% increase in [η] at pH 3.5. This suggests that if the same mechanism is responsible for both the first increase in [η] and the increase in α at pH 4.3, then a separate mechanism which does not involve the ultrasonic properties of the solution is responsible for the larger increase in [η]. Shear viscosity alone has been shown to be too small to account for the observed magnitude of the excess absorption coefficient. Tanford et al. (1955) proposes that the complete expansion of BSA occurs in at least three distinct stages. The first stage is an initial "all or none" structural change from the compact form to an "expandable form." The second stage is the actual expansion of the molecule, and the third stage which is accompanied by a small time varying increase in the viscosity at pH < 4. The last stage, not shown in Fig. 5-1, is attributed to possible slow aggregation of the molecules.

Aggregation has been observed by many investigations in aqueous BSA solutions at acid pH. Favorable conditions for the formation of

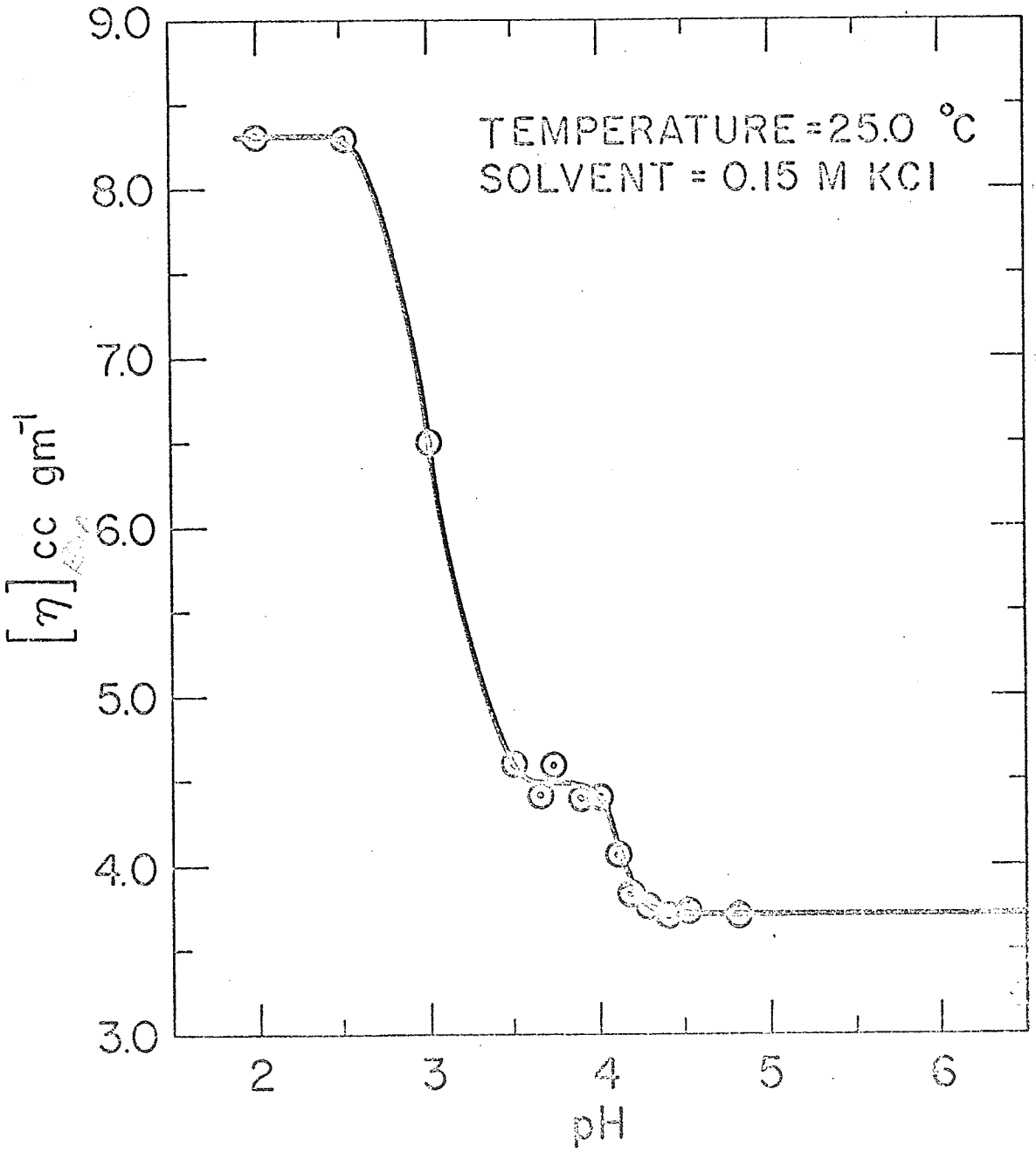

FIGURE 5-1

DEPENDENCE OF INTRINSIC VISCOSITY ON pH (Tanford, 1955)

aggregates are low pH, high concentration of BSA and high salt concentration. According to Williams and Foster (1959) the principle aggregate, that composed of two BSA molecules (dimer), is found to have a maximum concentration at pH 3.3. Below pH 3.0 or above pH 3.5, the rate and extent of dimerization diminishes and these investigators conclude that at low salt concentrations aggregation is not significant, and the turbidity, or cloudiness of the solution that occurs below the isoelectric point which is usually attributed to aggregation, is due, in fact, to the liberation of a lipid impurity that is carried along with the BSA molecule, probably stearic acid. The above evidence precludes the possibility that the abrupt change of the ultrasonic absorption is due to the perturbation of such an intermolecular equilibrium since the effects on the absorption coefficient do not occur at pH 3.3. The possibility exists that the lipid material itself is involved in the absorption process. Even in the purest crystalline fractions of BSA available there is more than one mole of stearic acid liberated per mole of protein at low pH. Techniques are available for completely removing the impurity (Foster, 1960) however, it is claimed that these may produce structural modifications of the molecule (Williams and Foster, 1960). In the present investigation, the fatty acid was released at about pH 4.6 and sometimes at slightly higher pH values, where no corresponding event was detected ultrasonically and therefore the presence of this impurity cannot be correlated with the principal absorption mechanism at this time.

The stepwise expansion process proposed by Tanford and more recent evidence of a two step change in the rotational relaxation time occurring at pH 4.1 and pH 3.6 (Riddiford and Jennings, 1966) lend support to the theory of the conformation changes to BSA proposed by Aoki and Foster

(1957a, 1957b) and Foster (1960) known as the N-F transformation. The N form of the molecule is the compact rigid form which exists at $4.3 < pH < 10.5$ and is thought to be composed of two pairs of globular subunits held together tightly with each member of a pair held to its partner by hydrophobic bonds. That is, a molecule which consists of many polar and many non-polar groups will assume a configuration in a polar solvent such that the number of polar groups of the molecule in contact with the solvent are minimized. The resulting forces which stabilize the intramolecular configuration are known as hydrophobic bonds. The two pairs of subunits are then bonded to one another electrostatically to make up a four unit globule. As the pH is reduced from the isoelectric point of the protein, electrostatic charge on each pair of subunits forces the molecule to separate into two globular subunits linked together by flexible chains. This is the so-called F' state or "intermediate F" form. The F' state formation corresponds to Tanford's "expandable form" and occurs in the same region as the observed ultrasonic effect. As the pH is reduced below 3.6, electrostatic forces overcome the hydrophobic bonds and each globular subunit separates. This state of the molecule which consists of four subunits linked by flexible linkages is known as the F state.

Weber and Young (1964) subjected acidified BSA to short enzymatic digestion and found that the BSA molecule was split into one large and two smaller globular fragments, a total of three instead of four subunits. With this evidence and with the hydrodynamic properties obtained by others, Bloomfield (1966) determined a suitable three subunit model for BSA which consists of a central sphere, of radius 26.6 Å and two flanking spheres of radius 19 Å in contact with the central sphere. The hydrodynamic properties of this model agree well with the experimentally

observed properties at pH 3.6. However, this model does not take into account the first step of the expansion process that occurs at pH 4.1. It is possible, however, that a combination of Bloomfield's model and Foster's could do so. For example, assume that the N state is composed of a single pair of hydrophobically bonded subunits which is electrostatically bonded to a third, larger subunit. Then the F' state and F state would correspond to Foster's model with the exception that the number of subunits is one less and the subunits are not all of equal size. The hydrophobically bonded subunits would then correspond to the flanking spheres of Bloomfield's model.

From Fig. 4-7, it is seen that the reduced velocity exhibits a minimum at pH 4.1. Assuming that the expansion of the molecule occurs simply by separation of the globular units without structural changes to the globular units themselves, as implied by the fragmentation experiments of Weber and Young (1964), it may be considered that the moduli and densities of these units remain constant. It then follows from (2-12) that there must be a net decrease in the volume fraction of molecules in solution, which leads to the conclusion that a reduction of the hydration layer must occur. This is reasoned physically as follows. In the N state, each gram of protein is associated with 0.2 gm of tightly bound hydration. If, when the molecule assumes the intermediate F' state, the hydration layer remains intact, then the internal rotational freedom possessed by the separated globular units (Riddiford and Jennings, 1966; Weber, 1952) would be suppressed and thus not be observed. At pH < 4.1, the velocity increases steadily and is due in part to the increased velocity in the solvent alone, not compensated for by subtracting off just the velocity of water. In a separate experiment, the velocity in water at pH 2.5 with

HCl was found to differ from pure water by less than 0.5 m/sec. The velocity of the solution however increases by 3.3 m/sec between pH 4.05 and pH 3.0. The additional increase in the velocity at low pH may be due in part, to a restructuring of hydration layers about each subunit as they become displaced far from each other and in part, to the increased binding by BSA of the chloride ions (Saroff, 1957) from the HCl.

The change in the ultrasonic absorption coefficient at pH > 10.5 is more difficult to correlate with molecular events than it is for pH < 4.3. Since very little experimental work on the nature of the alkaline expansion has been reported in the literature. Weber (1952) and Tanford et al. (1955) suggest that both the acid and alkaline expansions are similar, however, no experimental evidence has been presented to substantiate this. An abrupt decrease of the rotational relaxation time of BSA was observed by Weber (1952) to occur at pH 3.6 and pH 11.2. It has been observed (Foster, 1960) that at pH 3.6 BSA begins to expand rapidly with decreasing pH, and thus it is reasonable to assume that expansion is rapid with pH changes above 11.2. The ultrasonic titrations at acid pH and alkaline pH are similar in that the absorption coefficient begins to increase above pH 3.6 and below pH 11.2, i.e., before the molecule expands. At pH < 3.6, there is no correspondence of the expansion with the absorption coefficient, however, at pH > 11.2, the absorption coefficient is still increasing sharply. This implies that the mechanisms responsible for the increase in α in both pH regions may be different. Evidence which supports this is the sharp contrast between the titration of velocity at acid and alkaline pH. It is also shown that the changes in the intrinsic viscosity at alkaline pH do not correspond with the changes in the ultrasonic absorption coefficient. Tanford and Buzzel (1956) have measured [n]

up to pH 10.5 and found that no change in $[\eta]$ occurs between pH 9.3 and pH 10.5 whereas α increases over the same pH region by 17%. Further correlation of the ultrasonic absorption increase for pH > 10.5 must await further determination on the nature of the alkaline expansion.

B. Polyethylene Glycol

Hammes and Lewis (1966) investigated the ultrasonic absorption coefficient in aqueous solutions of PEG over the frequency range from about 10 MHz to 200 MHz for the two molecular weight fractions 20,000 and 7,500 and reported that their data was best described by a single relaxation mechanism. Previously, it has been shown that dextran, which is a molecule that also assumes a random coiling configuration in aqueous solution, was characterized by a wide distribution of relaxation times (Kessler, 1966; Hawley, 1966). In addition, the theoretical considerations of Zimm et al. (see Chapter 2) predict a distribution of relaxation times for long chain flexible polymers in solution. A single relaxation mechanism can be described by (2-15) or more simply by

$$\alpha/f^2 = \frac{A}{1 + (f/f_o)^2} + B \tag{5-1}$$

where A and B are constants, and f_o is the characteristic relaxation frequency. In order to determine how well (5-1) describes the present data, a least squares procedure developed by Andreae et al. (1965), was used to select, by trial and error, the optimum values for A, B, and f_o. The result, shown in Fig. 5-2, indicates clearly that a process more complex than a single relaxation process is occurring, in contrast to the previously reported result. However, in order to verify that above 10 MHz, a single relaxation does provide a good description of the data as

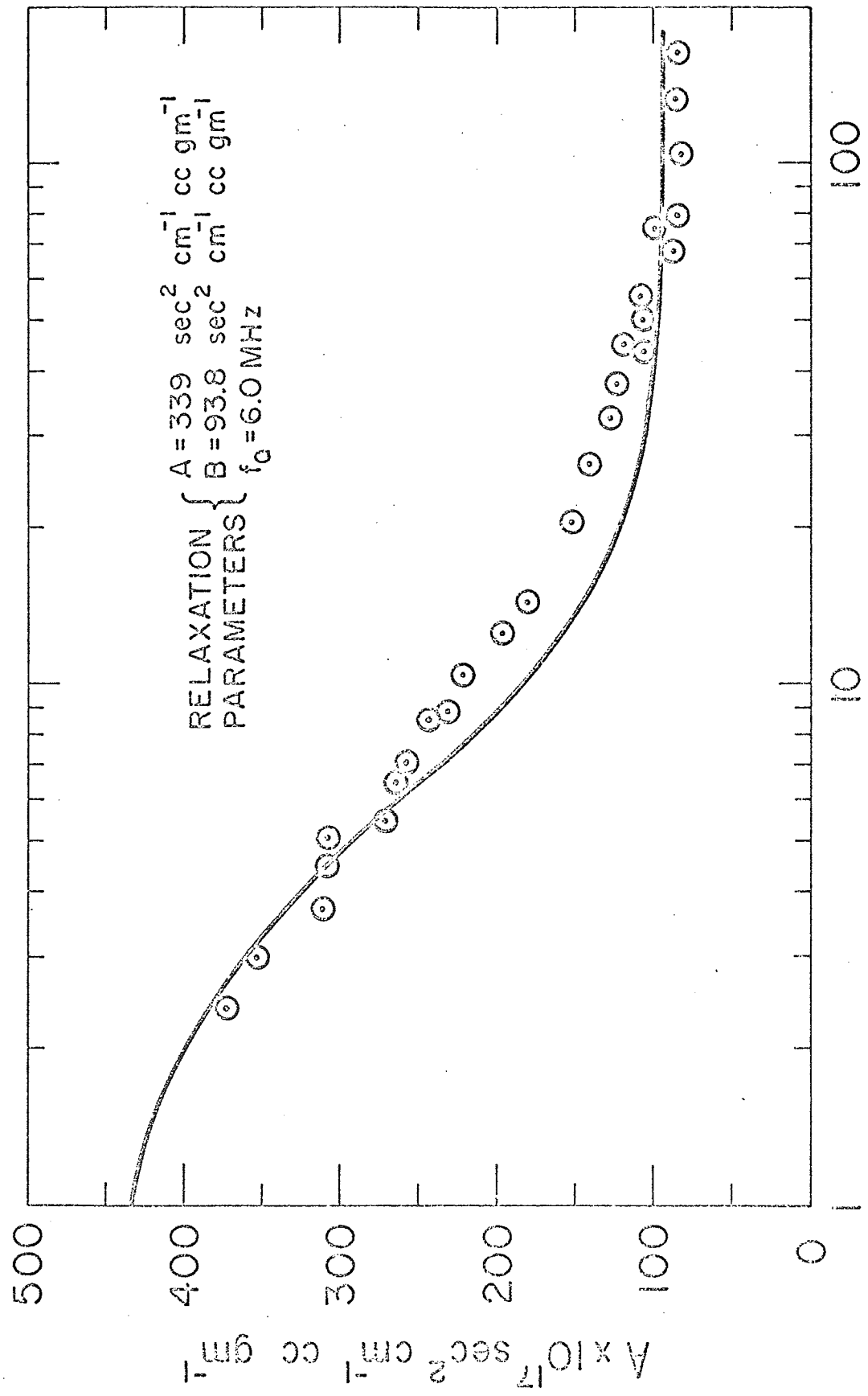

FIGURE 5-2

BEST FIT SINGLE RELAXATION CURVE (PEG, Mw 20,000 and 4,500)

stated by Lewis, the values of A between 10 MHz and 163 MHz only were used. The best fit single relaxation curve for the above conditions is shown in Fig. 5-3 from which it is clear that if the data below 10 MHz are ignored, a misleading conclusion regarding the relaxation nature of the process is easily drawn. Further evidence of the relaxation process extending below 10 MHz would be the presence of velocity dispersion in this frequency region. However several attempts to establish its presence resulted in only a statistical answer in the affirmative. Between 1 MHz and 10 MHz, five trials on separate occasions resulted in dispersions ranging from 0 to 0.5 m/sec and all of the correct sign.

In Chapter 4, it was shown that both the absorption coefficient and the velocity of sound varied linearly with concentration to at least 0.21 gm/cc. This indicates that interactions that may occur between polymer molecules in the concentrated solutions employed in this study are not important in determining the observed relaxation process; for if these interactions were important, a significant departure from linear dependence on concentration should result.

Referring to Fig. 4-19 several points can be made regarding the dynamic shear viscosity contributions to the absorption coefficient. The theory associated with dynamic shear viscosity of random coiled polymers in solution predicts a distribution of relaxation times corresponding to different modes of coordinated motion of the polymer chain (see Chapter 2). Fig. 4-19 shows that the relaxation times for Mw 20,000 and Mw 4,500 cannot be distinguished in the present frequency range, however the relaxation time for Mw 1,450 is definitely shorter in accordance with the theory. A conclusion reached by Lewis (1965) that the relaxation times predicted by the Zimm theory were more than an order of magnitude greater than the

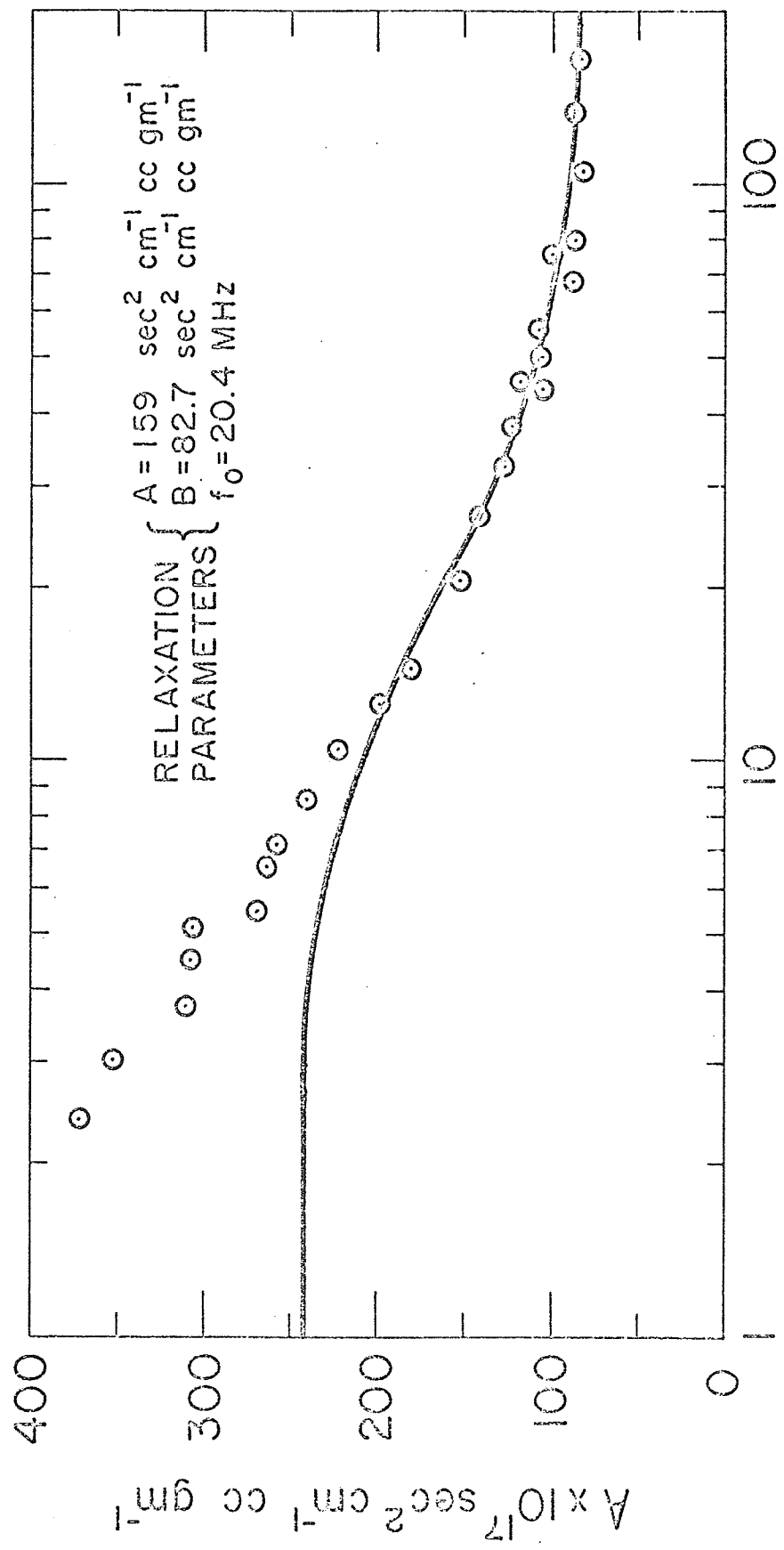

FIGURE 5-3

BEST FIT SINGLE RELAXATION CURVE ABOVE 10 MHz (PEG, Mw 20,000 and 4,500)

the observed values must be re-examined for the following two reasons. First, as seen in Fig. 5-2, using the best fit single relaxation curve, the present data in dicate f_o = 6.0 MHz whereas using only the data above 10 MHz as Lewis did, Fig. 5-3 shows f_o = 20.4 MHz, thus an apparent discrepancy of a factor of approximately 3. Second, in an apparent misunderstanding of (2-25), the solution viscosity was used in his calculations in place of the solvent viscosity and resulted in a theoretical relaxation time which was too large by the ratio η/η_s.

The dynamic shear viscosity contribution to the absorption coefficient is discussed below. For this analysis, the Bloomfield-Zimm theory, being the more general, is employed. PEG molecules are assumed to be extended, non-free draining, flexible polymers consisting of N + 1 beads. Each structural unit is assumed to be the monomer unit, although larger segments could also have been used (Tanford, 1961). Assuming no restrictions on bond rotations, a theoretical segment length b_o, was calculated from the individual bond lengths for single carbon-oxygen and carbon-carbon bonds and found to be 4.4 Å. The intrinsic viscosity was reported in aqueous solutions of PEG at 20.0° C by Sadron and Rempp (1958) and found to be related to the molecular weight by the following relationship

$$[\eta]_{observed} = 2.0 + 0.033\ Mw^{0.72} \tag{5-2}$$

The effective segment length, b_{eff}, is calculated from the ratio of the intrinsic viscosity, predicted on the basis of b_o for non-free draining coils, to the observed viscosity and b_{eff}. From (2-26)

$$\frac{[\eta]_o \text{ theoretical}}{[\eta]_o \text{ observed}} = \left(\frac{b_o}{b_{eff}}\right)^3 \tag{5-3}$$

In order to evaluate the expansion parameter ε, (2-27) is used. Table 5-1 contains the parameters to be used in the Bloomfield-Zimm theory and the values of λ_K' are listed in Table 2-1.

TABLE 5-1. PROPERTIES OF PEG POLYMER CHAINS

Mw	N	cc/gm $[\eta]_{SADRON}$	cc/gm $[\eta]_{theoretical}$	A° b_{eff}	ε	sec $\tau_K \times 10^{10}$
20,000	455	43.2	11.73	6.78	0.14	$8944./\lambda_K'$
4,500	102	15.1	5.48	6.29	0.15	$642.2/\lambda_K'$
1,450	33	8.38	3.16	6.07	0.184	$143.9/\lambda_K'$
400	9	4.46	1.63	6.16	0.306	$33.3/\lambda_K'$

In Table 5-2, the first four relaxation times are listed for each molecular weight and the contribution to the absorption coefficient is evaluated from the following equation

$$A_s = \frac{\Delta\alpha_s}{cf^2} = \frac{8\pi^2}{3\rho_o c_o^3}\left[\frac{\eta - \eta_s}{c}\right] \tag{5-4}$$

which reduces to

$$A_s = \frac{1}{M} \times 15.65 \times 10^{-5} \sum_{K=1}^{u} \frac{\tau_K}{1 + \omega^2 \tau_K^2} \tag{5-5}$$

The shear viscoelastic contribution to the absorption coefficient is shown in Fig. 5-4.

If the dynamic shear viscosity alone was responsible for the excess observed absorption, then according to Fig. 5-4 a definite measurable difference in the absorption coefficient should be detected between Mw 20,000 and Mw 4,500 within the frequency range covered by this investigation. However, since it was found experimentally that no such distinction

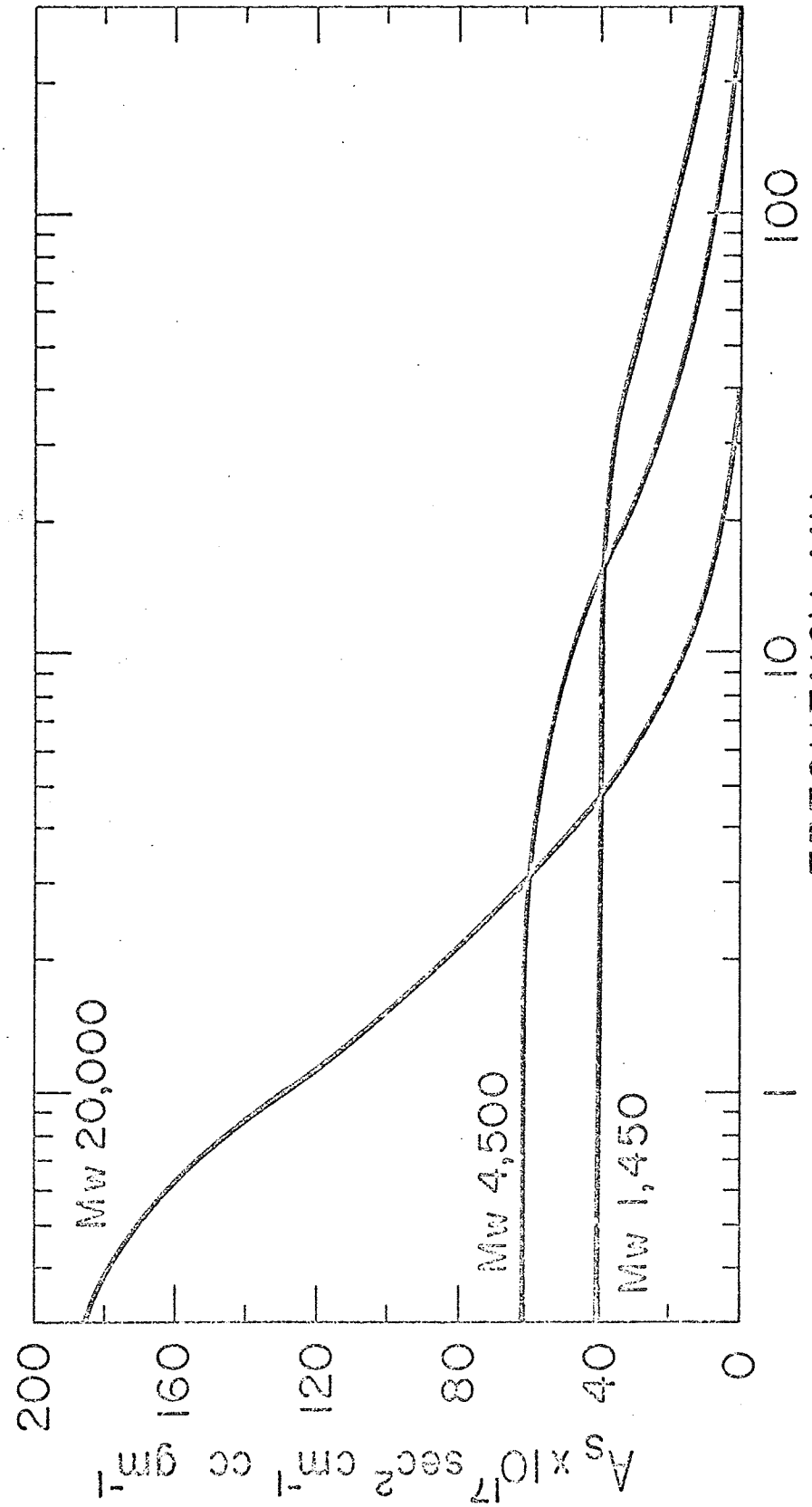

FIGURE 5-4

ABSORPTION DUE TO SHEAR VISCOSITY (ZIMM, BLOOMFIELD THEORY)

FIGURE 5-4

ABSORPTION DUE TO SHEAR VISCOSITY (ZIMM, BLOOMFIELD THEORY)

TABLE 5-2. RELAXATION TIMES FOR FIRST FOUR MODES OF VISCOELASTIC RELAXATION FOR NON-FREE DRAINING POLYMER CHAINS CALCULATED FROM THE BLOOMFIELD-ZIMM THEORY FOR EXTENDED POLYMERS

Mw	τ_1 sec	τ_2 sec	τ_3 sec	τ_4 sec
20,000	16.0×10^{-8}	4.92×10^{-8}	2.54×10^{-8}	1.59×10^{-8}
4,500	11.27×10^{-9}	3.44×10^{-9}	1.77×10^{-9}	1.11×10^{-9}
1,450	23.5×10^{-10}	7.14×10^{-10}	3.65×10^{-10}	2.28×10^{-10}
400	42.0×10^{-11}	12.4×10^{-11}	6.29×10^{-11}	3.8×10^{-11}

exists, shear processes may play only a minor role in determining the observed absorption. In addition, the shear viscosity theory predicts that A approaches zero at high frequencies. However, it was found to assymptotically approach a value of 87×10^{-17} cm^{-1} sec^2 cc gm^{-1}. This can be explained in terms of either a volume viscosity which is associated with the finite time required for the volume of the molecule to change in response to a uniform compressional stress or an internal viscosity which is associated with a time lag of orientation of one polymer segment with respect to another in response to a periodic shear stress. The internal viscosity of a polymer chain was shown by Peterlin (1967), to cause a non-vanishing viscosity and therefore non-vanishing absorption parameter A at infinitely high frequencies and cause very little effect at frequencies below that of the primary mode relaxation. On the other hand, a volume viscosity would be expected to add to the absorption coefficient at low frequencies as shown in (2-8).

Table 5-3 lists the classical values of α/f^2 for aqueous solutions of various molecular weight fractions of PEG of concentration 0.2 gm/cc and compares them to limiting values of observed α/f^2 at $f = 0$. The values of

α/f^2 in Table 5-3 represent the total absorption per frequency squared and the values of A were computed for direct comparison on the coordinate axis of Fig. 4-19. The viscosity of each molecular weight and concentration was obtained from a Dow Chemical Company publication (1962).

TABLE 5-3. CLASSICAL ABSORPTION COEFFICIENTS IN AQUEOUS SOLUTIONS OF PEG AT 20.7°C

Mw	Concentration gm/cc	Classical $\alpha/f^2 \times 10^{17}$	H_2O $\alpha/f^2 \times 10^{17}$	Classical* A $\times 10^{17}$
20,000	0.2	335.	24.8	1,550
4,500	0.2	63.2	24.8	192
1,450	0.2	25.3	24.8	2.45

$$*A_{classical} = \frac{[(\alpha/f^2)_{classical} - (\alpha/f^2)_{H_2O}]}{concentration}$$

Comparison of the classical absorption values with Fig. 4-19 shows that volume viscosity contribution is important since observed values of A are larger than classical at the low frequencies. Since the volume viscosity and internal viscosity cannot be separated, it is not possible to predict exactly the magnitude of a volume viscosity process as a function of frequency although it can be described by a distribution of relaxation times. Since thermal relaxation and dynamic shear viscosity have been ruled out as the important absorption mechanism, the remaining volume viscosity mechanism seems most likely. There are two lines of reasoning that can be pursued in this case. First, that η_V is due to a change in the conformation of the polymer itself, and second, that η_V is due to interaction between polymer and solvent. The latter has been proposed as the mechanism of excess absorption for PEG by Lewis (1965)

and for dextran by Hawley and Dunn (1968). With regard to the first suggestion, if the structural change in the molecular configuration is a simple rotational isomerism, then a single relaxation depicts the process (Lamb, 1965) and must therefore be ruled out. PEG is known not to exist in the helical form in aqueous solution so that a random coil to helix coil transition is not possible. However, it has been found that PEG can take on more than one configuration (Curme, 1952). The lower molecular weight polymers exist in the zig zag configuration, i.e.,

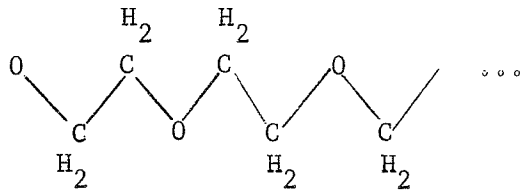

whereas the higher polymers take on the meandering form.

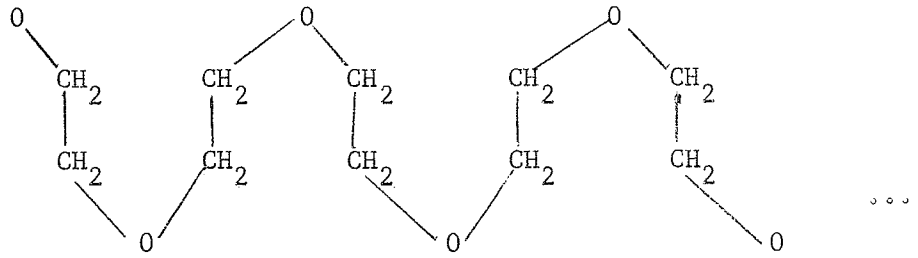

Unfortunately the terms "lower" and "higher polymers" are not specific and further investigation could not reveal more definitive description. However, it is probable that since the highest molecular weight PEG available is 20,000, this molecule assumes the meandering form. Furthermore, it is possible that both forms represent stable configurations which differ in energy levels and that the ultrasonic wave can perturb an equilibrium distribution between the two configurations. It would be expected that at some intermediate molecular weight the polymer chain would consist of

segments of both configurations in a state of equilibrium and that above some "threshold" polymer length all the polymers would exist in only one form. In this case, in the absence of other relaxation phenomena, the amplitude of the ultrasonic absorption coefficient would depend only on the number of relaxing units present and not on the molecular weight of the polymer. In Fig. 5-5, the frequency free absorption parameter A is plotted as a function of molecular weight. The curve is similar to that obtained by Hawley and Dunn (1968) for dextran with the exception that for aqueous dextran solutions at high frequencies the absorption coefficient approaches that of the monomer whereas at 163 MHz, the absorption coefficient in aqueous solutions of PEG has approached a limiting value. Additional relaxation mechanisms occurring in a higher frequency range are not ruled out and may correspond to the internal viscosity of the chain segments. According to Lewis (1965) the primary process being observed is most likely an interaction between the sound wave and the polymer solvent equilibrium. As the sound pressure varies the equilibrium distribution of the water molecules surrounding the polymer is shifted. Evidence presented in this study supports both the possibility of structural relaxation of the polymer molecule occurring and the possibility of solute-solvent interactions occurring which gives rise to the excess ultrasonic absorption.

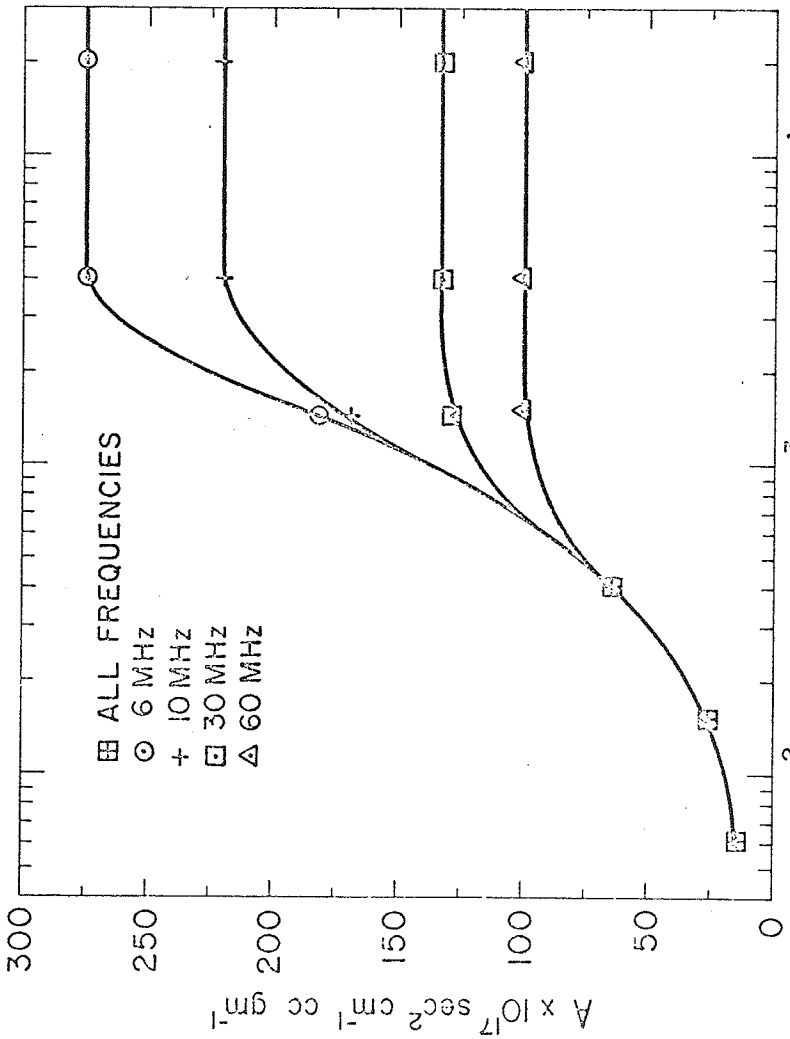

FIGURE 5-5

DEPENDENCE OF ABSORPTION ON MOLECULAR WEIGHT AT FES

CHAPTER 6

CONCLUSIONS

A. Bovine Serum Albumin

1) The ultrasonic absorption coefficient has been measured in aqueous solutions of BSA at concentrations approximately 0.05 gm/cc and 0.09 gm/cc at 20°C over a frequency range from 0.3 MHz to 163 MHz and indicates that a distribution of relaxation processes occurs in this region.

2) Velocity dispersion that is observed in the frequency range between 1 MHz and 13.4 MHz further indicates the occurrence of relaxation processes.

3) Only a small fraction of the observed ultrasonic absorption can be attributed to shear viscosity and relative motion between solvent and solute molecules. The excess absorption is attributed to the pertubation of the equilibrium distribution of solvent and solute molecules by the sound wave.

4) It is also shown that the effect on the absorption coefficient of the presence of salt in aqueous solutions of BSA at pH 7 is entirely due to the effect of the salt on the solvent.

5) The ultrasonic absorption coefficient abruptly increases over its value at neutral pH outside the range $4.3 < pH < 10.5$ and is reversible over the entire pH range investigated, i.e., $2.3 < pH < 11.8$.

6) The abrupt increase in the ultrasonic absorption coefficient at $pH < 4.3$ is associated with the pertubation by the sound wave of the hydration layer which undergoes structural alteration due to the N-F' transformation (Foster, 1960). There is no obvious correlation between the increase in intrinsic viscosity and that of the absorption coefficient.

7) At alkaline pH the increase in the ultrasonic absorption coefficient is shown not to correlate with changes in the intrinsic viscosity to pH 10.5, however, the nature of the structural change which the BSA molecule undergoes in an alkaline environment has not been characterized and further correlation is not possible at present.

8) Comparison with the observations of Weber (1952) shows that the increase in the ultrasonic absorption coefficient at pH ~ 4.3 is complete before the major portion of the molecular expansion occurs at pH < 3.6. However, the increase in the ultrasonic absorption coefficient at pH > 10.5 is not complete in the region of molecular expansion at pH > 11.2.

9) The increase in the absorption coefficient is more pronounced at the alkaline pH than at acid pH and in both titrations the effect is enhanced at the lower frequencies.

10) Much experimental work of a physical-chemical nature must be performed on the characterization of the alkaline expansion of the BSA molecule in order to correlate configurational changes with the observed ultrasonic absorption coefficient. In addition, other globular proteins which undergo configurational changes with changes of pH should be examined acoustically for comparison to BSA. Another suggestion is that the shear properties of BSA be investigated at ultrasonic frequencies as a function of pH to more adequately determine the volume viscosity contribution to the ultrasonic absorption coefficient.

B. Polyethylene Glycol

1) The ultrasonic absorption coefficient has been measured in aqueous solutions of polyethylene glycol of concentrations to 0.21 gm/cc over a frequency range from 0.3 MHz to 163 MHz. The absorption coefficient is

independent of molecular weights greater than about 4,500 over the frequency range investigated.

2) The absorption coefficient and velocity of sound vary linearly with concentration up to 0.21 gm/cc.

3) The absorption data are described by a distribution of relaxation processes for molecular weights 20,000, 4,500 and 1,450 and the excess absorption is not fully accounted for by the dynamic shear viscosity of the solution.

4) The excess absorption is attributed to a volume viscosity which can result from several possible mechanisms, for example, a structural relaxation of the polymer configuration or an interaction between solute and solvent molecules.

5) The absorption coefficient dependence on molecular weight of polyethylene glycol is similar to that of another random coil polymer, i.e., dextran, except that the parameter A for PEG does not approach zero. This could be due to an internal viscosity of the PEG molecule.

6) If the shear properties of aqueous solutions of PEG could be determined experimentally, the applicability of the dynamic shear viscosity theory can be verified, and the contributions to the observed absorption due to volume and local viscosities could be evaluated. In order to determine whether or not structural relaxation is occurring, more definite information must be obtained on the characteristics of the meandering form, and the free energy difference between this form and the zig zag form.

CHAPTER 7

SUMMARY

In order to investigate further the principle mechanisms responsible for the excess ultrasonic absorption observed in biological media, the absorption coefficient was measured in aqueous solutions of macromolecules that assume different spatial configurations. Bovine serum albumin, a globular protein which undergoes marked configurational change as a function of pH was investigated in aqueous solution over a frequency range from 0.3 MHz to 163 MHz and a pH range from 2.3 to 11.8. As the pH is varied outside the limits $4.3 < pH < 10.5$, the magnitude of the absorption coefficient increases sharply, and this effect is greater at the lower frequencies than at the higher frequencies. The absorption coefficient is reversible over the entire pH range covered. The increase in the ultrasonic absorption observed below pH 4.3 corresponds to the intermediate N-F' transition proposed by Foster (1960) and the change above pH 10.5 appears to correspond to the actual expansion of the molecule. The ultrasonic spectrogram is best described by a distribution of relaxation times and the magnitude of the absorption coefficient is attributed to pertubations of the solute-solvent equilibrium by the sound wave. The structural changes which occur to the serum albumin molecule are thought to enhance the interaction between the sound wave and the solute-solvent complex.

The ultrasonic absorption coefficient was also measured in aqueous solutions of polyethylene glycol (PEG) a flexible chain macromolecule which assumes a random coil configuration in aqueous solution. The ultrasonic absorption coefficients for this macromolecule as a function of molecular weight and frequency are compared to the data of another

macromolecule which assumes a similar spatial configuration in solution. The molecular weight range investigated was from highly polymerized, 20,000 to the monomer, 62. The absorption is linearly dependent on concentration to 0.21 gm/cc and it is observed that above molecular weight 4,500, the absorption coefficient is independent of molecular weight over the frequency range from 2.4 MHz to 163 MHz. Reconsideration is given to a conclusion by Hammes and Lewis (1966) that the dynamic shear viscosity predicted by Zimm (1956) is not responsible for the observed absorption in aqueous solutions of PEG. The basis for this conclusion was their observation of a single relaxation time which occurred more than an order of magnitude lower than that predicted by theory. The present study extends the frequency range of the previous investigation below 10 MHz and it is observed that the absorption data is best described by a distribution of relaxation times. In addition, an apparent error in their calculation of the theoretical relaxation time (Lewis, 1965) no longer precludes the importance of dynamic shear viscosity. The present investigation indicates that although the theory now predicts relaxation times of the correct order of magnitude, the excess absorption coefficient is still not attributed to the dynamic shear viscosity but rather to the pertubation of the solute-solvent equilibrium by the sound wave or a structural relaxation of the PEG molecule.

A comparison technique first described by Carstensen (1954) was employed in the design of an automated instrument for absorption and velocity measurements below about 10 MHz. This instrument was used along with a high frequency instrument (Hawley, 1966) to cover the total frequency range from 0.3 MHz to 163 MHz. A major improvement

in the pulsed interferometer technique (Hawley, 1966) has resulted in an automatic instrument which, at present, is capable of comparative velocity measurements to ± 0.5 m/sec and absolute measurements to ± 1 m/sec.

REFERENCES

Allis, J. W., and Ferry, J. D., (1965), J. Am. Chem. Soc., 87, 4681.

Andregg, J. W., Beeman, W. W., Shulman, S., and Kaesberg, P., (1955), J. Am. Chem. Soc., 77, 2927.

Andreae, J. H., Edmonds, P. D., and McKellar, J. F., (1955), Acustica, 15, 74.

Aoki, K., and Foster, J. F., (1957a), J. Am. Chem. Soc., 79, 3385.

Aoki, K., and Foster, J. F., (1957b), J. Am. Chem. Soc., 79, 3393.

Barthel, Romard, (1954), J. Acoust. Soc. Amer., 26, 227.

Bergmann, L., (1949), "Ultrasonics and their Scientific and Technical Applications," Bureau of Ships Navy Department, Washington, D.C., Navyships 900, p. 167.

Bloomfield, V., (1966), Biochem., 5, 684.

Bloomfield, V., and Zimm, B. H., (1966), J. Chem. Phys., 44, 315.

Carstensen, E. L., Li, K., and Schwan, H. P., (1953), J. Acoust. Soc. Amer., 25, 286.

Carstensen, E. L., (1954), J. Acoust. Soc. Amer., 26, 858.

Carstensen, E. L., and Schwan, H. P., (1959a), J. Acoust. Soc. Amer., 31, 185.

Carstensen, E. L., and Schwan, H. P., (1959b), J. Acoust. Soc. Amer., 31, 305.

Cerf, R., (1952), Compt. Rend. Acad. Sci., Paris, 234, 1549.

Cohn, E. J., Hughes, W. L., and Weare, J. H., (1947), J. Amer. Chem. Soc., 69, 1753.

Curme, G. O., (1952), "Glycols," Reinholt Publishing Co., New York.

Del Grosso, V. A., (1964), NRL Report No. 6026.

Del Grosso, V. A., (1965), NRL Report No. 6133.

Dow Chemical Company, (1962), "Polyethylene Glycols," Midland, Michigan.

Dunn, F., (1957), J. Acoust. Soc. Amer., 29, 395.

Dunn, F., (1958), Am. J. Phys. Med., 37, 148.

Einstein, A., (1920), Sitzber. Preus. Acad. Wiss. Phys., Kl, 380.

Epstein, P. S., (1941), "Theordore von Karman Anniversary Volume," Calif. Inst. Tech., Pasadena, Calif., 162.

Eyring, H., (1936), J. Chem. Phys., 4, 263.

Foster, J. F., (1960), "Plasma Proteins," ed. by F. W. Putnam, Academic Press, New York 1960, Chap. 6.

Foster, J. F., and Yang, J. T., (1955), J. Am. Chem. Soc., 77, 3895.

Fox, F., and Wallace, W., (1954), J. Acoust. Soc. Amer., 26, 994.

Frank, H. S., and Wen, W. Y., (1957), Disc. Faraday Soc., 24, 133.

Fry, W. J., (1952), J. Acoust. Soc. Amer., 24, 412.

Greenspan, M., and Tschiegg, C. E., (1962), "Underwater Acoustics," Plenum Press, Inc., New York, Chap. 5.

Greenspan, M., and Tschiegg, C. E., (1959), J. Acoust. Soc. Amer., 31, 75.

Hall, L., (1948), Phys. Rev., 73, 775.

Hammes, G. G., and Lewis, T. B., (1966), J. Phys. Chem., 70, 1610.

Hawley, S. A., (1966), Ph.D. Thesis, Univ. of Illinois, Urbana, Illinois.

Hawley, S. A., and Dunn, F., (1968), to be published.

Hawley, S. A., Kessler, L. W., and Dunn, F., (1965), J. Acoust. Soc. Am., 38, 521.

Herzfeld, K. F., and Litovitz, T. A., (1959), "Absorption and Dispersion of Ultrasonic Waves," Academic Press, New York.

Hirai, N., and Eyring, H., (1958), J. Appl. Phys., 29, 810.

Jeffery, G., (1922), Proc. Roy. Soc. Lon., A102, 161.

Jingensons, B., (1952), Arch. Biochem. Biophysics, 39, 261.

Kessler, L. W., (1966), M.S. Thesis, Univ. of Ill., Urbana, Illinois.

Kinsler, L. E., and Frey, A. J., (1950), "Fundamentals of Acoustics," Wiley, New York, p. 111.

Kinsler, L. E., and Frey, A. J., (1962), "Fundamentals of Acoustics," Wiley, New York.

Kirchhoff, G., (1868), Pogg. Ann. Phys., 134, 177.

Lamb, H., (1945), "Hydrodynamics," 6th ed., Dover, New York.

Lamb, J., (1965), in "Physical Acoustics," Vol. II, Part A, Chapter 4, ed. by W. P. Mason, Academic Press, New York, 1965, p. 203.

Lewis, T. B., (1965), Ph.D. Thesis, M.I.T., Cambridge, Mass.

Litovitz, T. A., (1963), in "Dispersion and Absorption of Sound by Molecular Processes," Proceedings of the International School of Physics, "Enrico Fermi," ed. by D. Sette, Academic Press, New York, 1963, pp. 133-174.

Litovitz, T. A., and Davis, C. M., (1965), in "Physical Acoustics," Vol. II, Part A, Chap. 5, ed. by W. D. Mason, Academic Press, New York 1965, p. 282.

Medeod, R. M., and Dunn, F., (1966), J. Acoust. Soc. Amer., 40, 1202.

Markham, J. J., Beyer, R. T., Lindsay, R. B., (1951), Revs. Mod. Phys., 23, 353.

Nemethy, G., and Scheraga, H. A., (1962a), J. Chem. Phys., 36, 3382.

Nemethy, G., and Scheraga, H. A., (1962b), J. Chem. Phys., 36, 3401.

Nemethy, G., and Scheraga, H. A., (1962c), J. Chem. Phys., 66, 1773.

Pellam, J. R., and Galt, J. K., (1946), J. Chem. Phys., 14, 608.

Perrin, F., (1934), J. Phys. Badium, 5, 497.

Peterlin, A., (1938), Z Physik, 111, 232.

Peterlin, A., (1967), J. Polymer Science A2, 5, 179.

Philippoff, W., (1965), in "Physical Acoustics," Vol. II, Part B, Chap. 7, ed. by W. P. Mason, Academic Press, New York, 1965.

Piccirelli, R., and Litovitz, T. A., (1957), J. Acoust. Soc. Amer., 29, 1009.

Pinkerton, J. M. M., (1949a), Proc. Phys. Soc. Lon., B62, 129.

Pinkerton, J. M. M., (1949b), Proc. Phys. Soc. Lon., B62, 286.

Riddiford, C. L., and Jennings, B. R., (1966), J. Chem. Soc., 88, 4359.

Rouse, P. E., (1953), J. Chem. Phys., 21, 1272.

Sadron, C., and Rempp, P., (1958), J. Polymer Science, XXIX, 127.

Saito, N., (1951), J. Phys. Soc., Japan, 6, 293.

Saroff, H. A., (1957), J. Phys. Chem., 61, 1364.

Scheraga, H., (1955), J. Chem. Phys., 23, 1526.

Schwartz, G., (1965), J. Mol. Biol., 11, 64.

Stokes, G. G., (1845), Trans. Cambr. Phil. Soc., 8, 287.

Sylvan, T. P., (1963), E.E.E., Sept., 1963, Issue.

Tanford, C., (1961), "Physical Chemistry of Macromolecules," Wiley, New York.

Tanford, C., and Buzzell, J. G., (1956), J. Phys. Chem., 60, 225.

Tanford, C., Buzzel, J. G., Rands, D. G., Swanson, S. A., (1955), J. Am. Chem. Soc., 77, 6421.

Urick, R. J., (1947), J. Appl. Phys., 18, 933.

Urick, R. J., (1948), J. Acoust. Soc. Amer., 20, 283.

Weber, G., and Young, L. B., (1964), J. Bio. Chem., 239, 1424.

Weber, G., (1952), Biochem. J., 51, 155.

Welkowitz, W., (1955), J. Acoust. Soc. Amer., 27, 1142.

Williams, E. J., and Foster, J. F., (1959), J. Am. Chem. Soc., 82, 3741.

Yang, J. T., and Foster, J. F., (1954), J. Am. Chem. Soc., 76, 1588.

Zana, R., Cerf, R., and Candou, (1963), J. Chim. Phys., 60, 869.

Zimm, B. H., (1956), J. Chem. Phys., 24, 269.

Zimm, B. H., (1960), Chapter in Rheology, Vol. 3, ed. by F. R. Eirich, Academic Press, New York 1960, Chapter 1.

APPENDIX A

DATA TABULATION

BOVINE SERUM ALBUMIN

Acid Titration 1

Temp = 20.0°C

pH	conc (gm/100cc)	freq (MHz)	$A(sec^2 cc\ cm^{-1} gm^{-1}) \times 10^{+16}$
7.0	4.36	8.87	220
7.0	4.36	14.79	143
7.0	4.36	26.65	99.1
7.0	4.36	50.43	59.4
5.0	4.32	8.87	220
5.0	4.32	14.79	143
5.0	4.32	26.65	95.0
5.0	4.32	50.43	58.3
4.6	4.30	8.87	220
4.6	4.30	14.79	142
4.6	4.30	26.65	93.6
4.6	4.30	50.43	57.7
4.25	4.29	8.87	228
4.25	4.29	14.79	142
4.25	4.29	26.65	96.9
4.25	4.29	50.43	61.1
4.0	4.27	8.87	237
4.0	4.27	14.79	151
4.0	4.27	26.65	98.3
4.0	4.27	50.43	62.5
3.9	4.25	8.87	246
3.9	4.25	14.79	160
3.9	4.25	26.65	102
3.9	4.25	50.43	63.0
3.6	4.22	8.87	248
3.6	4.22	14.79	157
3.6	4.22	26.65	102
3.6	4.22	50.43	63.1
3.2	4.18	8.87	246
3.2	4.18	14.79	150
3.2	4.18	26.65	97.2
3.2	4.18	50.43	57.2

BOVINE SERUM ALBUMIN

Acid Titration 1 (cont'd)

Temp = 20.0°C

pH	conc (gm/100cc)	freq (MHz)	A(sec^2 cc cm^{-1} gm^{-1}) x 10^{+16}
2.68	4.12	8.87	247
2.68	4.12	14.79	147
2.68	4.12	26.65	93.4
2.68	4.12	50.43	52.2
*5.2	3.95	8.87	214
*5.2	3.95	14.79	142
*5.2	3.95	26.65	95.9
*5.2	3.95	50.43	60.7
*6.65	3.92	8.87	222
*6.65	3.92	14.79	147
*6.65	3.92	26.65	97.6
*6.65	3.92	50.43	65.7

*Back Titrations

BOVINE SERUM ALBUMIN

Acid Titration 2

Temp = 20.0°C

pH	conc (gm/100cc)	freq (MHz)	A(sec^2 cc cm^{-1} gm^{-1}) x 10^{+16}
7.1	5.31	8.821	212
7.1	5.31	14.74	140
7.1	5.31	26.60	89.6
7.1	5.31	50.25	55.2
5.95	5.29	8.821	218
5.95	5.29	14.74	142
5.95	5.29	26.60	94.0
5.95	5.29	50.25	57.1
5.0	5.26	8.821	222
5.0	5.26	14.74	147
5.0	5.26	26.60	92.8
5.0	5.26	50.25	57.5
4.35	5.22	8.821	227
4.35	5.22	26.60	98.5
4.35	5.22	50.25	60.8
4.1	5.19	8.821	229
4.1	5.19	14.74	148
4.1	5.19	26.60	96.5
3.9	5.16	8.821	245
3.9	5.16	14.74	157
3.9	5.16	26.60	100
3.9	5.16	50.25	62.5
3.5	5.09	8.821	245
3.5	5.09	14.74	157
3.5	5.09	26.60	99.1
3.5	5.09	50.25	51.7
3.0	5.00	8.821	240
3.0	5.00	14.74	148
3.0	5.00	26.60	91.4
3.0	5.00	50.25	51.7
2.3	4.92	8.821	240
2.3	4.92	14.74	148
2.3	4.92	26.60	88.2
2.3	4.92	50.25	47.4

BOVINE SERUM ALBUMIN

Acid Titration 2 (cont'd)

Tem = 20.0°C

pH	conc (gm/100cc)	freq (MHz)	A(sec^2 cc cm^{-1} gm^{-1}) x 10^{+16}
*3.5	4.77	8.821	246
*3.5	4.77	14.74	155
*3.5	4.77	26.60	99.1
*3.5	4.77	50.25	59.1
*4.8	4.63	8.821	215
*4.8	4.63	14.74	141
*4.8	4.63	26.60	93.2
*4.8	4.63	50.25	59.0

*Back Titrations

BOVINE SERUM ALBUMIN

Acid Titration 3

Temp = 19.9°C

pH	conc (gm/100cc)	freq (MHz)	A(sec^2 cc cm^{-1} gm^{-1}) x 10^{+16}
7.0	9.18	4.424	336
7.0	9.18	2.392	484
6.55	9.14	4.426	343
6.55	9.14	2.392	496
5.05	9.01	4.426	365
5.05	9.01	2.392	547
4.5	8.92	4.427	376
4.5	8.92	2.392	559
4.3	8.56	4.426	379
4.3	8.56	2.392	602
4.05	8.75	4.426	421
4.05	8.75	2.392	668
3.9	8.66	4.426	447
3.9	8.66	2.392	709
3.45	8.51	4.426	449
3.45	8.51	2.393	712
3.05	8.22	4.426	419
3.05	8.22	2.392	685
*5.3	7.54	4.426	356
*5.3	7.54	2.392	528

*Back Titrations

BOVINE SERUM ALBUMIN

Alkaline Titration

Temp = 20.0°C

pH	conc (gm/100cc)	freq (MHz)	A(sec^2 cc cm^{-1} gm^{-1}) x 10^{+16}
6.9	4.48	8.870	216
6.9	4.48	14.79	142
6.9	4.48	26.65	96.8
6.9	4.48	50.43	56.6
8.1	4.46	8.870	216
8.1	4.46	14.79	138
8.1	4.46	26.65	91.5
8.1	4.46	50.43	55.8
9.7	4.44	8.870	211
9.7	4.44	14.79	140
9.7	4.44	26.65	91.9
9.7	4.44	50.43	54.8
10.0	4.43	8.870	223
10.0	4.43	14.79	145
10.0	4.43	26.65	97.2
10.0	4.43	50.43	57.1
10.35	4.41	8.870	239
10.35	4.41	14.79	155
10.35	4.41	26.65	101
10.35	4.41	50.43	61.0
10.7	4.40	8.870	270
10.7	4.40	14.79	173
10.7	4.40	26.65	106
10.7	4.40	50.43	60.6
11.0	4.37	8.870	327
11.0	4.37	14.79	198
11.0	4.37	26.65	119
11.0	4.37	50.43	65.6
11.2	4.34	8.870	381
11.2	4.34	14.79	222
11.2	4.34	26.65	128
11.2	4.34	50.43	65.9

BOVINE SERUM ALBUMIN

Alkaline Titration (cont'd)

Temp = 20.0°C

pH	conc (gm/100cc)	freq (MHz)	A(sec^2 cc cm^{-1} gm^{-1}) x 10^{+16}
11.6	4.30	8.870	483
11.6	4.30	14.79	267
11.6	4.30	26.65	140
11.6	4.30	50.43	72.8
*9.3	4.16	8.870	208
*9.3	4.16	14.79	135
*9.3	4.16	26.65	91.3
*9.3	4.16	50.43	56.1

*Back Titration

BOVINE SERUM ALBUMIN

A Vs frequency pH = 7.0 Temp = 19.9°C

Concentration = 9.18 gm/100cc

freq (MHz)	A(sec^2 cc cm^{-1} gm^{-1} x 10^{+16}
13.32	164
10.58	189
8.530	221
7.164	250
5.800	283
4.427	337
3.067	415
2.392	487
1.725	584
1.037	772
0.353	885

BOVINE SERUM ALBUMIN

A Vs frequency pH = 7.0 Temp = 20.0°C

Concentration = 3.53 gm/100cc

freq (MHz)	A(sec^2 cc cm^{-1} gm^{-1}) x 10^{+16}
163.14	22.6
104.1	32.4
74.95	43.3
45.50	62.8

POLYETHYLENE GLYCOL

Temp = 4.2°C

Mw = 20,000

Mw = 4,000

Averaged together

freq (MHz)	$A(sec^2 cc\ cm^{-1} gm^{-1}) \times 10^{+17}$
4.54	427
5.54	388
6.57	380
7.55	359
8.60	342
10.6	310
12.6	294
14.6	283
14.7	283
20.6	244
26.5	220
32.5	209
38.3	194
44.3	186
50.2	179
56.0	169
68.0	147
80.1	140

POLYETHYLENE GLYCOL

Temp = 20.7°C

Mw = 20,000

Mw = 4,000

Averaged together

freq (MHz)	A(sec^2 cc cm^{-1} gm^{-1}) x 10^{+17}
2.45	373
3.07	353
3.75	312
4.54	310
5.12	308
5.54	271
6.50	265
7.16	259
8.60	240
8.87	236
10.56	222
12.6	199
14.6	184
14.7	181
20.6	153
26.6	141
32.5	127
38.4	123
44.4	107
45.5	119
50.1	107
56	108
68	89.5
74.95	99.6
79.4	88.2
104.1	84.7
133.5	88.9
163.1	84.5

POLYETHYLENE GLYCOL

Temp = 32.2°C

Mw = 20,000

Mw = 4,000

Averaged together

freq (MHz)	A(sec^2 cc cm^{-1} gm^{-1}) x 10^{+17}
2.41	281
3.09	263
3.75	263
4.44	241
5.11	228
5.87	202
6.48	195
8.53	176
10.6	164
12.6	149
14.7	136
20.6	125
26.6	111
32.4	98.8
38.4	94.3
50.2	83.9
56.0	81.2
67.9	75.8
80.0	69.9

POLYETHYLENE GLYCOL

Temp = 20.7°C Mw = 1,450

freq (MHz)	A(sec^2 cc cm^{-1} gm^{-1}) x 10^{+17}
5.800	184
6.482	181
7.167	179
7.849	174
8.53	171
8.87	170
10.58	170
13.32	166
14.79	148
20.70	145
26.65	127
38.50	122
50.43	107

POLYETHYLENE GLYCOL

Temp = 20.5°C Mw = 400

freq (MHz)	A(sec^2 cc cm^{-1} gm^{-1}) x 10^{+17}
7.849	68.4
8.53	61.1
8.87	79.4
10.58	67.9
13.32	65.0
14.79	52.3
20.70	61.0
26.65	56.8
38.50	60.4
50.43	57.7

TRIETHYLENE GLYCOL

Temp = 20.5°C

Mw = 150

freq (MHz)	A(sec^2 cc cm^{-1} gm^{-1}) x 10^{+17}
20.70	26.5
26.65	25.5
38.50	27.9
50.43	25.4

ETHYLENE GLYCOL

Temp 20.5°C

Mw = 62

freq (MHz)	A(sec^2 cc cm^{-1} gm^{-1}) x 10^{+17}
20.70	14.2
26.65	14.2
38.50	20.5
50.43	15.6
68.32	14.1

APPENDIX B

ELECTRONIC INSTRUMENTATION

Oscillator (< 5 MHz):	Hewlett Packard Corp.; Palo Alto, Calif. Model 650A
Oscillator (> 5 MHz):	Measurements Corp.; Boonton, N.J. Model 80-R
Gated Amplifier:	Arenberg Ultrasonic Lab.; Boston, Mass. Model PG650-C
Receiver (Low Frequency System):	Arenberg Ultrasonic Lab.; Boston, Mass. Model WA600-D with PA 620L Preamplifier
Receiver (High Frequency System):	Matec Inc.; Providence, R.I. Model PR 201
Isolation Amplifier Wideband Amplifier	Hewlett Packard Model 460A or 460B
Pulse Generator:	General Radio Corp.; Concord, Mass. Model 1217C
Frequency Counter Interval Timer	System Donner Corp.; Concord, Calif. Model 1037
Logarithmic Recorder:	Sargent Co.; Chicago, Ill. Model SRL
Pulse Height Detector 1:	(Sylvan, 1963)

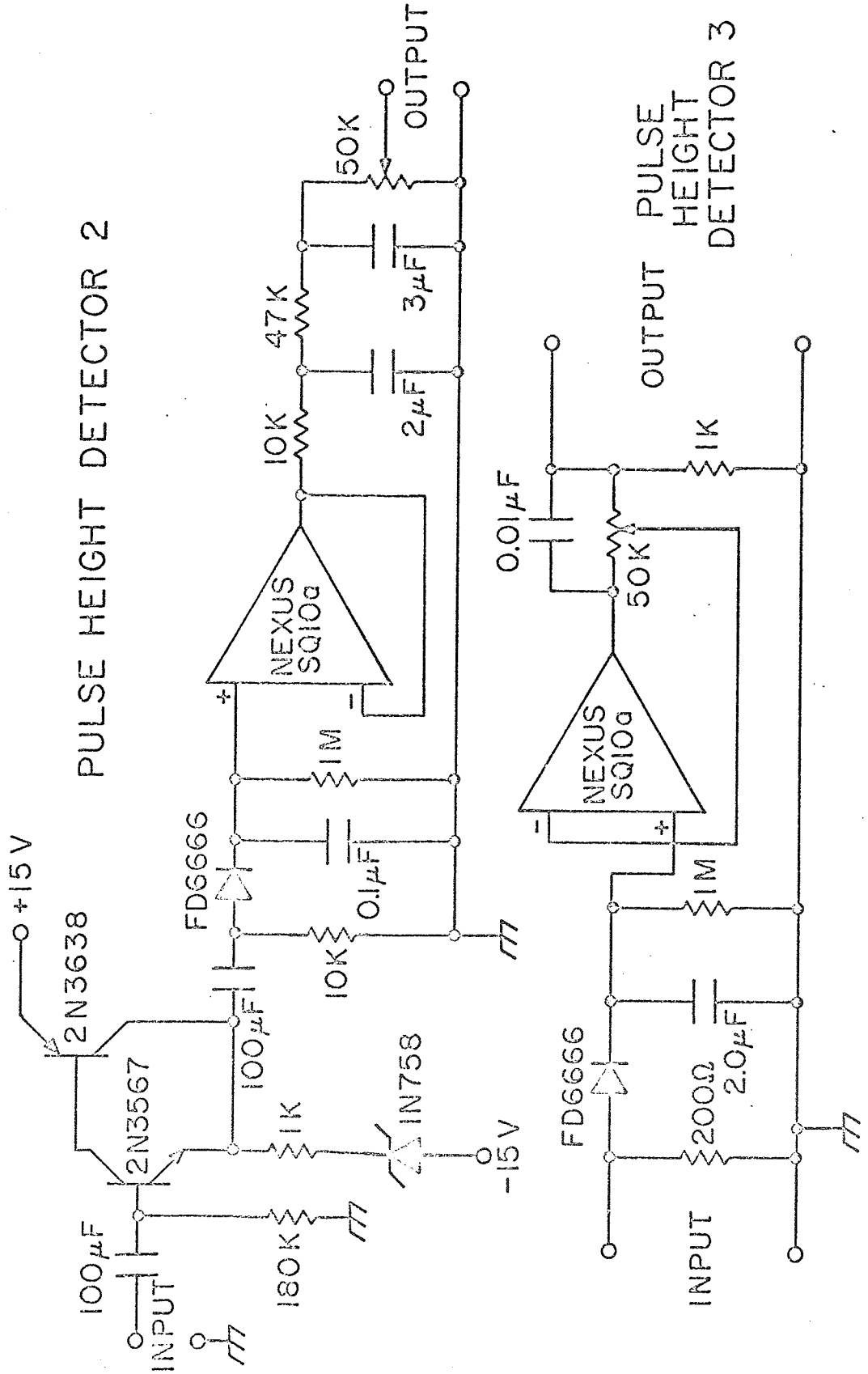
PULSE HEIGHT DETECTOR 2
+15 V
2N3638
2N3567
100μF
INPUT
180K
100μF
1K
IN758
-15 V
FD6666
10K
0.1μF
1M
NEXUS SQ10a
10K
47K
2μF
3μF
50K
OUTPUT
PULSE HEIGHT DETECTOR 3
0.01μF
50K
1K
NEXUS SQ10a
OUTPUT
1M
FD6666
200Ω
2.0μF
INPUT

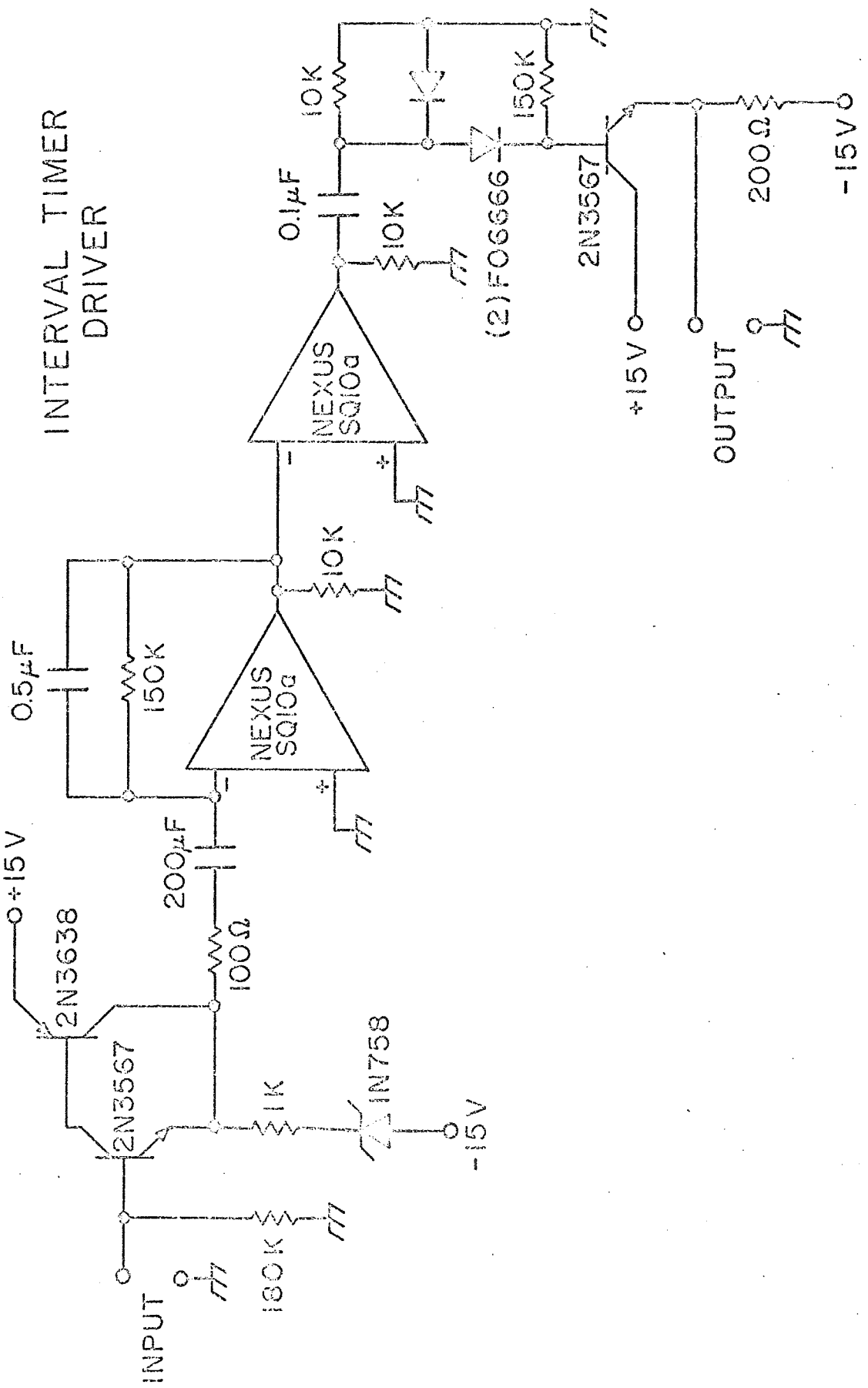
INTERVAL TIMER
DRIVER
INPUT
180K
2N3567
2N3638
+15V
100Ω
200μF
0.5μF
150K
NEXUS
SQ10a
10K
0.1μF
IN758
1K
-15V
(2) FOG666
150K
2N3567
+15V
OUTPUT
200Ω
-15V

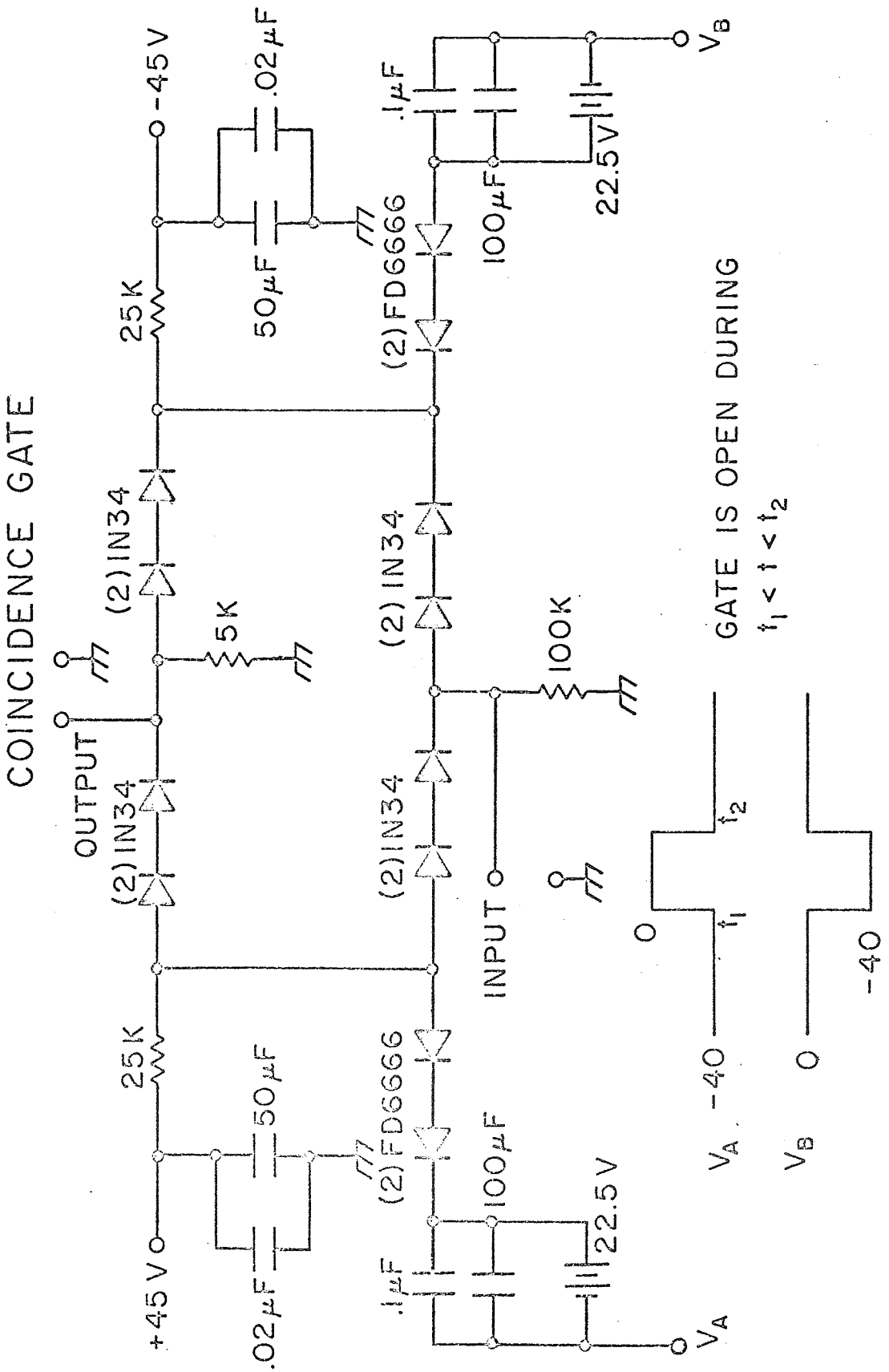
COINCIDENCE GATE
-45 V
.02 μF
50 μF
25K
(2) FD6666
.1 μF
100 μF
22.5 V
V_B
(2) IN34
5K
100K
OUTPUT
INPUT
+45 V
.02 μF
50 μF
25K
(2) FD6666
.1 μF
100 μF
22.5 V
V_A
GATE IS OPEN DURING
$t_1 < t < t_2$
t_1
t_2
0
-40
V_A
V_B

AUTOMATIC GAIN CONTROL AMPLIFIER

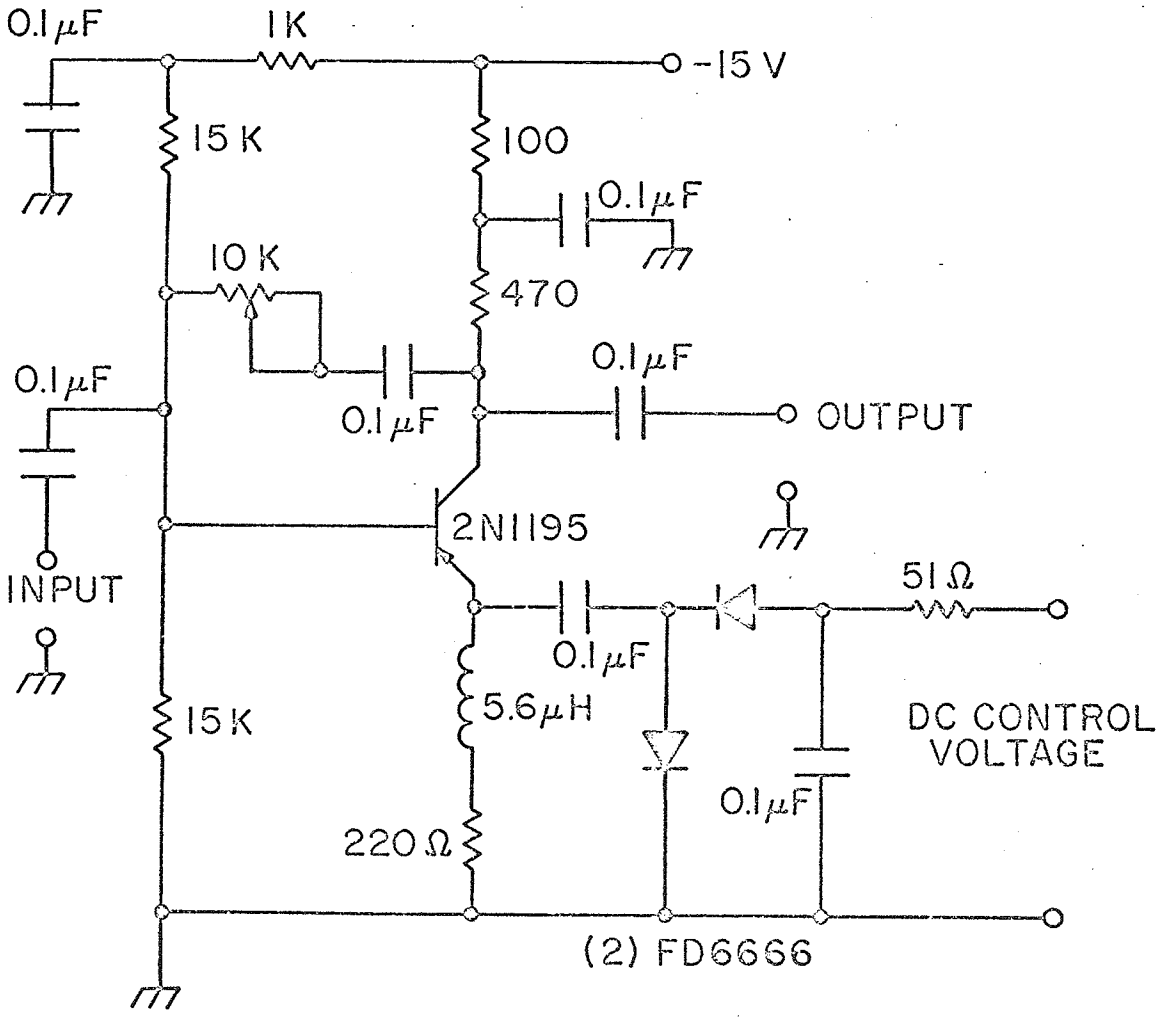

VITA

Lawrence Wolfe Kessler was born in Chicago, Illinois on September 26, 1942. After graduating from Senn High School in Chicago in 1960, he studied electrical engineering at Purdue University, West Lafayette, Indiana, and in his junior and senior years he received National Science Foundation fellowships. In 1964 Mr. Kessler entered the graduate school of electrical engineering of the University of Illinois and became interested in investigating the mechanisms of interaction between ultrasound and biological media. His M.S. thesis was entitled "The Absorption of Ultrasound in Aqueous Solutions of Dextran," and won honorable mention in the electrical engineering department yearly competition of M.S. theses. Mr. Kessler's minor subjects in graduate school were physiology and biophysics, and he has taught the laboratory section of a senior course in rf circuits. Mr. Kessler's interests lie in the fields of acoustics and bioengineering and he belongs to the following societies: Eta Kappa Nu, Sigma Xi, American Association for the Advancement of Science, and the Acoustical Society of America. He is coauthor of the following paper, "The Absorption of Ultrasound in Aqueous Solutions of Polysaccharides," S. A. Hawley, L. W. Kessler, and F. Dunn, J. Acoust. Soc. Amer., 38, 521, 1965 and has presented the following talk at the 73rd meeting of the Acoustical Society of America 1967: "Semiautomatic Ultrasonic Velocity and Absorption Instrumentation for Liquid Media," L. W. Kessler, S. A. Hawley, and F. Dunn.